PAEOECOLOGY AND PALEOENVIRONMENTAL RECONSTRUCTION OF THE LOWER SILURIAN QUSAIBA SHALE IN THE QASIM REGION

BY

PRAMUDYA RINENGGA DATU PERDANA

A Thesis Presented to the
DEANSHIP OF GRADUATE STUDIES

KING FAHD UNIVERSITY OF PETROLEUM & MINERALS

DHAHRAN, SAUDI ARABIA

In Partial Fulfillment of the
Requirements for the Degree of

MASTER OF SCIENCE

In

GEOLOGY

December 2017

KING FAHD UNIVERSITY OF PETROLEUM & MINERALS

DHAHRAN- 31261, SAUDI ARABIA

DEANSHIP OF GRADUATE STUDIES

This thesis, written by **PRAMUDYA RINENGGA DATU PERDANA** under the direction of his thesis advisor and approved by his thesis committee, has been presented and accepted by the Dean of Graduate Studies, in partial fulfillment of the requirements for the degree of **MASTER OF SCIENCE IN GEOLOGY.**

Michael A Kaminski

Prof. Michael A. Kaminski

(Advisor)

Dr. Abdulaziz Al-Shaibani

Department Chairman

Dr. Osman M. Abdullatif

(Member)

Prof. Salam A. Zummo

Dean of Graduate Studies

30/4/18

Date

Dr. Sedat Inan

(Member)

Dedication

To my beloved parents, wife, and daughter

ACKNOWLEDGMENTS

In the name of Allah, the most gracious, most compassionate, most merciful and all the praises and thanks be to Allah that have given me the opportunity and capability to finish my study in KFUPM.

I place on record my gratitude to KFUPM and NSTIP for giving me the opportunity to pursue my master's degree and conduct my research.

I am deeply indebted and most sincere appreciation goes to my advisor, Pof. Michael Kaminski, for knowledge, patience, encouragements, and guidance he has shown me over the past few years that I have been with this department, be it scientifically, personally, or academically.

I would like to express my gratitude to my thesis committee members, Dr. Osman Abdullatif and Dr. Sedat Inan for their precious support and guidance.

The help from Earth Sciences Department professors (Dr. Abdulaziz Shaibani, Dr. Ismail Kaka, Dr. Mustafa Hariri, Prof. Gavor Korvin, Prof. Ahmet Dogan, Dr. Muhammad Makawi, Dr. Khalid Ramadan, and many more) during my studies here are highly appreciated. Thanks also goes to Dr. Abduljamiu Amao, Septriandi, Muhammad Asif Abbas, Dr. Lamidi Babalola for the discussion and logistic support during field work and laboratory analyisis, and to KFUPM Indonesian community.

Thank you to my wonderful family: my parents for their endless pray, love and support; my brothers, Dika, and lastly — to my wife Maryam Al Azra, your endless love, support and encouragement has been most influential.

TABLE OF CONTENTS

ACKNOWLEDGMENTS ..... **IV**

TABLE OF CONTENTS ..... **V**

LIST OF FIGURES ..... **VIII**

LIST OF TABLES ..... **XI**

ABSTRACT ..... **XII**

ملخص الرسالة ..... **XIV**

CHAPTER 1 ..... **1**

1.1 Motivation **1**

1.2 Problem Statements and Objectives **3**

1.3 Study Area **5**

1.4 Thesis Structure **6**

CHAPTER 2 ..... **7**

2.1 Geological Setting **7**

2.2 Paleoenvironment Reconstruction **13**

2.2.1 Foraminiferal Biofacies Analysis 13

2.2.2 Geochemical Analysis 15

2.3 Previous Studies on the Qusaiba Shale **17**

CHAPTER 3 ..... **21**

3.1 Field Work **21**

3.2 Laboratory Work **21**

CHAPTER 4 ..... **28**

4.1. Lithofacies **28**

4.2. Facies Description and Interpretation **28**
4.2.1. Gray to dark gray Mudstone (Mdg) 28
4.2.2. Light gray Mudstone (Mlg) 30
4.2.3. Alternation of greenish-gray mudstone and reddish siltstone (Mzr) 32
4.2.4. Alternation of claystone to siltstone with fine to coarse-grained sandstone (Sfc 1) 34
4.2.5. Alternation of claystone to siltstone with fine to coarse grained sandstone (Sfc 2). 34

CHAPTER 5 ..... **37**

5.1. Foraminiferal Biofacies **37**
5.1.1. Foraminiferal Preservation 37
5.1.2. Foraminiferal Assemblages 38
5.1.3. Diversity Indices 44
5.1.4. Foraminiferal Morphogroups 47
5.1.5. Foraminiferal Wall Texture 51
5.1.6. Discussion 54

5.2. Graptolites **62**

CHAPTER 6 ..... **67**

6.1. Introduction **67**

6.2. XRD Results **67**

6.3 XRF Results **73**
6.3.1 Major Elements 73
6.3.2 Trace elements 77
6.3.3 Cross Plot Analysis 78

6.4 Environmental Proxies Analysis **80**
6.4.1 Sediment flux proxy 80
6.4.2 Paleoredox Proxy 82
6.4.3 Paleoproductivity Proxies 83

6.5 Framboidal pyrite **86**

6.6 Paleoecology and Paleoenvironmental Reconstruction **87**

CHAPTER 7 91

7.1 Conclusions 91

7.1 Recommendations for further study 93

REFERENCES 94

APPENDICES 117

A. Systematic Palaeontology 117

B. Plate Explanations 154

C. Recoverable Conodonts 176

D. SEM-EDS 177

Curriculum Vitae 180

LIST OF FIGURES

Figure 1: Ordovician and Lower Silurian Succession in Saudi Arabia (Craigie et al., 2016). Our studied section is illustrated with red rectangle of the Qusaiba and Sharawra Foramtion. 2
Figure 2: Paleozoic Paleolatitude Position of the Arabian Plate (Golonka et al., 2006). The transition during the clockwise rotational process, might be conceive essential transformation of geology, ecology, or environment aspect. Studying characteristics of the Lower Silurian succession may shed light on processes taking place during deposition. 2
Figure 3: Location of section 1 and 2 (base map after Zalasiewicz et al. 2007). 5
Figure 4: Stratigraphic column of the Qalibah Group (Mahmoud, et al., 1992) and updated version of Saudi Stratigraphic Committee (2012). 9
Figure 5: Depositional setting in the Lower Silurian of the Arabian Plate (Konert et al., 2001). 10
Figure 6: Chitinozoan zonation of the Qusaiba Formation represents the Rhuddanian – Telycian stage (Paris et al., 2015). 12
Figure 7: Morphogroups analysis of modern agglutinated foraminifera (Murray et al., 2011). 14
Figure 8: Morphogroup Model for Agglutinated Foraminifera (Setoyama et al., 2013). 15
Figure 9: PANanalytical Empyrean XRD at the Haliburton Technology Center. 24
Figure 10: PANanalytical Energy Dispersive XRF at Haliburton Technology Center. .. 25
Figure 11: Cressington Sputter Coater for preparing SEM samples. Shale samples were coated using Platinum. 26
Figure 12: SEM-EDS (JSM 6610LV). 27
Figure 13: A-B. Photograph of dark gray mudrock showing intense fissicility. C. SEM photomicrograph of clay minerals D. Lithology of the Mdg facies are classified as clay-rich argilaceous mudstone to silica-rich argillaceous mudstone. The classification was modified after Gamero-Diaz et al. (2013). 29
Figure 14:A-B. Photograph of light gray mudrock showing intense fisscility. C. SEM photo micrograph of clay minerals D. Lithology of the Mlg facies are classified as clay-rich argilaceous mudstone. The classification was modified after Gamero-Diaz et al. (2013). 31
Figure 15: A-B. Photograph of alternation of greenish-gray mudstone and reddish siltstone. C. SEM photomicrograph of clay minerals. D. Lithology of the

Mzr facies are classified as clay-rich argilaceous mudstone. The classification was modified after Gamero-Diaz et al. (2013). 33
Figure 16: A-B. Photograph of alternation of clay to siltstone with fine to coarse grain sandstone. C. SEM photomicrograph of clay minerals D. Lithology of the Sfc2 facies are classified as clay-rich argilaceous mudstone. The classification was modified after Gamero-Diaz et al. (2013). 35
Figure 17: Lithofacies description of Section 1. 36
Figure 18: Proportion of foraminiferal ordesrs and genera in the recovered samples. 39
Figure 19: Lithostratigraphy and occurrences of common species in the secton 1. 42
Figure 20: Lithostratigraphy and occurrences of common species in the secton 2. 43
Figure 21: Vertical distribution of diversity indices. 46
Figure 22: Rarefaction curves of foraminiferal assemblages from the section 1. 46
Figure 23: Foraminiferal morphogroups showing three groups and five subgroups or morphotypes. 50
Figure 24: Temporal distribution of the foraminiferal morphotypes in section 1. 51
Figure 25: Vertical distribution of group of foraminiferal wall textures in section 1. 54
Figure 26: Vertical distribution of common taxa. 57
Figure 27: Location of previously studied Lower Silurian foraminiferal assemblages (Golonka et al., 2006). A= Central United States (Moreman 1930); B= Bolivia (Gagnier et al. 1996); C= western Ireland (Kaminski et al. 2016); D= Czech Republic (Holcová 2002); E= Baltic region (Eisenack 1954); F= Western Australia (Bell et al. 2000); G= this study. 59
Figure 28: Representative species of recovered graptolite from section 1. A. *Normalograptus scalaris* (?); B. *Pristiograptus regularis;* C. *Pristiograptus renaudi;* D. *Normalograptus scalaris;* E. *Metaclimacograptus bohemicus;* F. *Pristiograptus variabilis;* G. *Metaclimacograptus hugesi;* H. *Neolagarograptus rickardsi;* I. *Normalograptus trifilis* (?); J. *Normalograptus ajjeri*. 65
Figure 29: Mineral distribution acquired from XRD in section 1. 69
Figure 30: A. Mineral percentages obtained from XRD B. Clay minerals percentage obtained from XRD. 71
Figure 31: Clay content distribution of section 1. 72
Figure 32: Major element oxide distribution obtained from XRF. 75
Figure 33: Crossplot analysis between Al_2O_3 and other oxides of the major elements. 79
Figure 34: Detrital proxies distribution of section 1. 81
Figure 35: Paleoredox proxies distribution of section 1. 83
Figure 36: Paleoprodctivity proxies distribution of section 1. 85
Figure 37: Two representatives of ramboidal pyrite recovered from the bottom part of the section 1. Scale bars are 100 µm. 87

Figure 38: Paeloenvironmental model of the Aeronian Qusaiba Formation in the Qasim Region, based on sedimentology, foraminiferal biofacies, and framboidal pyrite contents. Sedimentary depositional model was modified after Senalp and Al Duaji (2001). 90

LIST OF TABLES

Table 1: Taxonomic assignments of the recovered species. 39
Table 2: Diversity indices of foraminiferal assemblages in section 1. 45
Table 3: Comparison of the occurrence of genera at studied Silurian localities. 60
Table 4: Statistical parameters of mineral contents in shale samples. 68
Table 5: Statistical parameters of clay contents in shale samples. 70
Table 6: Statistical parameters of clay contents in shale samples. 71
Table 7: Statistical parameters of major elements obtain from XRD. 74
Table 8 : Statistical parameters of trace elements. 77

ABSTRACT

Full Name : [Pramudya Rinengga Datu Perdana]

Thesis Title : [Paeoecology and Paleoenvironmental Reconstruction of the Lower Silurian Qusaiba Shale in the Qasim Region]

Major Field : [Geology]

Date of Degree : [December, 2017]

The basal Qusaiba Formation especially “Qusaiba Hot Shale” is a prolific source rock in the Middle East and North Africa, and studies of its sedimentology and biostratigraphy utilizing graptolites, chitinozoa, achritarchs, and microspores were extensively carried out both in outcrop as well as in the subsurface. On the other hand, our foraminiferal study of the midle to upper Qusaiba Formation has obtained the first discovery of agglutinated foraminiferal assemblages in the Middle East.

Despite agglutinated foraminifera having been previously reported from the Lower Silurian succession in Laurasia and Baltic paleocontinents, as well as from carbonate successions in the Czech Republic, Australia and Bolivia, there is no previously published report of foraminifera in clastic deposits from the Gondwana paleocontinent. This first record of agglutinated foraminifera consists of an abundant assemblage consisting of 24 genera; *Ammobaculites, Ammovertella, Amphitremoida, Bathysiphon, Blastammina, Ceratammina, Hemisphaerammina, Hyperammina, Lagenammina, Psammosphaera, Rhabdammina, Saccammina, Saccamminita, Sorosphaera, Stacheia, Turritellella,*

Tolypammina, Thurammina, Thuramminoides Webbinelloidea, and 77 species. Some of the species are new to science. Compared with the described faunas in North America and Europe, this assemblage is more diverse.

The stratigraphic distribution of the foraminiferal assemblages exhibits low abundance in the lower part of the succession. This interval characterized by a low detrital influx of the quartz, Ti/Al, Zr/Al, high clay content, as well as high V/Cr, Co/Al, Fe/Al and P/Ti, Ba/Al ratio, may indicate dysoxic to suboxic conditions with high paleoproductivity in an offshore environment. On the contrary, in the middle of the section, a high diversity of foraminiferal assemblages comprising monothalimids, tubothalimids with smooth wall texture, and sparse multichambered forms, bloomed and reflect better paleo-oxygenation conditions. In the uppermost part of the studied section, globothalamid forms disappeared and were replaced by monothalamid assemblages with a medium-grained wall texture, indicating oxic conditions with a higher hydrodynamic energy in a lower shoreface paleoenvironment.

ملخص الرسالة

الاسم الكامل : فرموديا رنينغا داتو فيردانا

عنوان الرسالة **:** دراسة البيئة القديمة لصخور الطفلة بمتكون قصيبة ذات العمر السيلوري، منطقة القصيم

التخصص **:** الجيولوجيا

تاريخ الدرجة العلمية : ديسمبر – 2017

الجزء السفلي من متكون قصيبة يعد وافراً بصخور المنشأ في الشرق الأوسط والشمال الأفريقي. تم بعمق دراسة الرسوبية والطبقية لهذه الصخور باستخدام الخطيات، أكريتاركس، والأبواغ المجهرية في كلا من المنكشفات الصخرية والصخور التحت السطحية. في هذه الداسة تم لأول مرة في الشرق الأوسط اكتشاف تجمعات من المنخربات الملتحمة في الجزء اللأوسط والعلوي من متكون قصيبة. بالرغم من أن المنخربات الملتحمة تم اكتشافها من قبل في الطبقات ذات العمر السيليوري السفلي في كلا من لوراسيا وبانوتيا، كما تم رصدها في الصخور الجيرية باستراليا، بوليفيا وجمهورية التشيك، لم يسبق وأن تم أي ذكر للمنخربات في الصخور الفتتاتية بقارة غندوانا القديمة. وهنا تم رصد منخربات ملتحمة من تجمعات تتكون من أربعة وعشرين جنسا: أموباكوليتس، أموفرتيلا، أمفيتريمويدا، باثيسيفون، بلاستامينا، سيراتامينا، هيميسفايرامينا، هيبيرامينا، لاجينامينا، بساموسفيرا، رابدامينا، ساكامينا، ساكامينيتا، سوروسفيرا، ستاتشيا، توريتليلا، توليبامينا، ثورامينا، ثورامينويدس وبينيلويديا، و سبعة وسبعين نوعا. بعض هذه الأنواع تذكر لأول مرة . بالمقارنة بتجمعات أوروبا وأمريكا الشمالية، التجمعات في هذه الدراسة أكثر تنوعا. التوزيع الطبقي لتجمعات المنخربات يوضح وفرة قليلة في الجزء السفلي من الطبقات. هذا الجزء يتصف بقلة في التدفق الفتاتي من الكوارتز، ونسبة Zr/Al،Ti/Al ووفرة في المحتوى الطيني ونسبة Ba/Al، P/Ti، Fe/Al،Co/Al،V/Cr . وذلك يشير إلى ظروف قليلة الأكسجين مع علو في الانتاجية في بيئة بعيدة عن الشاطئ. ويتصف الجزء الأوسط من الطبقات بتنوع عالي في تجمعات المنخربات مونوثاليميدس وتوبوثاليميدس والذي يعكس بيئة قديمة ذات محتوى أكسجيني أعلى من السابق. في

الجزء العلوي من الطبقات، اختفت تجمعات الجلوبوثالاميد واستبدلت بتجمعات من المونوثلاميد، مشيرة إلى وفرة في الأكسجين و هيدروديناميةعالية في بيئة قديمة لسطح شاطئ سفلي.

CHAPTER 1

INTRODUCTION

1.1 Motivation

The Silurian Qusaiba shale Formation of the Qalibah Group is one of the important rock records in Saudi Arabia, containing a basal hot shale that is a world-class source rock of the Paleozoic petroleum system in the Arabian Peninsula (Abu-Ali et al., 1991; Mahmoud, et al., 1992; Jones and Stump, 1999; Luning et al., 2000, Inan et al., 2016, Inan et al., 2017). The generation of this sedimentary record coincides with an Oceanic Anoxic Event that occurred after the Hirnantian glaciation (Melvin, 2015), and is reflected as Maximum Flooding Surface (MFS) S10 (Sharland, 2001) (Fig.1).

The uniqueness of the Silurian deposition in Saudi Arabia, not only on the basis that this succession rests on glaciogenic deposits of the Sarah Formation that represents a change in environment, but also a hiatus is present on the upper part of this Silurian deposit that is interpreted as due to the Caledonian Orogeny (Mahmoud, et al., 1992). Moreover, during Silurian time the Arabian Plate underwent a clockwise rotation of about 100° without any significant latitudinal change (Konert et al. 2001) (Fig. 2). Therefore, the Silurian period has a fundamental contribution to global phenomena in northern Gondwana.

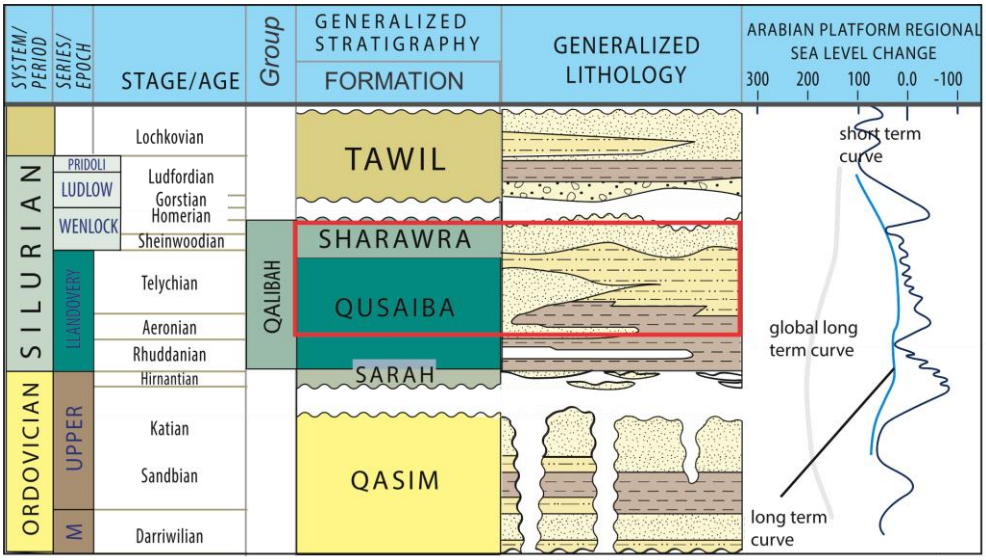

Figure 1: Ordovician and Lower Silurian succession in Saudi Arabia (Craigie et al., 2016). Our studied section is illustrated with red rectangle of the Qusaiba and Sharawra Formation.

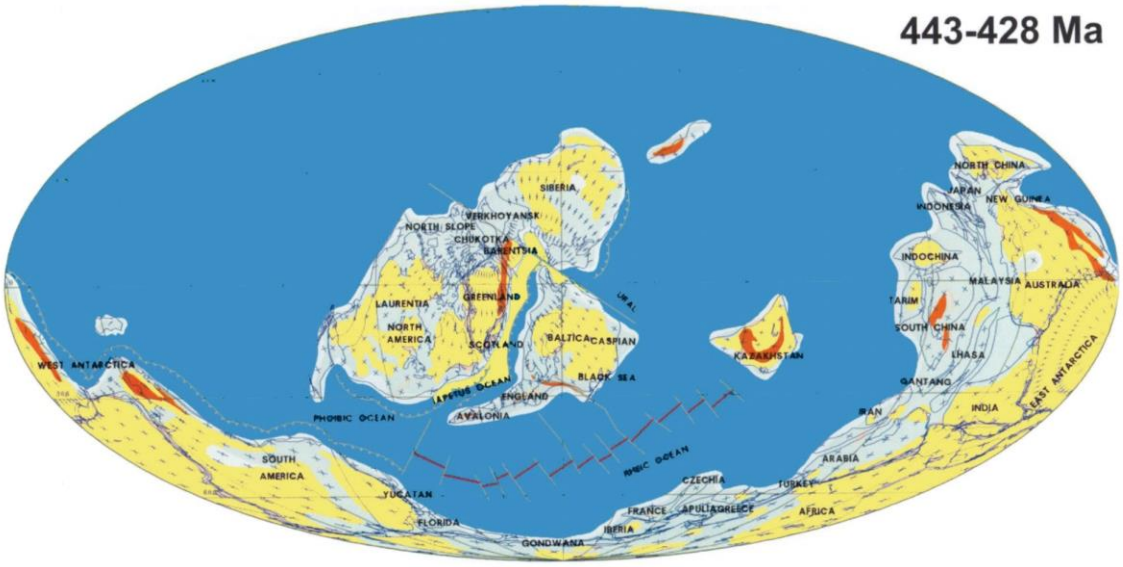

Figure 2: Paleozoic paleolatitude position of the Arabian Plate (Golonka et al., 2006). The transition during the clockwise rotational process, might be conceived as an essential transformation of geology, ecology, or environment aspect. Studying characteristics of the Lower Silurian succession may shed light on processes taking place during deposition.

1.2 Problem Statements and Objectives

Owing to its status as a world-class prolific Paleozoic source rock in the Arabian Peninsula and North Africa, extensive research has been done on the basal Qusaiba Formation “Qusaiba Hot Shale” (Mahmoud et al., 1991; Jones et al. 1999; Miller and Melvin, 2005; Inan et al., 2016a; Inan et al., 2017; Hayton et al., 2017). Studies of sedimentology, stratigraphy, organic geochemistry, and rock characterization try to reveal how this formation and its correlative sequence was deposited, generated, as well as its potential as a source rock and even as an unconventional reservoir rock. Moreover, paleontological studies, including macrofauna such as graptolites, and microfossils and palynomorphs such as chitinozoa, achritarch, microspores, were also conducted to recognize its relative age to correlate lateral successions in the Arabian Peninsula and northern Africa (Luning et al., 2000), and reveal the paleoenvironment in which this sequence was deposited.

Detailed investigations on the graptolites (El-Khayal, 1987; Aoudeh and Al Hajri, 1995; Zalasiewicz et al., 2007; Williams et al., 2016) and palynomorphs (Miller and Melvin, 2005; Wellman et al., 2005; Le Herisse et al., 2014; Paris et al. 2015; have been relatively well-established. However, the study of the benthic fauna is only restricted to the nature of the ichnofossil assemblage, and no benthic foraminiferal studies have been performed on this sequence. Therefore, this study is the first investigation on benthic foraminifera in the Gondwana region in the Lower Silurian Qusaiba or its correlative formations in North Africa.

Benthic foraminiferal study on the Qusaiba Formation will be suggested as a new alternative method for inferring and reconstructing the paleoenvironment and paleoecology of the Lower Silurian succession. This benthic foraminiferal study on the Lower Silurian succession will give a contribution on how the foraminifera evolved and adapted during this age, since studies about the fauna of this age are still very limited compared to the Mesozoic, Cenozoic, and modern records.

On the other hand, not only studies of benthic foraminifera, but also integrated studies that combine benthic fauna with organic and inorganic geochemistry to reveal paleooxygenation, paleoenvironment, and paleoecology of the Lower Siluran have an essential role. Thus, these two methods will become a fundamental key to reveal environmental change after the Hirnantian deglaciation, coinciding with an Oceanic Anoxic Event (OAE) in the intial transgression.

Therefore, the main objectives of this thesis are summarized as follow:

1) Identification of the foraminiferal species and biofacies in the gray-warm shale unit of the Qusaiba and Sharawa formations of the Qalibah Group in outcrop
2) Analysis of foraminiferal morphotypes and inferred life style (i.e., epifaunal, shallow infaunal, deep infaunal) based on morphogroup interpretations.
3) Determining the temporal succession of paleo-oxygenation based on major and trace elements.
4) Reconstructing the paleoecology & paleoenvironment of the middle to upper Qusaiba Formation in the Qasim Region.

1.3 Study Area

The study area is located in the Qusaiba depression, near the abandoned Old Qusaiba village, Qasim Region Central Saudi Arabia (Fig. 3). The first section, corresponding to Section 1 of Abbas et al. (2017) is exposed along an unpaved road that leads up the face of the cuesta from Old Qusaiba Village (N 26° 51’35” E 43° 34’19”). The second section, corresponding to Section 2 of Abbas et al. (2017) is located about a kilometer to the south of the road outcrop (N 26° 50’ 2.8”, E 43°, 36’ 00”). Both sections are considered as a middle to upper part of the Qusaiba Foramation.

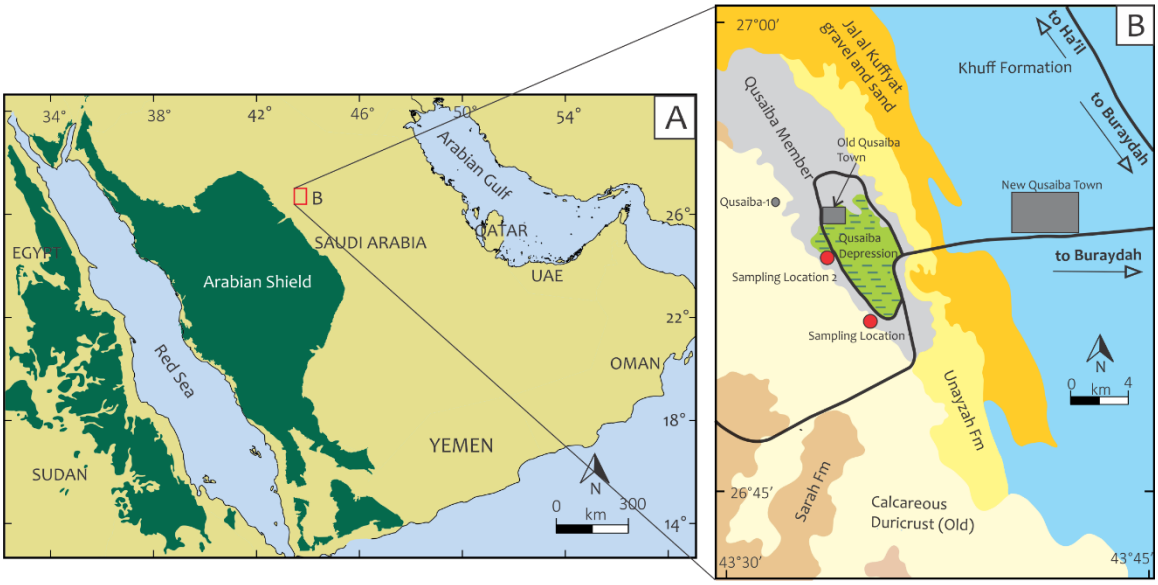

Figure 3: Location of section 1 and 2 (base map after Zalasiewicz et al. 2007).

1.4 Thesis Structure

This master thesis constitutes six chapters, the first Chapter provides the motivation, problem statement, and objectives of this thesis, the second chapter provides information in the form of a literature review including the geological setting of the Silurian succession in Saudi Arabia, an overview about foraminiferal morphogroups in regard to paleoenvironmental reconstruction, as well as geochemical analysis as a tool for interpreting paleoredox and paleoproductivity that controls the formation of the rock records. The third chapter elaborates the methodology followed in this research including field work and laboratory work, the fourth chapter informs the obtained results of this research, comprising the sedimentological description, micropaleontological identifications, and geochemical analysis of the major, minor, and trace elements. The fifth chapter is a discussion devoted to elaborate the correlation of results and the main objectives of this research. Moreover, the final chapter addresses and answers the main objectives stated in the first chapter, followed by recommendations for future work.

CHAPTER 2

LITERATURE REVIEW

2.1 Geological Setting

The Qalibah Group is subdivided into the Qusaiba and Sharawra formations (Saudi Stratigraphic Committee) (Fig. 4). The Qusaiba Formation consists of dominant laminated shale and mudstone with thin interbedded of siltstone and sandstone at its top. This member is pyritic, rich in organic matter, and contains graptolites in the lower part, with detrital sand and mica content gradually increasing toward the top. The richness of organic matter of the basal Qusaiba Formation classifies it as a hot shale (Mahmoud et al., 1992; Cole et al., 1994; Luning et al., 2000), which has gamma ray value more than 150 API. This hot shale is usually 9–31 m thick, less bioturbated than the overlying unit, and considered as the main source rock of the Paleozoic Petroleum System in Saudi Arabia (Jones and Stump, 1999; Cantrel et al., 2014).

The Sharawra Formation comformably overlies the Qusaiba Formation with a gradational contact, which is mostly sandstone with interbedded siltstones and mudstones with rich mica content. In the outcrop reference section, between Tayma and Al Qalibah towns, the Qusaiba Formation rests disconformably on the Sarah Formation, and the Sharawra Formation is overlain disconformably by the Tawil Formation with truncation on the uppermost part of this formation. The thickness of the Qalibah Group in the reference section is approximately 499 m, with 256 m of the Qusaiba Formation and 243 m of the Sharawra Formation (Mahmoud et al., 1992).

On the regional point of view, the Lower Silurian Qusaiba and Sharawra formations exhibit a clastic progradational succession that is interpreted as broad continental shelf deposition during rising sea level due to ice melting after the Hirnantian glaciation in northern Gondwana (Fig. 5). However, a hiatus in the uppermost part of the succession in the Upper Silurian is suggested as a result of uplift associated with the Caledonian Orogeny (Mahmoud et al., 1992).

As a continental shelf deposit, the absence of carbonate deposition in the Lower Silurian Qusaiba and Sharawra succession is suggested as a result of the high latitude position of the Gondwanan continent during the Silurian period. Furthermore, the high rate of sediment supply that is represented by a thick progradational clastic sequence also inhibited carbonate buildup (Mahmoud et al., 1992).

Based on the Qusaiba Formation sedimentological features and fauna content, which is the presence of the abundant and diverse benthic fauna in the gray shale of this formation, and its coarsening upward succession with thin interbedded silt and sand, has been interpreted as a shoaling upward depositional setting (Jones and Stump, 1999). The abundance of bioturbation is interpreted as oxygenated or partially oxygenated water column above the surface of the sediment. However, the absence of bioturbation in this deposit in eastern and central Saudi Arabia is interpreted as anaerobic conditions when the organic-rich shale was deposited (Melvin, 2015).

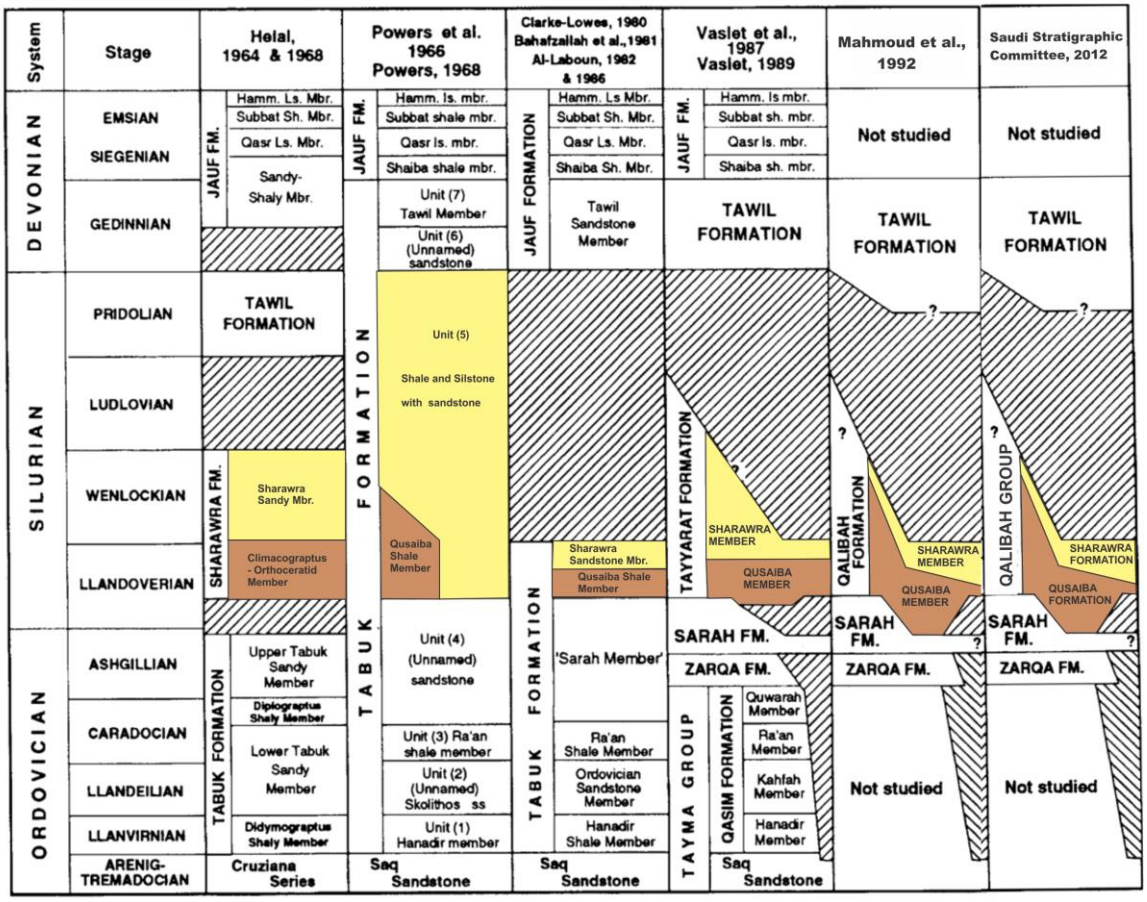

Figure 4: Stratigraphic column of the Qalibah Group (Mahmoud, et al., 1992) and updated version of Saudi Stratigraphic Committee (2012).

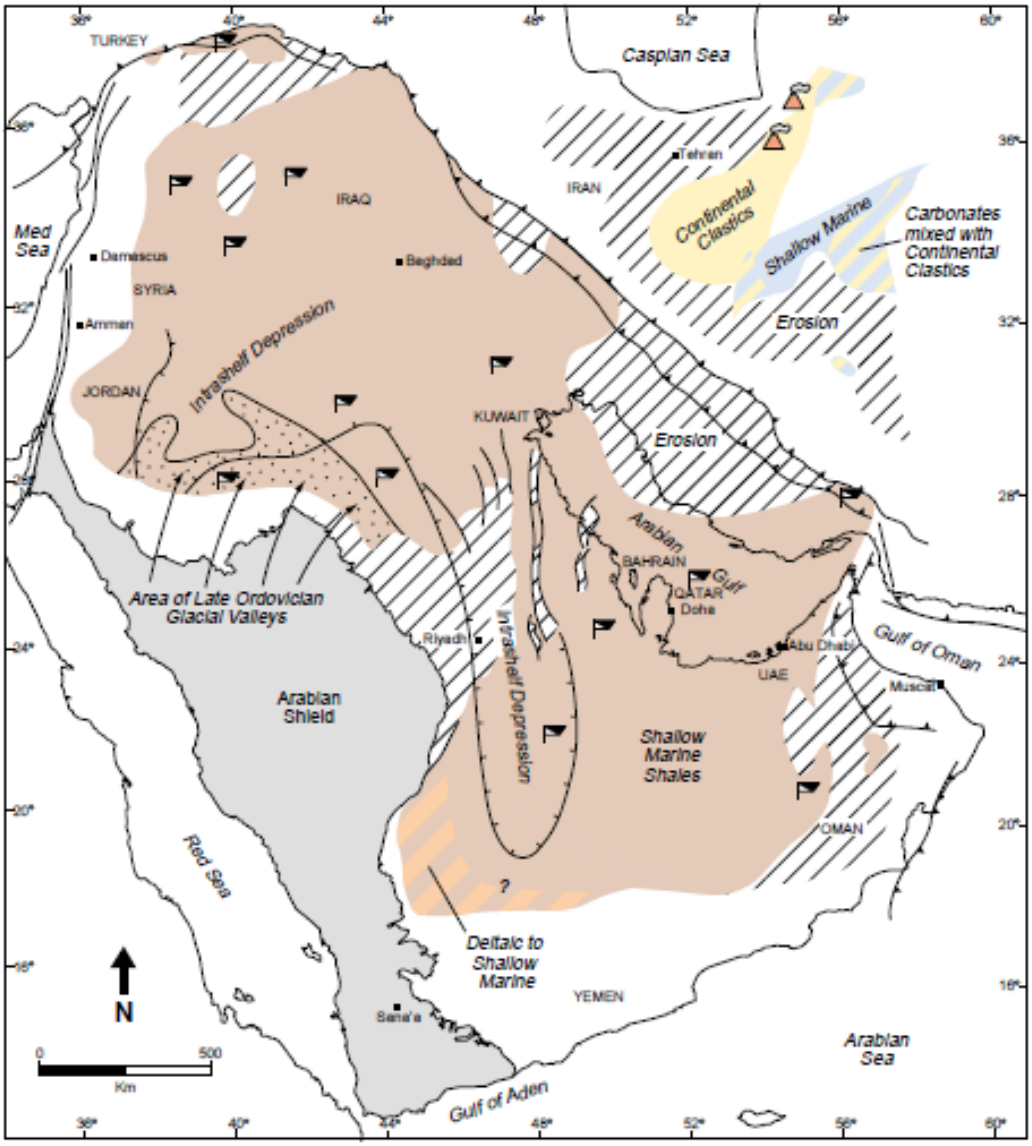

Figure 5: Depositional setting in the Lower Silurian of the Arabian Plate (Konert et al., 2001).

The age of the lower part of the Qalibah Group, based on the basal Qusaiba Formation is considered as early Rhuddanian–Telychian based on the recognition of the garaptolite and chitinozoans zones (Fig. 6). In the upper part, the age of the Sharawra Formation is determined as Pridolian based on the identification of palynomorphs (Mahmoud et al., 1992) in the Udaynan-1 well, and not younger than Early Devonian of the overlying Tawil Formation. From the graptolite analysis, Williams et al. (2016) classified the graptolite biozonation in Saudi Arabia into 12 biozones, which are *N. lubricus, A. ascensus–P. acuminatus, C. vesiculosus, C. cyphus, D. triangulates, N. thuringiacus, P. lepotheca, L. convolutus, S. sedgwickii, S. halli, S. guerichi, S. turriculatus*. On the other hand, based on the chitinozoan identification, Paris *et al.* (1995) subdivided the local chitinozoan stratigraphy into 8 biozones, *S. fragillis, B. postrobusta, L nuayyimensis, A. qusaibaensis* (Rhuddanian); *C. Alargada / P. paraguayensis* (Aeronian); *S. solitu / A.hemeri, A. hemeri,* and *A. macculerei* (Telychian).

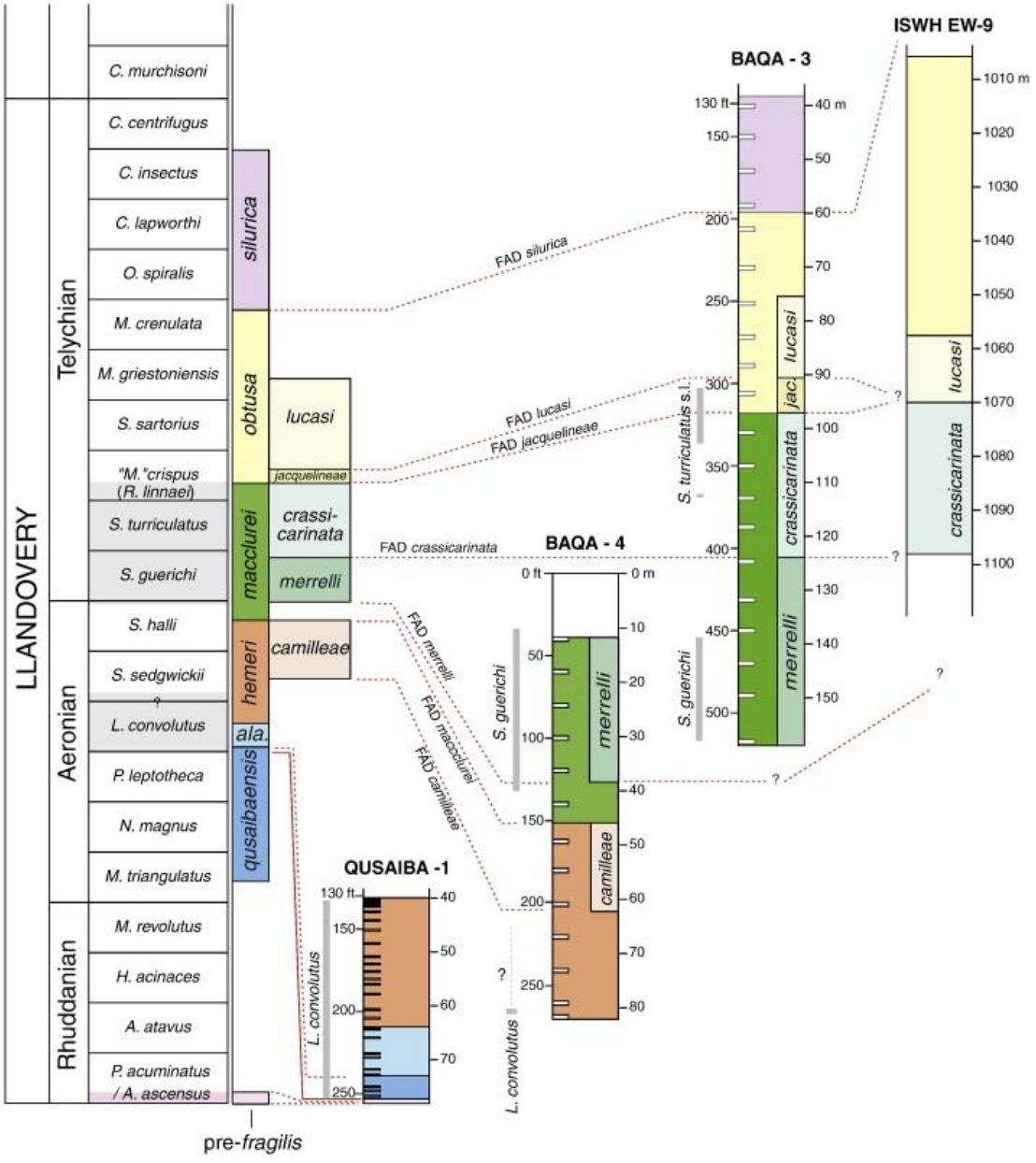

Figure 6: Chitinozoan zonation of the Qusaiba Formation represents the Rhuddanian – Telycian stage (Paris et al., 2015).

2.2 Paleoenvironment Reconstruction

There are some approaches to identify paleoenvironment and paleooxygenation of the ancient sediment. Those techniques include paleobiological and geochemical analysis of the sedimentary record. Integrating both of these approaches will provide more reliable answers for many questions related to shale and mud rock deposited in the paleoenvironment.

2.2.1 Foraminiferal Biofacies Analysis

Fossil benthic foraminifera are extensively applied as paleoenvironmental indicators based on comprisons with their modern representatives. Their habitats are influenced by biological, physical, and chemical conditions either in the short term or over long term periods of the interaction (Kuhnt et al., 1994). Therefore, by reversing the methodology by using the fossil record, the physical, biological, and chemical conditions in ancient environments can be inferred.

One of the basic approaches can be used in interpreting the paleoenvironment is morphogroup analysis. This approach that based on the foraminiferal morphology function, comes with the assumption that different test shape has different life habit, therefore changes in the relative abundance of these groups exhibit specific environment (Corliss, 1985; Jones and Charnock, 1985; Murray et al., 2011) (Fig.7).

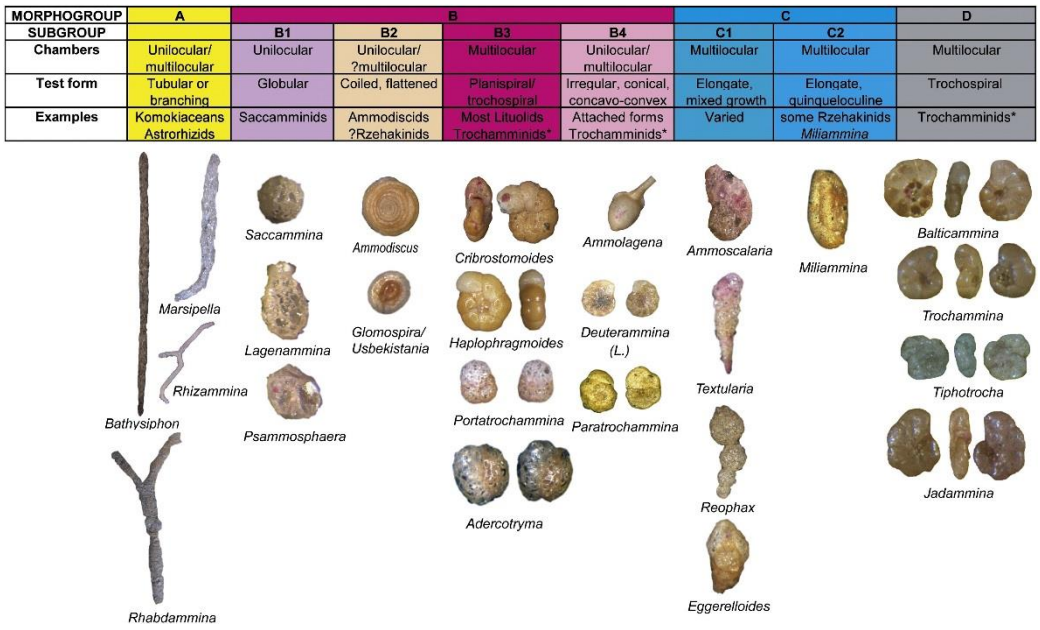

Figure 7: Morphogroup analysis of modern agglutinated foraminifera (Murray et al., 2011).

This method is widely applied for benthic foraminifera either on shallow environment or deep environment, with both agglutinated and calcareous shells, thus it is a well established method for assessing paleoenvironment, paleo-oxygenation, and paleobathymetrical conditions without the need for analyzing the paleoenvironment of every species (Jones and Charnock, 1985; Bernhard, 1986; Corliss and Chen, 1988; Tyszka and Kaminski, 1995; Nagy et al., 1992, 1995, 2009; Kaminski and Gradstein, 2005; Reolid et al., 2008, 2013; Setoyama et al. 2012, 2013).

Morpho-group		Morpho-type	Test form	Life position	Feeding habit	Environment	Main genera
M1			Tubular	Erect epifauna	Suspension feeding	Tranquil bathyal and abyssal with low organic flux	*Arthrodendron* *Nothia* *Psammosiphonella* *Rhizammina* *Tolypammina*
M2	M2a	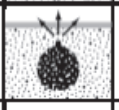	Globular	Shallow infauna	Suspension feeding and/or Passive deposit feeding	Common in bathyal and abyssal	*Caudammina* *Hyperammina* *Placentammina* *Psammosphaera* *Saccammina*
	M2b	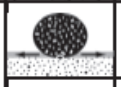	Rounded trochospiral and streptospiral	Surficial epifauna	Active deposit feeding	Shelf to deep marine	*Recurvoides* *Thalmannammina*
			Planoconvex trochospiral				*Trochammina*
	M2c		Elongate keeled	Surficial epifauna	Active deposit feeding	Shelf to marginal marine	*Plectoeratidus* *Spiroplectammina*
M3	M3a		Flattened trochospiral	Surficial epifauna	Active and passive deposit feeding	Lagoonal to abyssal	not in this study
			Flattened planispiral and streptospiral				*Ammodiscus* *Arenoturrispirillina* *Glomospira* *Repmanina* *Rzehakina*
	M3b		Flattened irregular	Surficial epifauna	Suspension feeding	Upper bathyal to abyssal	*Ammolagena*
	M3c		Flattened streptospiral	Surficial epifauna	Active and passive deposit feeding	Upper bathyal to abyssal	*Ammosphaeroidina* *Paratrochamminoides* *Praecystammina* *Trochamminoides*
M4	M4a		Rounded planispiral	Surficial epifauna and/or shallow infauna	Active deposit feeding	Inner shelf to upper bathyal	*Buzasina* *Evolutinella* *Haplophragmoides*
	M4b	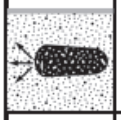	Elongate subcylindrical	Deep infauna	Active deposit feeding	Inner shelf to upper bathyal with increased organic matter flux	*Gerochammina* *Rectogerochammina* *Verneuilinoides*
		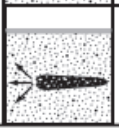	Elongate tapered				*Ammobaculites* *Hormosina* *Pseudonodosinella* *Reophax* *Subreophax*

Figure 8: Morphogroup Model for Agglutinated Foraminifera (Setoyama et al., 2013).

2.2.2 Geochemical Analysis

Geochemical analysis of marine sedimentary deposits may provide essential information about the environment conditions where sedimentation took place. In terms of identifying paleo-oxygenation conditions, there are several approaches that can be applied, such as the Vanadium and Nickel ratio (Lewan and Maynard, 1982; Arthur and Sageman, 1994),

the Degree of Pyritization (DOP) (Raiswell et al., 1988; Arthur and Sageman, 1994), and redox-sensitive element analysis (Co, Cr, Mo, Pb, U, Th) (Wignal and Mayers, 1988; Tribovillar et.al, 2006; Yilmaz et al., 2010; and Reolid et al., 2012).

The Vanadium and Nickel ratio is based on the assumption that Vanadium is fixed with organic matter and Nickel will be removed in anoxic water conditions. Therefore, rising concentration of Vanadium over Nickel may exhibit euxinic conditions, and the [V/(V+Ni)] ratio will describe water column paleo-oxygenation (Arthur and Sageman, 1994). Another alternative method is the Degree of Pyritization defined as the ratio between iron in sulfide minerals and total reactive iron. The parameters that can be utilized to infer oxic bottom water when the DOP is less 0.45, restricted bottom water conditions is suggested when the DOP value is between 0.45 and 0.75, and when the value is greater than 0.75, euxinic water conditions are inferred. (Arthur and Sageman, 1994). In addition, for redox sensitive trace element approach, assumed to be relatively abundant under low oxygen state as a result of less soluble when reducting condition occur (Reolid et al., 2012). Thus, the concentration of these elements will be higher under poorly oxygenated conditions and lower in oxic conditions.

In understanding paleoenvironmental conditions, estimating the paleoproductivity of the ancient marine setting also has an essential role. It can be correlated to paleo-oxygenation and preservation of organic matter. There are some geochemical techniques to determine paleoproductivity conditions such as the Barium to Aluminium ratio, Calcium to Aluminum ratio, Strontium to Aluminium ratio, and Phosphorus to Titanium ratio (Reolid

et al., 2012). In these techniques, the concentration of Ba, Ca, Sr, or P represents a biological influx to the sea floor; therefore, high values of these element ratios will indicate higher levels of paleoproductivity. In this study, P/Ti and Ba/Al ratio were calculated.

2.3 Previous Studies on the Qusaiba Shale

Previously, the Silurian succession was defined together with underlying Ordovician and overlying Lower Devonian clastic successions in the Tabuk area as the Tabuk Formation by Powers et al. (1966) and Powers (1968). On the other hand, Helal (1964) suggested separating the Lower Silurian succession as an independent formation using the more reliable type section as Sharawra Formation.

Based on Powers (1968), Bahafzallah et al. (1981) and Al-Laboun (1986) recognized a disconformity at the upper boundary of the Upper Silurian succession. However, they failed to mention the disconformity below the Qusaiba. In that work, Al-Laboun (1986) regarded the Qusaiba and Sharawra as members of the Tabuk Formation.

In a further study, Vaslet et al. (1987) redefined this Lower Silurian clastic succession as the Tayyarat Formation that consists of two members, Qusaiba and Sharawra. However, because the Tayyarat Formation was similar and already in use in Iraq as a Cretaceous succession (Dunington et al., 1959), Mahmoud et al. (1992) introduced this formation as the Qalibah Formation with Qusaiba and Sharawra as members.

Janjou et al. (1996), based on the mapping of the Qalibah Formation, in the Qalibah Quadrangle, northwestern Saudi Arabia, suggested that the Qalibah Formation should be elevated to a group, and the Qusaiba and Sharawra to formations. This new nomenclature is still debatable, some researchers from Saudi Aramco (Sharland, 2001; Miller and Melvin, 2005; Melvin, 2015) are still applying the previous status, while other researchers (Alsharhan and Nairn, 1997; Inan et al. 2016a) and the Saudi Stratigraphic Committee are using the new nomenclature. In this thesis, I follow the usage adopted by the Saudi Stratigraphic Committee (SSC).

Some layers of the Qusaiba Formation are rich in graptolites. The first study of graptolites was conducted by Steineke et al. (1958), who found *Climatograptus* in Tabuk. In a further study, Rickards and Koren (1974) identified graptolites of the *Monograptus convolutus* Zone. Some researchers (McClure, 1978, 1988; Ekren et al., 1987; El-Khayal, 1987; Vaslet, 1987) also studied graptolites that they found during their field work in the Qasim region. In a recent study in the Qusaiba Formation, Zalasiewicz et al. (2007) identified three graptolite biozones (convolutus, sedgwickii, and guerichi biozones) that were tied to the standard Silurian chronostratigraphy.

Other extensive paleontological studies of the Qusaiba Formation use chitinozoans (McClure, 1988; Aoudeh and Al-Hajri, 1995; Paris and Al-Hajri, 1995; Paris et al., 1995; Al-Hajri and Paris, 1998; Paris et al., 2008, Paris, et al., 2015). The goal of these studies was to define the age of the Qusaiba Formation and refine the chitinozoan biozonation in northern Gondwana. In the most recent study, Paris et al. (2015) subdivided the Qusaiba

into the *qusaibaensis, alagrada, hemeri, macclurei, obtuse, silurica* Zone, and *camilleae, merrelli, crassicarinata, jacquelineae and lucasi* Sub-zones.

Acritarchs (Le Hérissé et al., 1995, 2008, 2014) and spore assemblages (Steemans et al., 2000) have also been studied in the Qusaiba Formation. A resent study of acritarchs by Le Hérissé et al. (2014) found *Dorsennidium polorum,* which is an indication of the Rhudanian interval. In other hand, in a study of spore assemblages, Steemans et al. (2000) reported that unornamented hillate and trilate believed first appear in the Llandovery.

As a petroleum source rock, studies on the subject of organic geochemistry, such as total organic carbon (TOC), Hydrogen Index, Thermal Alteration Index (TAI), kerogen, Rock-Eva1 pyrolysis, ^{13}C isotopic composition, and biomarkers, have been conducted (McGillivray et al., 1992; Cole et al., 1994; Jones and Stump, 1999; Abu-Ali et al., 1991, 1999, 2005, Inan et al., 2016). In addition, Cole et al. (1994), conducted a study of graptolite reflectance to substitute vitrinite reflectance in terms of maturation analysis. Moreover, integrated thermal maturity analysis had been applied to infer source rock maturity and petroleum generation history (Inan et al., 2016; Inan et al., 2017; Schimdt-Mumm and Inan, 2016). From those studies it is inferred that the Lower Silurian Qusaiba hot shale is a prominent Paleozoic source rock in Saudi Arabia. On the other hand, inorganic geochemistry was conducted by Craigie (2016) to establish a chemostratigraphic zonation of the Qusaiba Formation. This technique is an effort to assist biostratigraphic methods in this succession.

Miller and Melvin (2005) developed a high-resolution biostratigraphic zonation based on palynomorph analysis (cryptospores, acritarchs, and chitinozoans of the Qusaiba Formation using subsurface data. Based on his work, these authors concluded that the Maximum Flooding Surface (MFS) is related to the occurence of *Papulogabata*, associated with a palynological diversity spike and starved sediment indicators.

Melvin (2015) conducted a study on the lithostratigraphy and depositional history of the Upper Ordovician – Lower Silurian succession using a shallow core with a total depth of 551 ft from the Qusaiba depression near the abandoned Qusaiba village in the Qasim region. He identified the lower part of the Qusaiba Formation as Rhuddanian age (2.5 ft; 0.75 m) with 15 cm subfissile sandy mudstone, 20 cm grey to dark grey fissile mudstone to 40 cm carbonaceous sandy shale, dark grey in color, contain bioturbation (*Chondrites*, *Zoophycos*, *Teichichnus*, *Palaeophycus*, and *Helminthopsis*), that decreasing upward to the presence of *Thalassinoides*. The Carbonaceous shale in this core is considered as a condensed section which represents the initial phase of a marine flooding surface caused by the retreat of the Hirnantian ice sheet. Moreover, the overlying succession was considered as Aeronian age (23.5 ft), coinciding with the graptolite convolutus biozone (Zalasiewicz et al., 2007). This part is suggested as a marine shelf setting, and the graptolites contained in it are reported to be shelf-marine cratonic invaders.

CHAPTER 3

METHODOLOGY

3.1 Field Work

This fieldwork included the following:

1. Sedimentological and stratigraphical investigations and measurements were conducted on two sections to construct a high-resolution vertical succession from the selected representative outcrops on the cuesta near Old Qusiaba village.
2. The investigated sections were divided into a control or reference section in which detailed sedimentological, stratigraphical, paleontological, and geochemical investigations have been performed, and another section as a complementary section in which only sedimentology, stratigraphy, and micropaleontological analysis was carried out to compare the lithofacies and foraminiferal biofacies with the reference/control section and understand their lateral distribution within the outcrop.
3. The samples in the reference section were collected in a specific order every 20–50 cm or to some extent based on the representative lithofacies. On the other hand, in the complimentary section, samples were collected based on the representative lithofacies.

3.2 Laboratory Work

Collected samples from Old Qusaiba Village were prepared for micropaleontological and geochemical analyses as follows:

3.1 Micropaleontological analysis

For the micropaleontological preparation and analysis, samples were treated as follows:

1. Samples were prepared in 500-400 grams weight and agitated to obtain small fragments of about 1 mm in diameter.
2. Small fragments of a sample were soaked in a pot with adding sufficient water and detergent to obtain a small fraction.
3. Small disaggregate fraction of samples were washed using a 63 μm sieve and dried at low temperature (40–50 ºC).
4. Dried samples were sieved with 500, 250, 125, and 63 μm mesh, and transferred in a small labeled bottle, and picked under a binocular microscope based on the stop counting approach. An MPE Microsplitter was utilized to split samples in order to obtain a manageable number of specimens.
5. Foraminifera specimens were picked and sorted into micropaleontological slides, documented using a Nikon SMZ 1500 light setereo microscope, and identified to the species level.
6. Species assemblages, relative abundance, and diversity were determined to interpret their lifestyle and morphogroups
7. Paleoenvironment and paleooxygenation proxies were defined in the vertical succession using formaminiferal morphogroups and geochemical data interpretation.

3.2 Graptolite Analysis

1. The collected sedimentological samples were investigated for recognizing graptolite specimens.

2. Recognized graptolites were identified using the light microscope and analyzed in order to develop a graptolite biozonation and compared with the existing zonation of Zalasiewicz et al. (2007).
3. Graptolite specimens were photographed using a Nikon SMZ 1500 stereo microscope.

3.3 Conodont and Framboidal Pyrite Analysis

1. Conodonts and framboidal pyrite were collected following standard foraminiferal sample preparation.
2. Recovered conodonts were identified, analyzed, and plotted along the vertical succession to understand their temporal distribution.
3. Framboidal pyrite were investigated and analyzed as a complementary variable in interpreting paleooxygenation conditions.
4. Conodonts and representative specimens of framboidal pyrite were photographed using a Light stereo microscope Nikon SMZ 1500.

3.4 Geochemical Analysis

1. X-ray Diffraction Analysis

- Shale samples were prepared mechanically by grinding about 100 grams sample into a powder less than 0.15 mm for the purpose of semiquantitative mineral determinations.
- Powder samples were identified utilizing a PANanalyitical Empyrean X-Ray Diffractometer (XRD) at the Halliburton Technology Center (Fig. 9).

- The XRD spectrum, which is the result of scanning the shale samples was analyzed using International Center for Diffraction Data (ICDD) to determine the mineral composition.
- Glycol treatment was conducted to differentiate between smectite and mixed layer (smectite/illite).

Figure 9: PANanalytical Empyrean XRD at the Haliburton Technology Center.

2. X-ray Fluorescence (XRF) analysis was carried out by using powdered samples in order to determine major and trace elements. The powder samples were analyzed using Energy Dispersive XRF (Fig. 10).
3. Obtained results were then processed using the Omnian quantitative software at Halliburton Technology Center.

Figure 10: PANanalytical Energy Dispersive XRF at Haliburton Technology Center.

4. Scanning Electron Microscopy (SEM) was performed to validate the geochemical analysis that has been acquired by XRD and XRF. The samples were prepared using a Cressingtone Sputter Coater at the Research Institue of King Fahd University of Petroleum & Minerals (Fig. 11), by coating a small fragment of shale using platinum. SEM images were obtained by JSM 6610LV SEM (Fig. 11), and elemental mapping was conducted for every sample utilizing EDS.

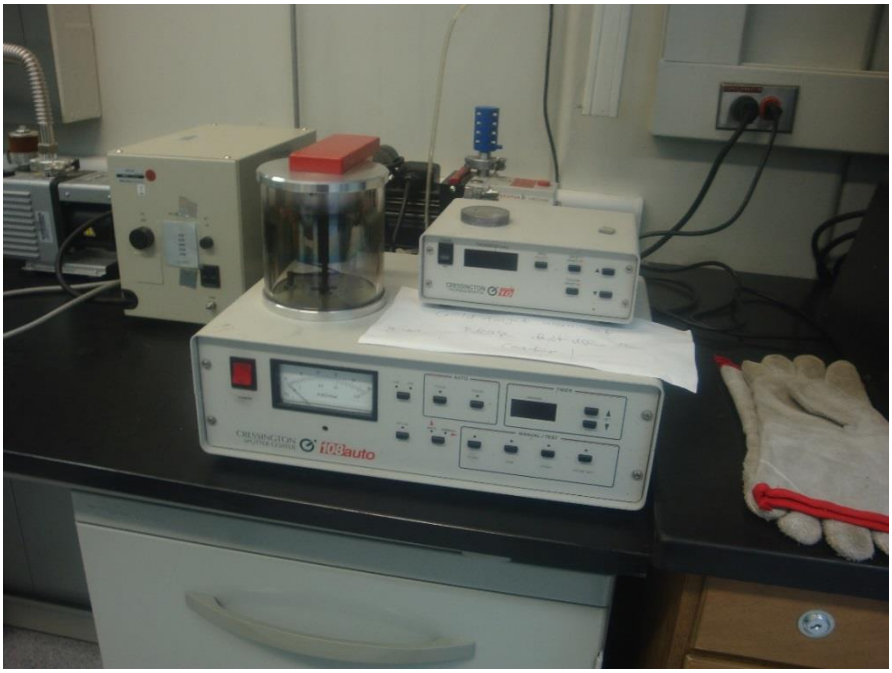

Figure 11: Cressington Sputter Coater for preparing SEM samples. Shale samples were coated using Platinum.

Figure 12: SEM-EDS (JSM 6610LV).

CHAPTER 4

LITHOFACIES

4.1. Lithofacies

Lithofacies analysis, which mainly based on the identification of distinctive properties of a sedimentary rock record, is greatly fundamental as a starting point for advanced subsequent analysis.

In this chapter, high-resolution siliciclastic lithofacies investigation was utilized to develop a depositional environment model. The lithofacies are mainly based on field descriptions, which are supplemented with SEM and geochemical data such as XRD and XRF.

4.2. Facies Description and Interpretation

The high-resolution study of the Qusaiba outcrop has revealed four siliciclastic lithofacies. The subsequent part of this chapter provides a description and interpretation of the lithofacies in the studied outcrop.

4.2.1. Gray to dark gray Mudstone (Mdg)

Facies Mdg is located at the basal part of the succession which consists mainly of light gray mudstone with an intercalation of thin laminae of dark mudstone (Fig. 13). The thickness of this lithofacies is about three meters. Intense fissile structure was shown from this lithofacies, and no sign of bioturbation and few graptolites have been encountered. Based on the mineralogy analysis conducted by XRD, the common mineral content this lithofacies was composed of quartz 36–55%, clay minerals (30–48%) which is dominated by kaolinite, and potassium feldspar 9–18%. Therefore, the mudstone of this lithofacies

can be classified as silica-rich argillaceous mudstone to clay-rich siliceous mudstone (Gamero et al., 2013) (Fig.13). Lithofacies Mdg is interpreted as an offshore environment.

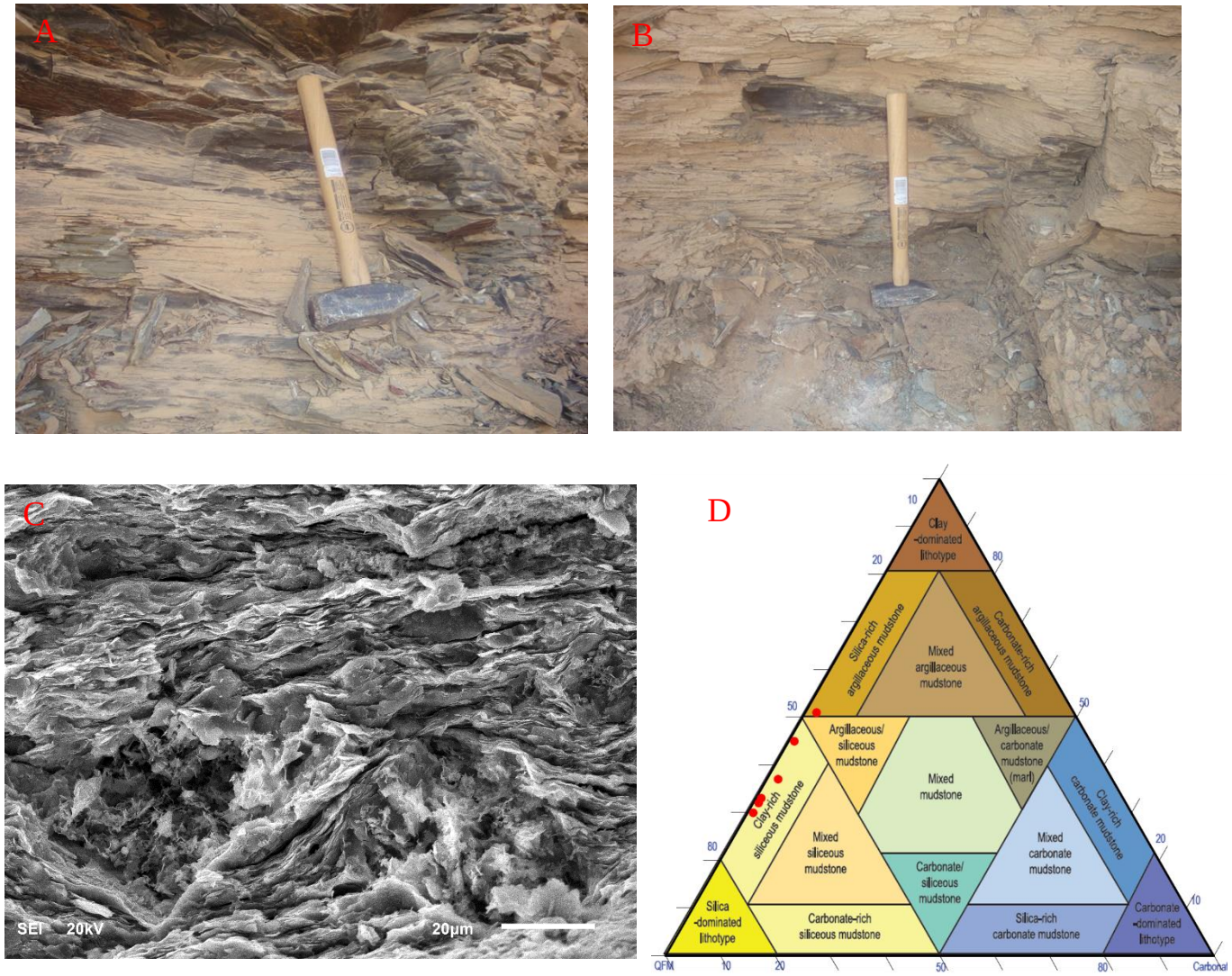

Figure 13: A-B. Photograph of dark gray mudrock showing intense fissicility. C. SEM photomicrograph of clay minerals D. Lithology of the Mdg facies are classified as clay-rich argilaceous mudstone to silica-rich argillaceous mudstone. The classification was modified after Gamero-Diaz et al. (2013).

4.2.2. Light gray Mudstone (Mlg)

This lithofacies overlies the facies Mdg, about 5.5 m in thickness, which exhibits fissile light gray mudstone, with a few intercalations of a thin layer of siltstone to fine grained sandstone (Fig.14). The transition between lithofacies Mdg and Mlg is characterized by the absence of the intercalation of dark gray mudstone. The lithology of this facies is classified as clay-rich siliceous mudstone (Gamero et al., 2013) (Fig. 14), with the dominant mineral including quartz, clay minerals dominated by kaolinite, and k-feldspar about 47–59%, 21–37%, and 11–22% respectively. The graptolite content in this lithofacies shows the highest abundance, which is comprised of *Normalograptus scalaris*, *Pristiograptus reckardsi*, *Metaclimacograptus hughesi*, and *Pristiograptus regularis*. Despite the absence of the index species *Lituograptus convolutus*, this part was considered as part of the Lituograptus convolutus graptolite biozone, in accordance with the abundance of *Normalograptus scalaris* and the presence of *Pristiograptus reckardsi.* This lithofacies was deposited in the shallower offshore environment.

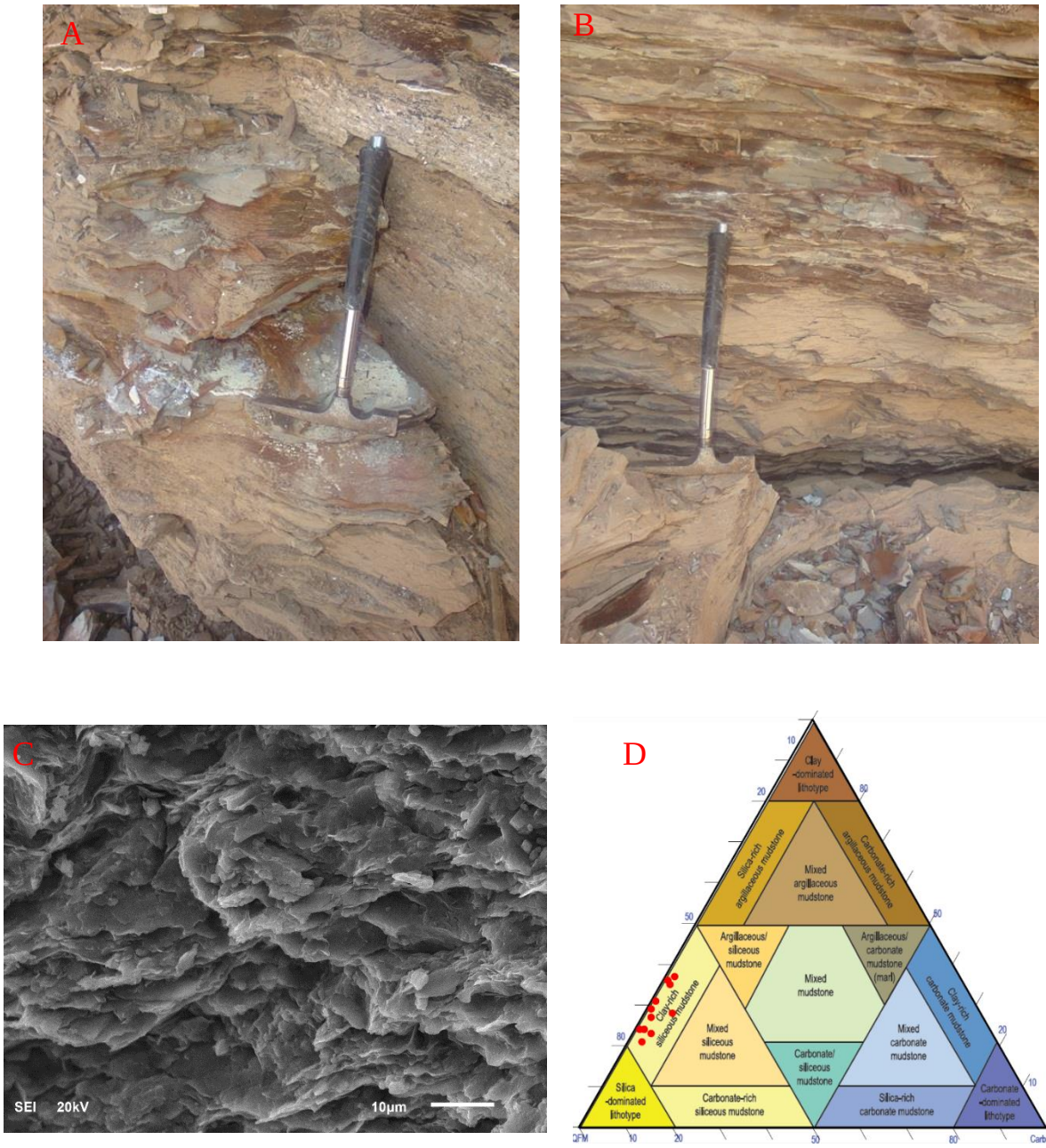

Figure 14:A-B. Photograph of light gray mudrock showing intense fisscility. C. SEM photo micrograph of clay minerals D. Lithology of the Mlg facies are classified as clay-rich argilaceous mudstone. The classification was modified after Gamero-Diaz et al. (2013).

4.2.3. Alternation of greenish-gray mudstone and reddish siltstone (Mzr)

Facies Mzr is underlain by Mlg, located in the transition of mudstone to sandstone-dominated lithology, with a thickness of about two meters. The transition between Mlg and Mzr is indicated by gradational change of the light gray mudstone to the presence of the intercalation of reddish siltsone to fine grained sandstone, and the uppermost contact of this Mzr and the overlain lithofacies is indicated by the presence of a 10-20 cm thick coarse-grained sandstone. The lithology of this facies is composed of an alternation of greenish mudstone and reddish siltstone to fine-grained sandstone (Fig. 15). In the 10 cm reddish siltstone to fine-grained sandstone, in the middle of this lithofacies, nodular gypsum is recognized. This evidence is consistent with the XRD result that some samples of this lithofacies possess 3–10% gypsum. With respect to the mineral content, the clay-silt lithology of this facies exhibits the highest percentage of quartz, ranging from 48–64%, clay minerals which consist exclusively of kaolinite (10-30%), and is classified as clay-rich siliceous mudstone to silica-dominated lithotype (Gamero et al., 2013) (Fig.15). Graptolite investigation of this facies shows a sparse abundance of *Pristiograptus regularis* and some poorly preserved specimens that cannot be identified. This lithofacies interpreted as a transition between offshore and lower shorface environment deposit.

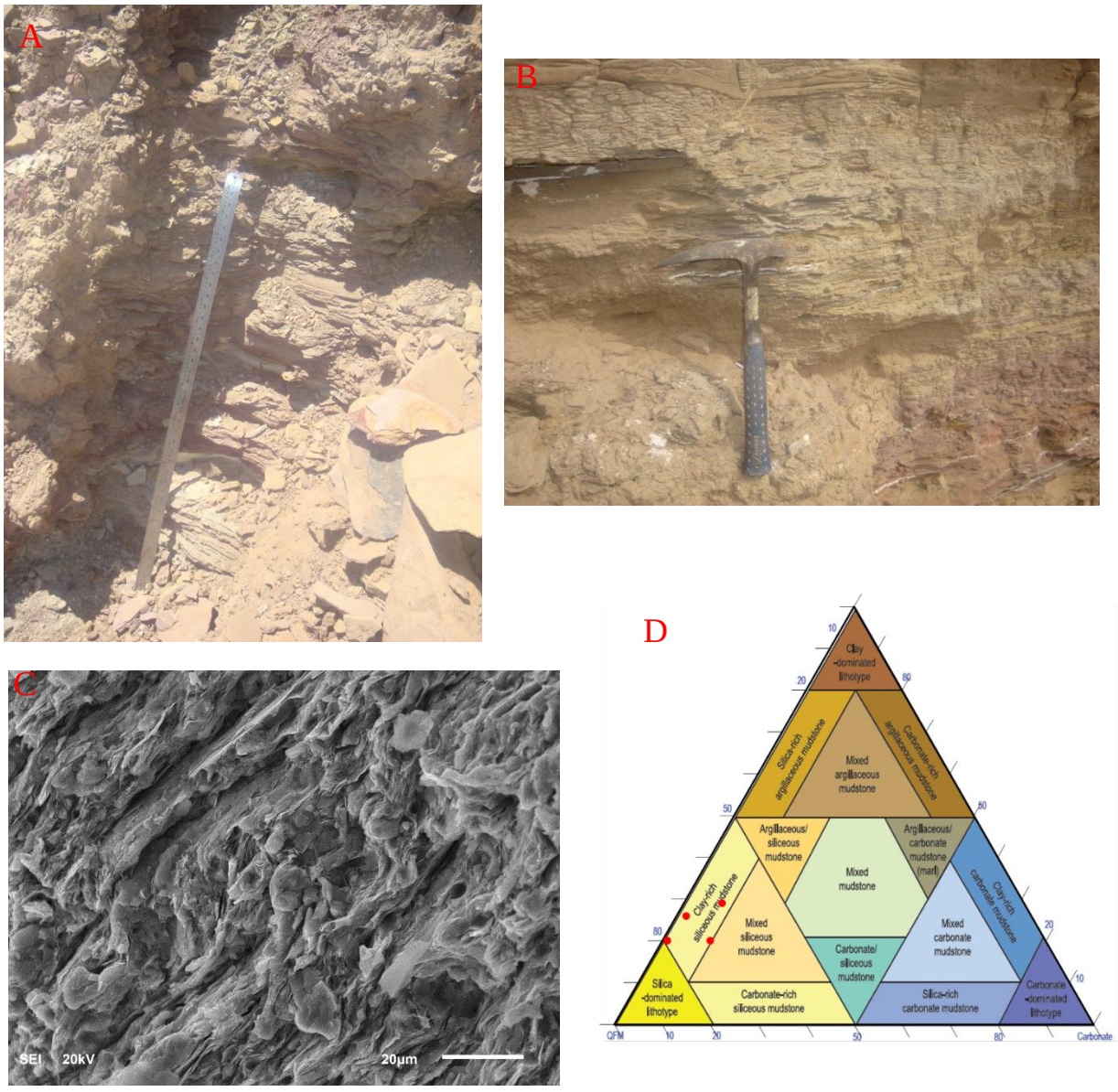

Figure 15: A-B. Photograph of alternation of greenish-gray mudstone and reddish siltstone. C. SEM photomicrograph of clay minerals. D. Lithology of the Mzr facies are classified as clay-rich argilaceous mudstone. The classification was modified after Gamero-Diaz et al. (2013).

.

4.2.4. Alternation of claystone to siltstone with fine to coarse-grained sandstone (Sfc 1)

Lithofacies Sfc 1 overlays the Mzr with a thickness of about 1.8 meters. This lithofacies is mainly composed of claystone to siltstone alternating with fine to coarse-grained sandstone (Fig. 16). The claysone and siltstone is greenish gray in color with a layer thickness of about 10-20 cm. The sandstone lithology is increasing the grain size and thickness toward the upper part of the exposure. The thickness of the sandstone is 10 to 30 cm, which shows lamination, and no graptolites have been found. The sandstone in this lithofacies is classified as a quartz arenite of the Sharawra Formation (Abbas et al., 2017). The upper part of this lithofacies is represented by 30 cm coarse grained laminated sandstone. This lithofacies is interpreted as a lower shoreface environment deposit.

4.2.5. Alternation of claystone to siltstone with fine to coarse grained sandstone (Sfc 2).

The Sfc2 lithofacies is mostly similar to Sfc1, but differs in having hummocky cross-stratification structure in the uppermost beds. To some extent, the sandstone also exhibits increasing thickness, in which beds are thicker compared to Sfc1. Facies Sfc 2 is characteristic of a lower shoreface environment sediment.

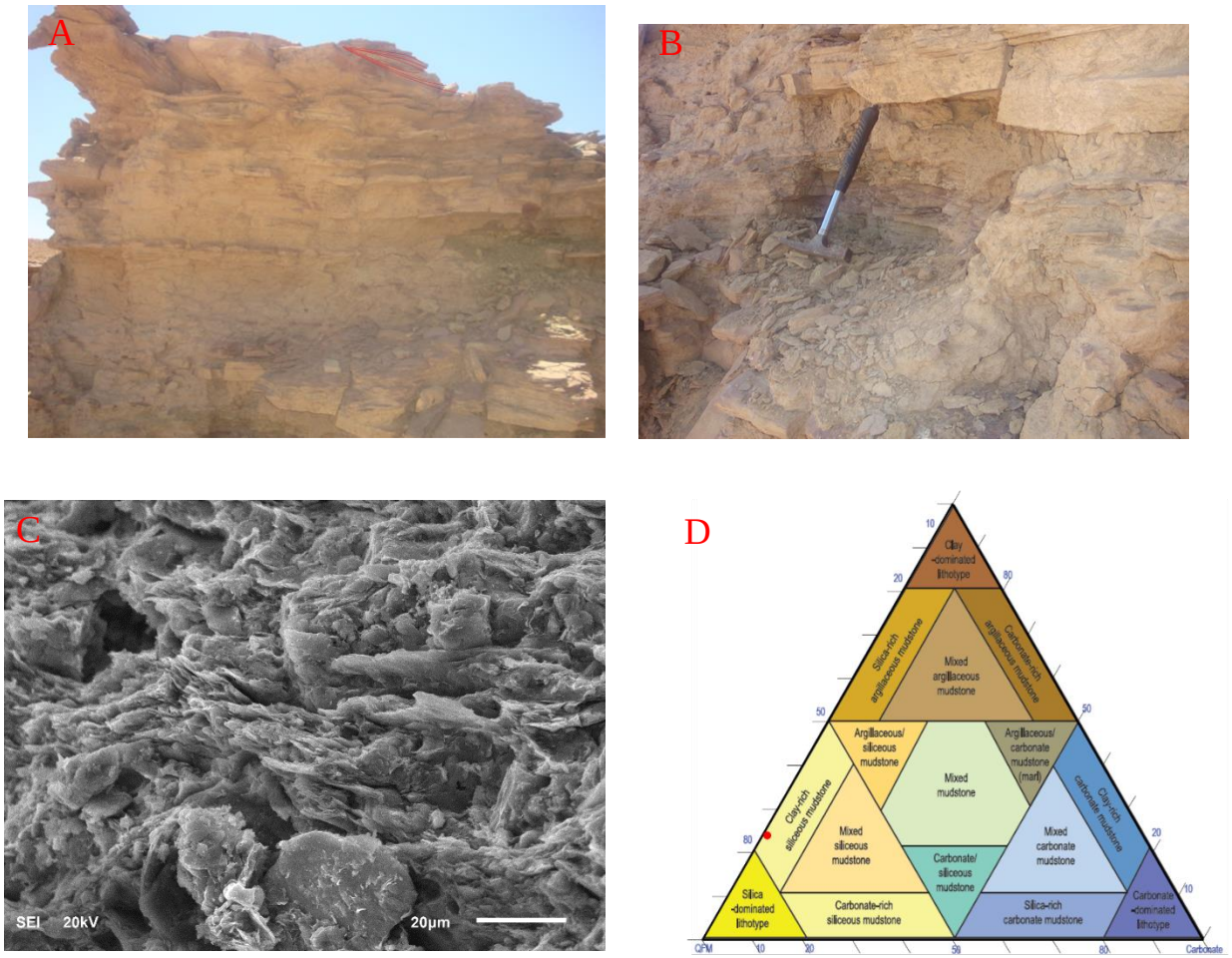

Figure 16: A-B. Photograph of alternation of clay to siltstone with fine to coarse grain sandstone. C. SEM photomicrograph of clay minerals D. Lithology of the Sfc2 facies are classified as clay-rich argilaceous mudstone. The classification was modified after Gamero-Diaz et al. (2013).

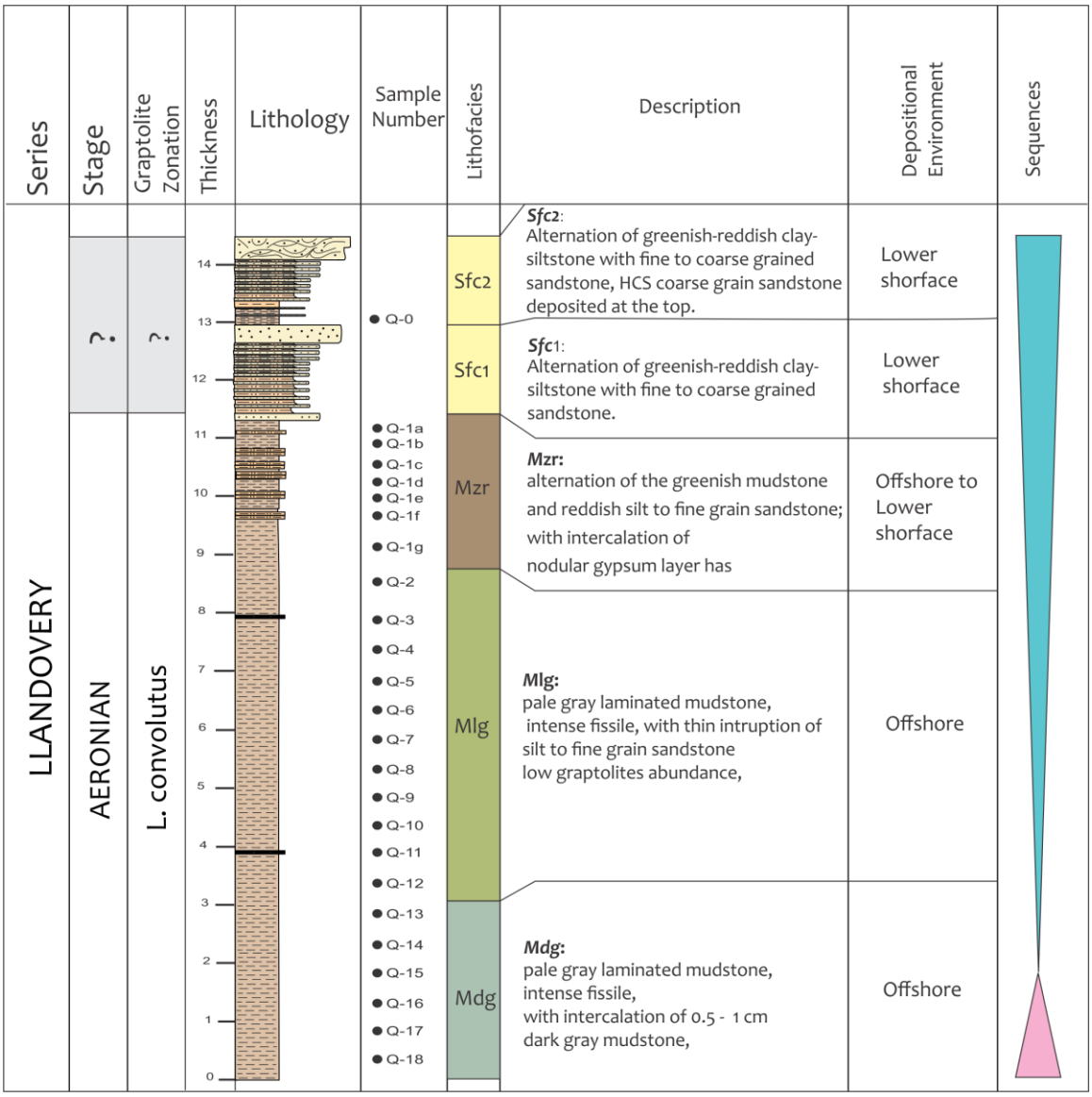

Figure 17: Lithofacies description of Section 1.

CHAPTER 5

BIOSTRATIGRAPHY

5.1. Foraminiferal Biofacies

This chapter presents broad paleontologic coverage of smaller benthic Foraminifera, graptolites, conodonts, and incertae sedis fauna in the Lower Silurian of Saudi Arabia. This chapter elaborates the fauna found in the Qusaiba succession and attempts a reconstruction of the paleoenvironment and paleoecology of the Qusaiba shale during the Early Silurian, in the Qasim Region of Saudi Arabia.

5.1.1. Foraminiferal Preservation

The recovered foraminifera generally exhibit moderate to good preservation, with several truncations encountered at the final and or initial stage of tubular and tubotalamamid forms. Delicate features of the monotalamid foraminifera such as the test periphery, aperture(s), and protuberances remain preserved, and only rare evidence of abrasion or erosion can be recognized. Our specimens also demonstrated no evidence of redeposition, which suggests the recoverable materials are preserved as autochthonous components in fine-grained sediments in an environment with low hydrodynamic energy.

5.1.2. Foraminiferal Assemblages

The studied Early Silurian foraminiferal assemblages from the upper Qusaiba and lower Sharawra formations consist exclusively of agglutinated foraminifera. A total of 5312 specimens were recovered in our samples. The specimens were identified and classified as belong to three orders, 13 families, 24 genera and 77 species (Table 1). In terms of species number, the foraminiferal assemblages from the studied sections are more diverse than any previously described Lower Silurian assemblage.

The assemblages recovered from the Upper Qusaiba and Lower Sharawra formations are dominated by monothalamous forms of Astrorhizida, comprising 95.58% of the assemblage, followed by tubotalamids belonging to the Hippocrepinida and Ammodiscida (4.14%), and finally globothalamids consisting of Lituolida (0.28%) (Fig. 18). Flattened and discoidal morphotypes of *Psammosphaera*(?) and *Thuramminoides* are the dominant genera. Other common genera include *Amphitremoida*, *Stegnammina*, *Lagenammina*, *Thurammina,* and *Tolypammina* (Fig. 18). The multichambered lituolids occur as rare components in assemblages consisting mostly of monothalamids.

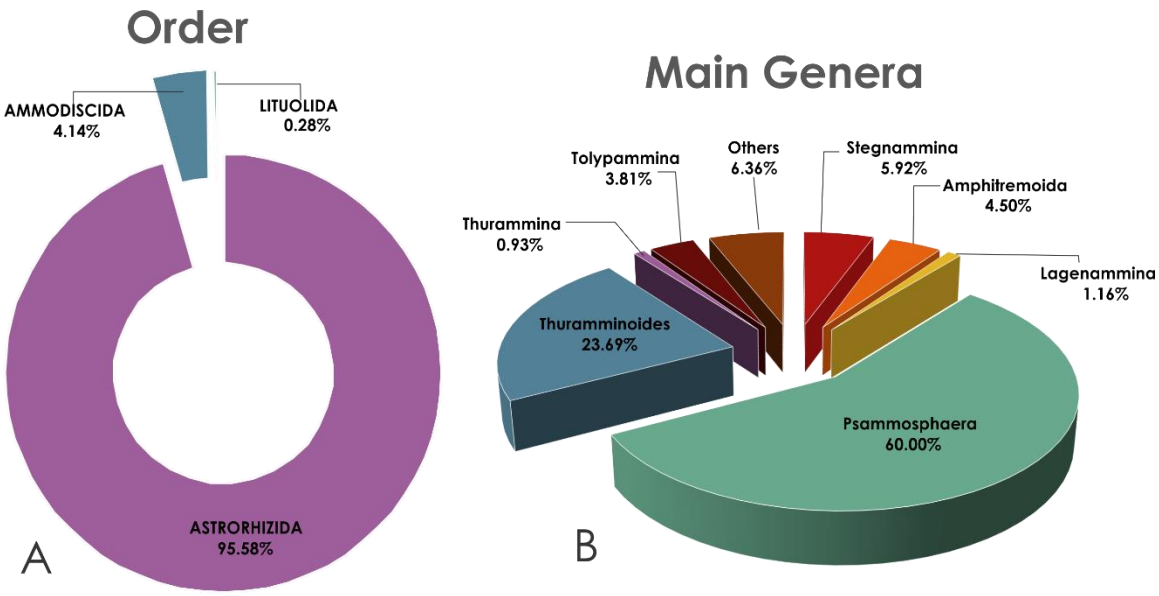

Figure 18: Proportion of foraminiferal ordesrs and genera in the recovered samples.

Table 1: Taxonomic assignments of the recovered species.

ORDER	FAMILY	GENUS	SPECIES
ASTRORHIZIDA	RHABDAMMINIDAE	*Rhabdammina*	*Rhabdammina trifurcata*
	BATHYSIPHONIDAE	*Bathysiphon*	*Bathysiphon* sp. 1
			Bathysiphon sp. 2
			Bathysiphon sp. *3*
	HIPPOCREPINELLIDAE	*Amphitremoida*	*Amphitremoida citroniforma,*
			Amphitremoida eisenacki
			Amphitremoida sp.1
			Amphitremoida sp. 2
			Amphitremoida sp.3
	STEGNAMMINIDAE	*Blastammina*	*Blastammina vulgaris*
		Ceratammina	*Ceratammina cornucopia*
			Ceratammina sp.1
			Ceratammina sp.*2*
		Raibosammina	*Raibosammina aspera*
		Stegnammina	*Stegnammina contorta*
			Stegnammina elongata
			Stegnammina sp. 1
			Stegnammina sp. 2
			Stegnammina sp.3

			Stegnammina sp. 4
		Thuramminoides	*Thuramminoides sphaeroidalis*
			Thuramminoides plumerae
			Thuramminoides sp.1?
			Thuramminoides sp.2
	HEMISPHAERAMMINIDAE	*Hemisphaerammina*	*Hemisphaerammina battalleri*
			Hemisphaerammina sp.1
			Hemmisphaerammina sp. 2
			Hemisphaerammina sp.3
	SACCAMMINIDAE	*Lagenammina*	*Lagenammina cumberlandiae*
			Lagenammina ligula
			Lagenammina silnica
			Lagenammina sp. 1
			Lagenammina sp.2
			Lagenammina sp. 6
		Saccammina	*Saccammina aspera*
			Saccammina sp.1
		Saccamminita	*Saccamminita galinae*
		Thurammina	*Thurammina arcuata*
			Thurammina holcovae
			Thurammina papilata
			Thurammina pentagona
			*Thurammina?*sp.1
	PSAMMOSPHAERIDAE	*Psammosphaera*	*Psammosphaera gracilis*
			Psammosphaera sp.1
			Psammosphaera(?) sp.1
			Psammosphaera(?) sp.2
		Sorosphaera	*Sorosphaera bicella*
			Sorosphaera tricella
	LACUSTRINELLIDAE	*Webbinella*	*Webbinella* sp. 1
AMMODISCIDA	HIPPOCREPINIDAE	*Kechenotiske*	*Kechenotiske expansa*
	HYPERAMMINIDAE	*Hyperammina*	*Hyperammina sinuosa*
			Hyperammina sp. 1
			Hyperammina sp. 2
			Hyperammina sp. 3
	AMMODISCIDAE	*Ammovertella*	*Ammovertella* sp. 1?
			Ammovertella sp. 1
			Ammovertella sp. 2
			Ammovertella sp. 3
			Ammovertella sp. 4

			Tolypammina aihemerensis
			Tolypammina bulbosa
			Tolypammina howchini
			Tolypammyna jackobchapelensis
			Tolypammina serpens
			Tolypammina tornella
		Tolypammina	*Tolypammina tortuosa*
			Tolypammina sp. 1
			Tolypammina sp. 2.
			Tolypammina sp. 3
			Tolypammina sp.4
			Tolypammina sp. 5
			Tolypammina sp. 6
		Turritellella	*Turritellella* sp.1.
LITUOLIDA	LITUOLIDAE	*Ammobaculites*	*Ammobaculites qusaibaensis*
		Simobaculites	*Simobaculites* sp. 1
	PLACOPSILINIDAE	*Stacheia*	*Stacheia trepeilopsisformis*
			Stacheia sp. 1
			Stacheia sp. 2

The distribution of the common foraminiferal species in the upper part of the Qusaiba Formation and the lower Sharawra Formation in the studied sections are shown in Figures 19–20, and the quantitative species counts are given in the appendix (supplementary material). In the stratigraphic succession, a change is observed from a *Psammosphaera*-dominated assemblage in the upper part of the Qusaiba shale to a less diversified assemblage with species of *Stegnammina* and *Amphitremoida* in the shale interbeds within the lower part of the Sharawra Formation. The lack of comparable foraminiferal studies in Gondwana means that additional sections need to be studied in order to assess the stratigraphic utility of the species from the studied section.

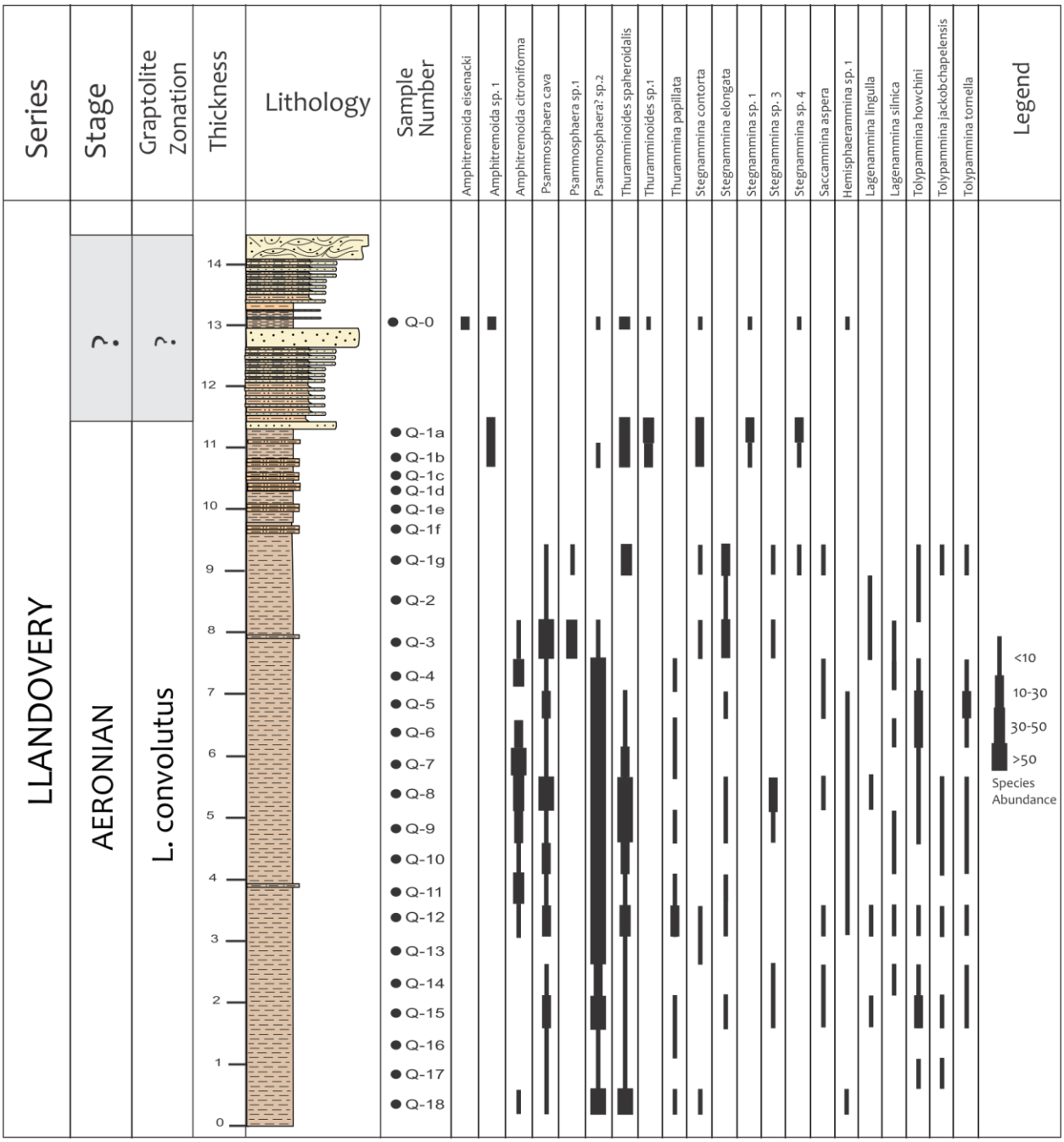

Figure 19: Lithostratigraphy and occurrences of common species in the secton 1.

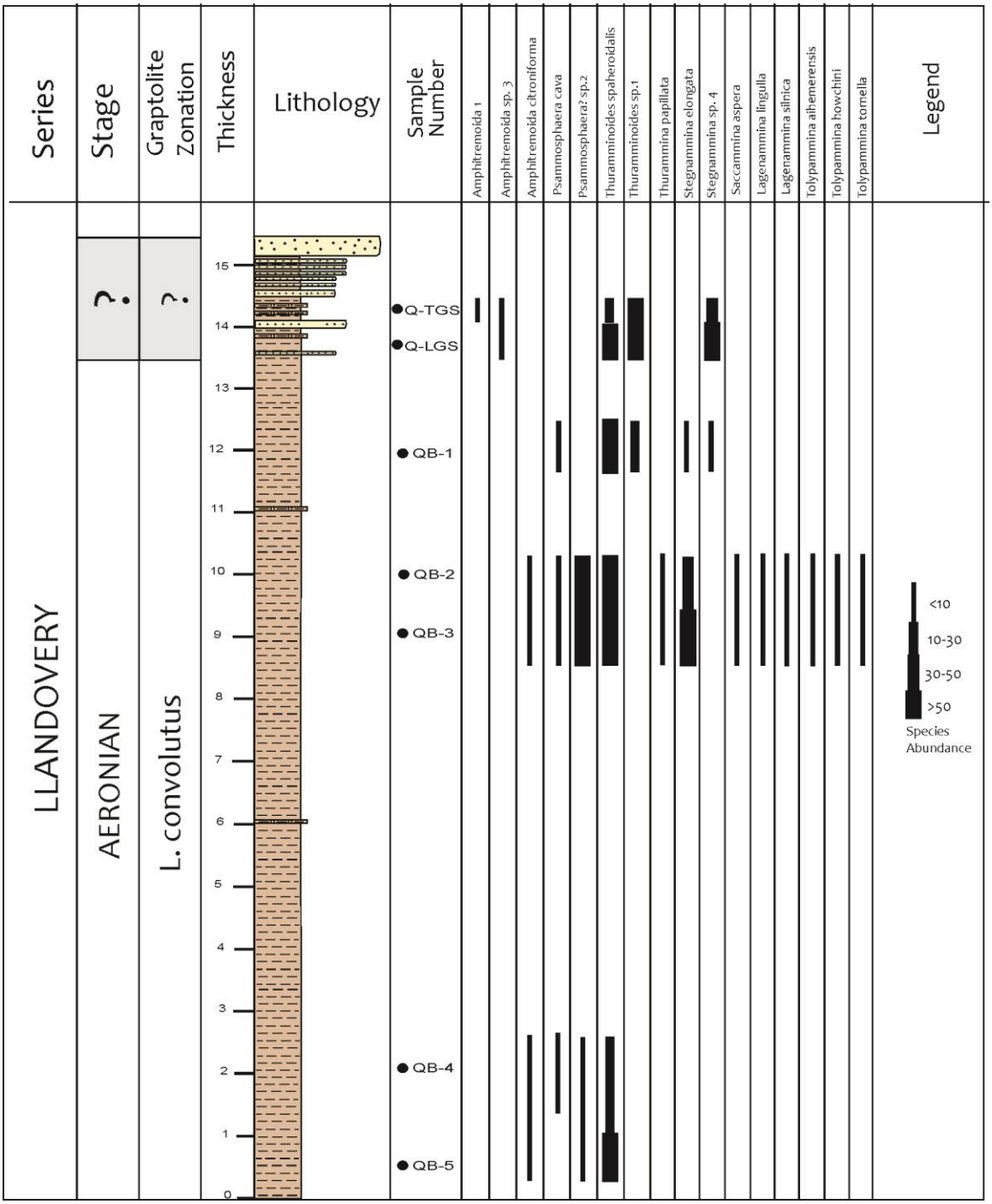

Figure 20: Lithostratigraphy and occurrences of common species in the secton 2.

5.1.3. Diversity Indices

Foraminiferal assemblages in section 1 generally exhibit dominance by some taxa, which is characterized by the high Dominance_D indicator (> 0.5) (Figure 21, Table 5.2). General trend of the assemblages shows fluctuating diversity, which generally reaches the peak in the lithofacies Mlg. The lowest diversity shows at the lithofacies Mdg and barren at the transition between mud dominated mudrock and sand dominated mudrock (Lithofacies Mzr). The highest diversity is encountered during the deposition of the light gray mudrock lithofacies (Mlg), which is indicated by a high number of specimens, number of species, and the diversity indices such as Fisher α, Shannon-H, and Chao-1 (Figure 21, Table 2). The highest diversity in this interval also characterized by high species richness (Figure 22). On the other hand, low diversity of the assemblages is associated with the present of coarser-grained material wich is related to the high hydrodynamic energy that may rework or erode the micro habitat, and disrupt the food supply in the suspension. In addition, the exceptionally low-diversity assemblages at the bottom of the succession (Fig. 21, Table 2) is related to the low dissolved oxygen (dysoxic environment) in the water column and in the sediment. These phenomena also can be recognized in the rarefaction curves. (Fig. 22)

Table 2: Diversity indices of foraminiferal assemblages in section 1.

	Taxa_S	Individuals	Shannon_H	Fisher_alpha	Chao-1
Q0	18	276	1.521	4.312	20.5
Q1A	8	200	1.624	1.668	8
Q1B	9	141	1.791	2.142	9
1D	0	0	0	0	0
1E	0	0	0	0	0
1F	0	0	0	0	0
Q1G	20	135	2.521	6.489	25
Q2	11	352	0.5006	2.156	13.5
Q3	17	191	1.735	4.51	20.75
Q4	27	320	1.638	7.032	34.2
Q5	14	360	1.111	2.899	15.5
Q6	22	370	1.055	5.124	31.17
Q7	9	395	0.9207	1.64	9
Q8	22	403	1.894	4.997	27.6
Q9	24	465	1.434	5.365	31.5
Q10	13	355	0.7812	2.65	13.6
Q11	10	180	1.114	2.283	10.33
Q12	28	464	1.374	6.551	46.33
Q13	5	230	0.2674	0.9016	5
Q14	14	58	2.057	5.862	15
Q15	21	335	0.9491	4.97	26.6
Q16	5	9	1.465	4.632	8
Q17	7	19	1.813	4.003	7
Q18	9	294	0.8933	1.755	9.6

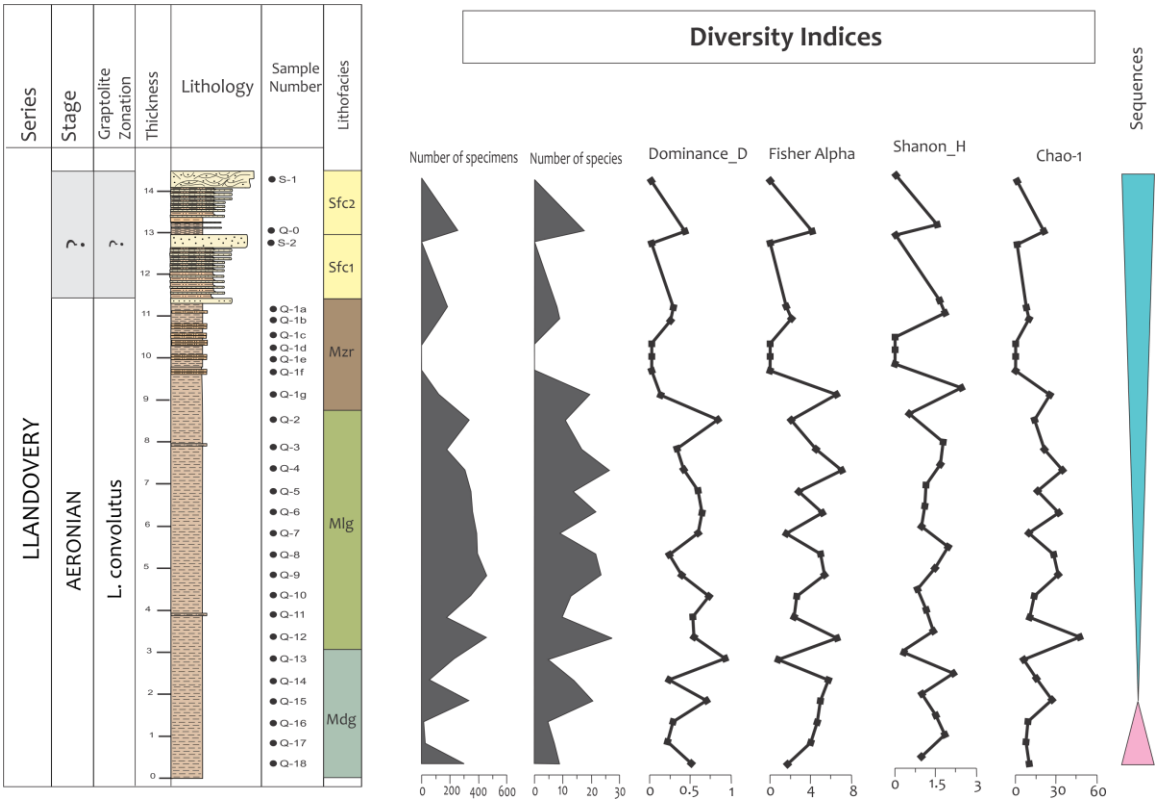

Figure 21: Vertical distribution of diversity indices.

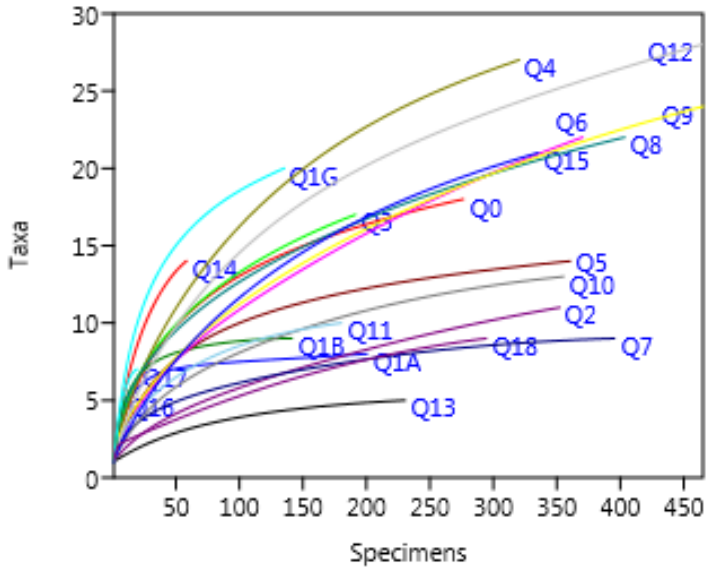

Figure 22: Rarefaction curves of foraminiferal assemblages from the section 1.

5.1.4. Foraminiferal Morphogroups

The foundation of the description and classification of the foraminiferal morphotypes utilized in the morphogroup analysis of this study were compared mainly to the studies of Devonian (Holcova and Slavik, 2013), Jurassic (Nagy, 1992; Tyszka, 1994; Nagy et al. 1995; Reolid et al., 2008a; Reolid et al., 2008b), Cretaceous (Cetean et al. 2011; Setoyama et al., 2013) and modern agglutinated foraminiferal morphogroups (Jones and Charnock, 1985; Murray et al. 2011).

Based on the morphogroup analysis, the Early Silurian foraminifera from the Old Qusaiba Village were subdivided into three morphogroups and six subgroups, or morphotypes.

5.1.4.1. Morphogroup A

This morphogroup includes tubular and unilocular foraminiferal shells, which can be divided into two subgroups (A1 and A2).

Subgroup A1 comprises straight tubular uniserial, and branched forms (Fig. 23). This subgroup is equivalent to the comparable subgroup of Jones and Charnock (1985), Tyszka (1994), Nagy et al. (1995), Reolid et al. (2008 a) Reolid et al. (2008b), and Nagy et al. (2009), Murray et al. (2011), Holcova and Slavik (2013), and Setoyama et al. (2013). The genera representing of this subgroup including *Bathysiphon, Hyperammina, Kechenotiske, Raibosammina, Rhabdammina and Stegnammina*. This subgroup is generally interpreted as suspension feeders, and represents erect epifauna. On the basis of the temporal distribution, subgroup A1 can be found prevalently along the whole succession (Fig. 24). However, the maximum assemblage of this group can be recognized from the upper part

of Mzr and mudstone part of Sfc lithofacies, which is interpreted as representing a muddy part of lower shorface environment.

Subgroup A2 including tubular, irregular, and spiral coiled test form, which has a feeding strategy as a passive herbivore or also suspension feeder. The life mode of this subgroup is interpreted as sessile epifauna to erect epifauna (Fig. 23). This type is comparable to the morphotype classification of Tyszka (1994), Nagy et al. (1992), Reolid et al. (2008a), Reolid et al. (2008b), Holcova and Slavik (2013), and Setoyama et al. (2013). The genera representing this subgroup consist of *Tolypammina, Ammovertella*, and *Turritellella*, which are present in offshore part (lithofacies Mdg and Mlg), but are absent at the top of the succession (lithofacies Mzr and Sfc) (Fig. 24).

4.2.5.2. Morphogroup B

The morphogroup B in this study represents monochambered, globular, spherical, subspherical, flattened, and discoidal test morphology, which consists of three subgroups (B1, B2, B3).

Foraminifera in subgroup B1 are characterized by globular to subglobular forms, with or without a neck and aperture (Fig. 23). This subgroup is equivalent to globuloar unilocular morphotype in the morphogroup classification of Nagy et al. (1995), Kaminski et al. (2005), Kender et al. (2008), Murray et al. (2011), Holcová & Slavík (2013), and Setoyama et al. (2013). The life style of the foraminifera in this group interpreted as shallow infauna and the feeding habit is indicated as a suspension and/or passive deposit feeder. The subgroup B1 encompasses the genera *Amphitremoida, Blastammina, Lagenammina, Saccammina,* and *Psammosphaera.* The B1 subgroup shows a homogenous distribution

throughout the section, and has a maximum relative abundance at the upper part of the offshore facies (Fig. 24).

Subgroup B2 is typified as spherical and hemispherical, and fusiform test morphology of the genera *Hemisphaerammina, Sorosphaera, Thurammina,* and *Webbinelloidea*. The life habit of this subgroup is characterized by surficial epifauna, and they may be representatives of passive deposit to suspension feeding foraminifera (Fig. 23). This B2 subgroup also comparable to the previous classification of Reolid et al. (2008a), Reolid et al. (2008b), and Holcová & Slavík (2013). A higher proportion of this morphotype is shown at the Mdg and Mlg facies, followed by its gradual decrease toward the upper part of lithofacies Mzr and Sfc (Fig. 24).

The B3 subgroup includes discoidal and flattened forms of surficial epifaunal foraminifera which have a passive detritivore feeding strategy (Fig. 23). The morphogroup division in this study is in agreement with that of Nagy et al. (1995), Reolid et al. (2008a), Reolid et al. (2008b), Nagy et al. (2009), and Holcová & Slavík (2013). The genera belonging to this morphotypes are *Thuramminoides* and *Psammosphaera*(?), which are the most dominant types found in this investigation (Fig. 24).

4.2.5.2. Morphogroup C

The morphogroup is indicated by the very rare multichambered foraminifera found in the Silurian record. The morphogroup can be compared with the studies of Tyszka (1994), Kaminski and Kuhnt (1995), Nagy et al. (1995), Reolid et al. (2008a), Reolid et al. (2008b), this morphogroup represents a shallow to deep infaunal mode of life (Cetean et al. 2011; Setoyama et al., 2013; Holcova and Slavik, 2013) (Fig. 23). Unlike the other

morphogroups, this morphogroup is only represented by a few specimens of *Ammobaculites*, and *Simobaculites*. This kind foraminiferal morphogroup is first discovered in the Silurian succession of this study.

Morpho-groups	Sub-groups	Life habit	Life Strategy	Feeding Habit	Environment	Main Genera
A	A1	Tubular, branching, elongated	Erect epifauna	Suspension feeder	Lower shoreface to offshore	 Bathysiphon Stegnammina Hyperammina Rhabdammina
	A2	Tubular or hemitubular meandering	Sessile epifauna to erect epifauna	Passive herbivore ? suspension feeder	Offshore	 Ammovertella Tolypammina Turritellella
B	B1	Globular to subglobular	Shallow infauna to epifauna	Suspension to passive deposit feeder	Common in offshore	 Lagenammina Psammosphaera Saccammina
	B2	Spherical hemispherical fusiform	Surficial epifauna	Passive deposit to suspension feeder	Common in offshore	 Sorosphaera Thurammina Hemisphaerammina
	B3	Discoidal flattened	Surficial epifauna	Passive detritivor	Lowershoreface to offshore	 Thuramminoides Psammosphaera(?) Thuramminoides
C		Multilocular palinspiral to uniserial	Shallow to deep infauna	Active deposit feeder	Offshore	 Ammobaculites Simobaculites

Figure 23: Foraminiferal morphogroups showing three groups and five subgroups or morphotypes.

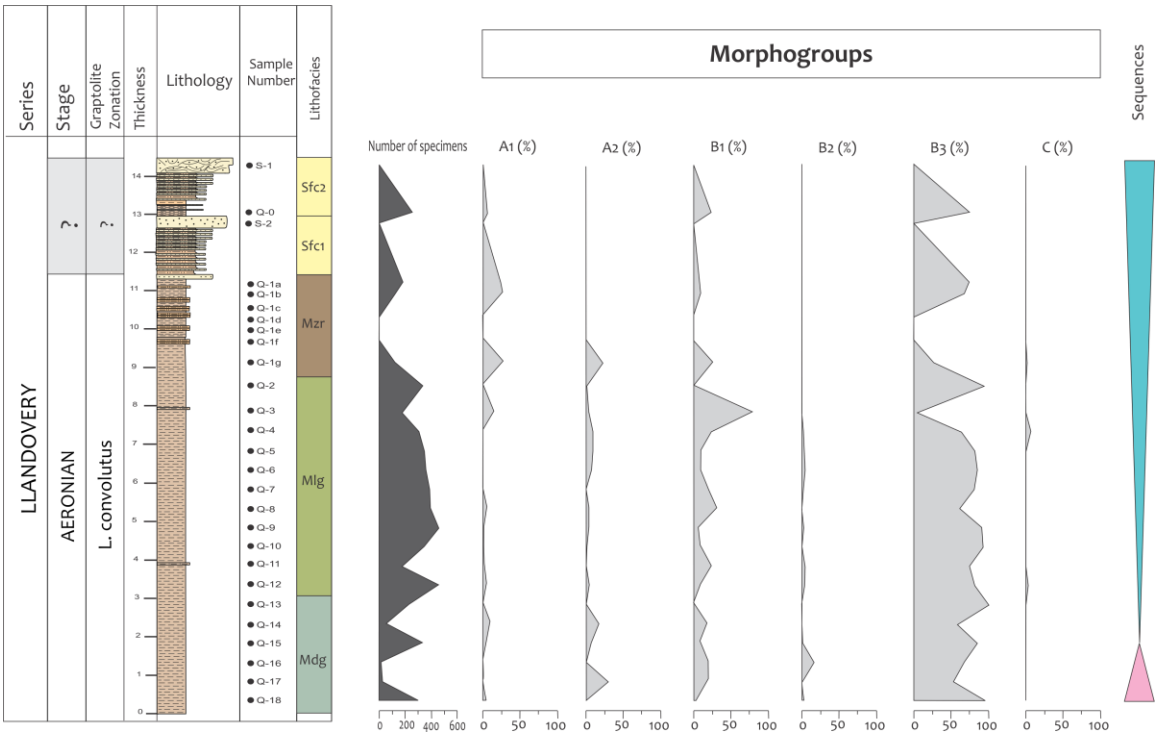

Figure 24: Temporal distribution of the foraminiferal morphotypes in section 1.

5.1.5. Foraminiferal Wall Texture

Application of the foraminiferal wall structure and texture is widely used in the classification of both planktic (Hemleben et al., 1991; Olsson et al., 1992; Hemleben et al., 2006) and benthic foraminifera (Loeblich and Tappan, 1992; 1994; Mikhalevich, 2004; Kaminski, 2004; 2014). In the agglutinated foraminiferal topic, studies on wall texture and structure have been applied on the basis of grain selection and the type of cement used in constructing their wall (Bender, 1995; Loeblich and Tappan, 1987, 1988, 1992;) and also have been used to interpret environmental variables (du Châtelet et al. 2013). In this section, wall texture identification was performed on the base of wall surface roughness, which is represented by the grain size of the materials used in wall construction. This attempt was conducted owing to the taxonomical classification of the genera that can

display variable wall roughness. Therefore, a classification was carried out with the purpose of interpreting physical and paleoenvironmental conditions during the life of the foraminifera. According to the roughness of the wall texture, recoverable foraminifera in this study can be classified into three groups:

Rough Wall Surface

This group is indicated by thick and rough foraminiferal wall surface, which is constructed of medium to coarse siliciclastic material. Grain shapes used in this wall are dominantly spherical and rounded. Represented species of this group include *Raibosammina aspera*, *Stegnammina contorta*, *Stegnammina* sp. 1, *Stegnammina* sp. 3, *Thuramminoides* sp. 1, *Ampitremoida eisenacki*, *Amphitremoida* sp. 1, *Amphiteromida* sp. 3, as well as some *Hyperammina* and *Lagenammina* species. Foraminifera with a rough wall surface are concentrated in the upper part of the Mzr and Sfc facies, which inhabit the muddy part of the lower shoreface environment. Only a small proportion (<5%) inhabited the lower part of the succession (Figure 25).

Thuramminid Wall Surface

The thuramminid wall surface represents fine to moderate wall roughness, which is constructed of platy or flattened thin siliceous materials. Almost all *Thurammina*, *Hemisphaerammina*, and *Sorosphaera* taxa are grouped in this classification. This group is mostly inhabited mud dominated lithofacies of Mdg and Mzr which were deposited in the offshore paleoenvironment (Figure 25).

Smooth Wall Surface

Smooth wall surface foraminifera are characterized by a thick to medium wall that is constructed of very fine to fine rounded siliceous grains. The typical species of this group include *Tolypammina*, *Turritellella*, *Ammovertella*, *Stacheia*, *Thuramminoides sphaeroidalis*, *Psammosphaera cava*, *Psammosphaera*(?) sp. 2, *Bathysiphon*, *Rhabdammina*, and some species of *Saccammina*, *Lagenammina*, and *Hyperammina*. This group is distributed in both sand and mud dominated lithology with high proportion (>40%) (Fig.25). However, the proportion of this group in the upper part of the sampled section is lower compared with the underlying succession.

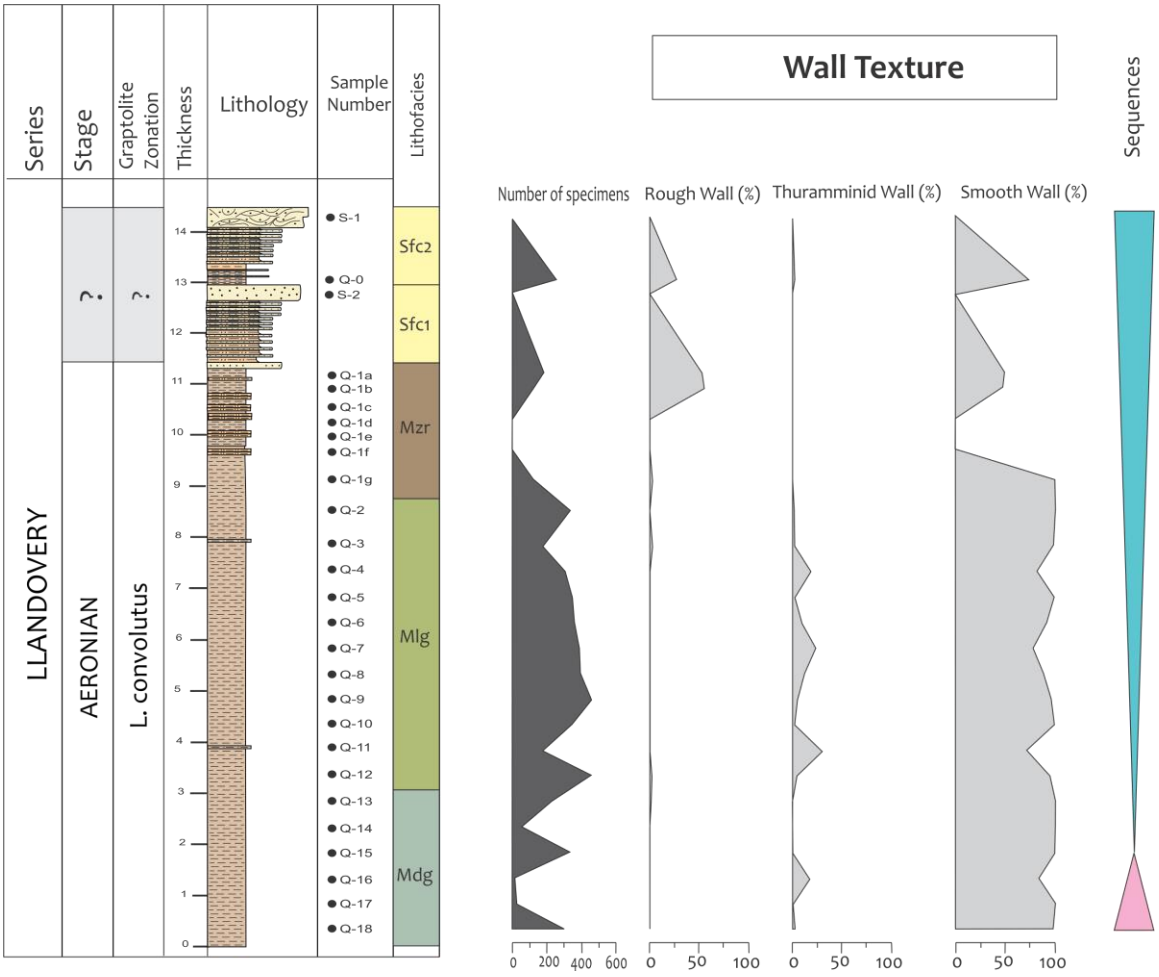

Figure 25: Vertical distribution of group of foraminiferal wall textures in section 1.

5.1.6. Discussion

5.1.6.1. Paleoenvironments

Morphogroups vs Paleoenvironment

Based on the modern foraminiferal analog, living representatives of subgroup A1 are not common in continental shelf areas (Murray et al., 2011). The genera belonging in this subgroup include rhabdamminids, hyperamminids, and *Bathysiphon*, which favor inhabiting a continental slope and deeper environment (Jones & Charnock, 1985). The

ancient studies on this subgroup also represent low current area, which mostly indicator of the bathyal and deeper environment reached by food supply (Holcova and Slavik, 2013). The high abundance of the tubular morphotype may also indicate enrichment of the food supply in suspension, which may come from increased terrigenous influx or planktonic productivity. In contrast, in this study, the highest relative abundance of subgroup A1 is shown in the upper part of the homogenous shale of upper offshore to alternating shale and sandstone of the lower shore face environment. This phenomenon is subjected to the dominant proportion of *Stegnamminia*, which is exhibits a rough wall surface in the lower shoreface succession and a smooth surface in the uppermost part of the offshore. This phenomenon supports the study of foraminifera from the Waldron Shale, which suggests that *Stegnammina contorta* and *Raibosammina* prefer a mixed and higher energy environment (McClellan, 1966).

The ecology of the subgroup A2 can be interpreted on the basis of life habit of the tolypamminids. The genus *Tolypammina* favor warm, shallow, and alkaline conditions, which can be considered as a characteristic of a nearshore setting with calcium-rich sediments (Conkin, 1961). Commonly, this genus appears as a dominant foraminiferal taxon, that is usually found in sediments that lack other organisms (McClellan, 1973) and prefers areas where calcareous muds and fine grain shale were deposited (Conkin, 1961). This study also demonstrated that the tolypamminids are absent in the high-energy water current environment, and inhabited the offshore environment.

Uniformly distributed B1 and B3 morphotypes along the succession may indicate opportunistic taxa within both subgroups. The *Psammosphaera* and *Thuramminoides spaheroidali*s are well acknowledged as taxa that can survive in many different

environments ranging from the lower shoreface environment, characterized by higher hydrodynamic condition, to the further offshore. Those taxa also able to adapt in both environments rich in clastic input and carbonate precipitation (Conkin, 1961, McClellan, 1966). On the other hand, morphogroup B2 and C exhibit lower proportions which occur in the quiet water current environment. Subgroup B2 is represented by *Thurammina* which is interpreted generally as a sessile and vagile behavior (Reolid et al. 2008b). However, the low proportion of this taxon may indicate that the B2 group were not able to compete with the opportunistic taxa. Meanwhile, the rare occurrence of morphogroup C, which is interpreted as infaunal, may indicate that a food source preserved in the sediment is poorer than that suspended in the water column, and the oxygen concentration beneath the sediment-water interface is low or anoxic.

5.1.6.2. Competition within opportunistic taxa

There are several taxa that can be classified as opportunists: *Psammosphaera, Thuramminoides sphaeroidalis,* and *Psammosphaera cava.* These taxa are present in most of the types of lithofacies that reflect variations in the paleoenvironment. The abundance of these opportunist genera in the succession most likely is influenced by the dominance of *Psammosphaera*(?). Figure (5.8) shows that high abundance of *Psammosphaera*(?) is indicated by the absence of *Thuramminoides spaheroidalis* and *Psammosphaera cava*, and vice versa (Fig.26). That condition is demonstrated when the *Psammosphaera*(?) are absent during unfavorable conditions, other opportunistic foraminifera start radiating. It clearly shows the competition within the opportunistic taxa that should be able to adapt and

tolerate to a stressed environment. In fact, only single taxa can survive and there is no evidence of sharing food and space, which is characterized by high diversity and low dominance indices. Competition can be recognized also among *Psammosphaera*(?) and other main species of *Tolypammina* and *Thurammina* found in the Qusaiba succession (Fig.26). It exhibits that *Tolypammina* and *Thurammina* bloom at the bottom of the studied section, which followed by decreasing numbers of *Psammosphaera*(?) upsection.

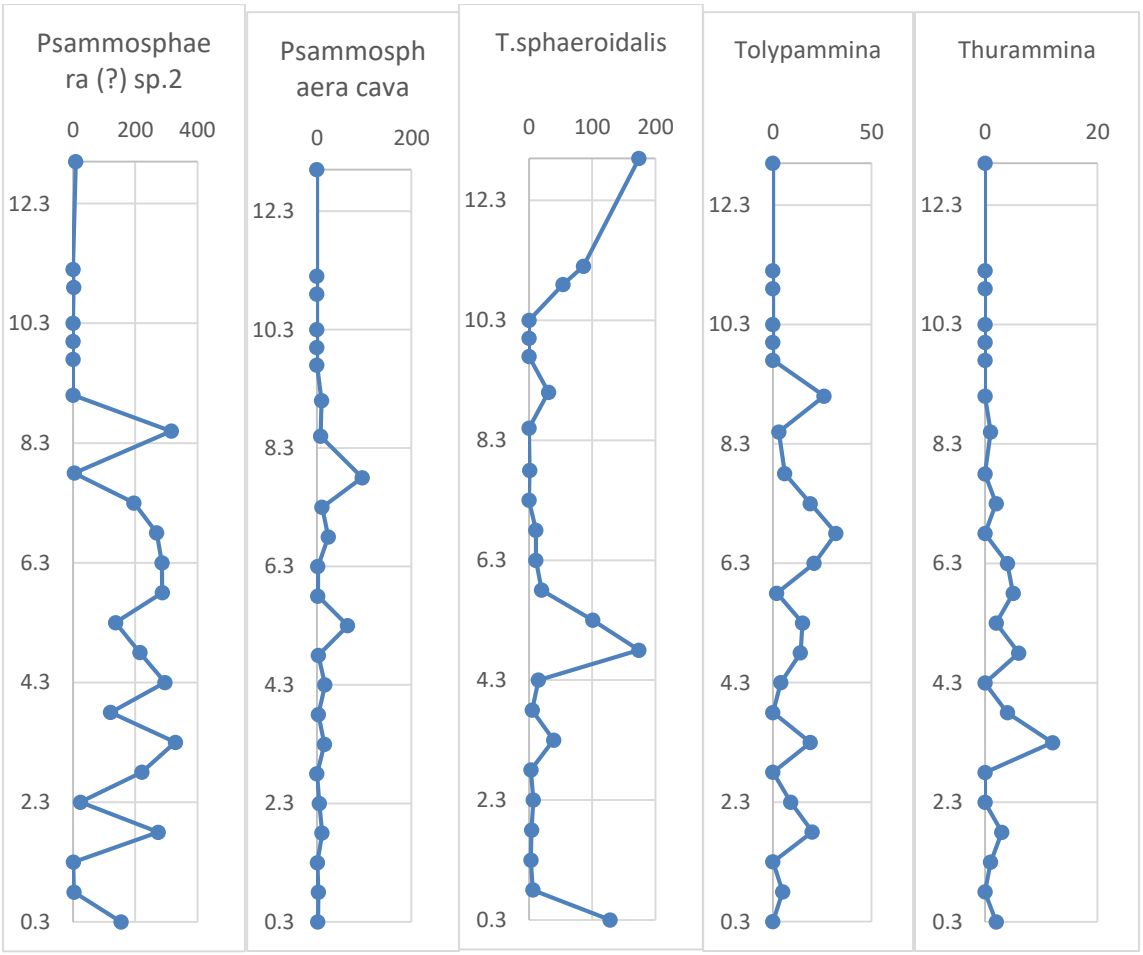

Figure 26: Vertical distribution of common taxa.

5.1.6.3. Paleogeography

A comparison of the palaeogeographical distribution of Aeronian agglutinated foraminifera from Saudi Arabia and other areas is carried out in an attempt to delineate faunal provinces. The previously studied regions include the Gondwanan continents, i.e., Australia (Bell et al. 2000), Bolivia (Gagnier et al. 1996), the peri-Gondwanan terraines, i.e., the Czech Republic (Holcová 2002), the Laurantian continent – North America (Moreman 1930; Grubbs 1939; Stewart and Priddy 1941; Dunn 1942; Ireland 1966; McClellan 1966; Watkins et al. 1999)), Avalonia (Aldridge et al. 1979; Mabillar and Aldridge 1982; Kircher and Brasier 1989; Kaminski et al. 2016), and Baltica (Eisenack 1938, 1954, 1969). The spatial distribution of foraminifera during the Silurian (Table 2) was compiled to infer the relationship between palaeolatitude and possible palaeoenvironments that favour particular foraminiferal associations. The comparison of the foraminifera is only applied to the genus level, since limited comparative studies have been conducted for Silurian foraminifera. A more comprehensive synthetic study needs to be carried out to map faunal provinces at the species level.

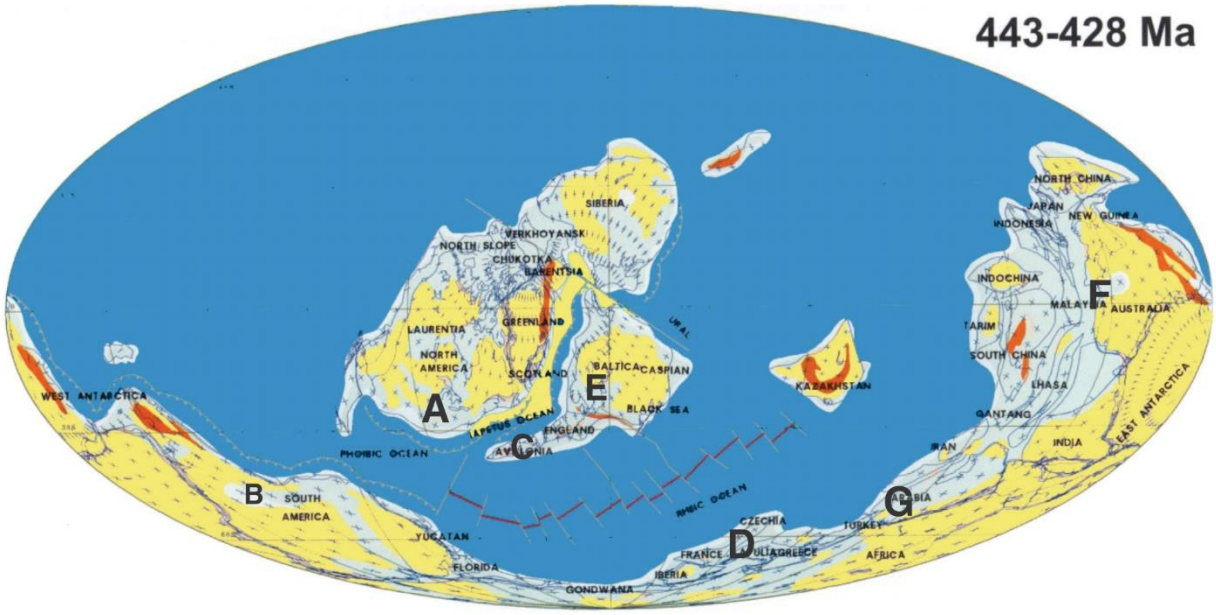

Figure 27: Location of previously studied Lower Silurian foraminiferal assemblages (Golonka et al., 2006). A= Central United States (Moreman 1930); B= Bolivia (Gagnier et al. 1996); C= western Ireland (Kaminski et al. 2016); D= Czech Republic (Holcová 2002); E= Baltic region (Eisenack 1954); F= Western Australia (Bell et al. 2000); G= this study.

Several species of Lower Silurian foraminifera present in Saudi Arabia exhibit a wide global distribution (Fig.27). These taxa can be classified as cosmopolitan foraminifera, which are represented by *Psammosphaera, Thuramminoides, Hyperammina, Lagenammina, Thurammina, Saccammina, Sorosphaera, Webbinelloidea*. Generally speaking, we recognize two faunal provinces: The Austral (Gondwanan) province consists of monothalamid foraminifera with rare tubothalamids and globothalamids, whereas the tropical province (Laurentia and Avalonia) contains abundant tubothalamids and lacks globothalamids. Lower Silurian assemblages from western Ireland are numerically dominated by ammodiscids (*Rectoammodiscus*), with subdominant hyperamminids (Kaminski et al. 2016). Likewise the Lower Silurian assemblage from the Welsh borderlands and English West Midlands is reported to be a diverse *Ammodiscus* assemblage (Kircher and Brazier 1989). The so-called cosmopolitan taxa of *Ammodiscus,*

Rectoammodiscus, *Glomospira*, *Lituotuba* and *Tholosina* that are common in various parts of North America (Conkin and Conkin 1982), and Europe have not been found in Saudi Arabia.

Table 3: Comparison of the occurrence of genera at studied Silurian localities.

	Australia	**Bolivia**	**Czech**	**Baltic**	**North America**	**British Avalonia**	**Saudi Arabia**
Ammodiscus					X	X	
Ammosphaeroides					X		
Ammovolummina			X				
Amphitremoida			X				X
Anictosphaera					X		
Areniconulus				X			
Arenosiphon				X	X		
Aschemonella					X		
Atelikamara					X	X	
Bathysiphon					X		X
Bifurcammina					X		
Blastammina				X			X
Ceratammina						X	X
Colonammina			X		X		
Crithionina					X		
Gastroammina					X		
Glomospira		X	X		X		
Glomospirella			X				
Hyperammina	X	X	X		X	X	X
Ketchentoiske							X
Lagenammina		X	X		X	X	X
Lituotuba	X				X		
Marsipella					X		

Ordovicina					X		
Oryctoderma					X		
Parathurammina	X						
Placopsillina					X		
Proteonina					X		
Psammosphaera	X	X	X		X	X	X
Raibosammina					X		X
Rhabdammina	X				X		X
Saccammina			X		X	X	X
Saccamminitta							X
Serpenulina			X				
Sorosphaera	X		X		X	X	X
Stacheia							X
Stegnammina					X	X	X
Stomasphaera						X	
Storthosphaera						X	
Thekammina					X		
Tholosina		X			X	X	
Thurammina	X	X	X		X	X	X
Tolypammina	X	X			X	X	X
Turitellella					X		X
Webbinelloidea		X	X		X	X	X
Nodosinellidae			X				
Paratikhinellidae			X				
Thuramminoides	X		X				
Ammobaculites							X
Sculptobaculites							X

5.2. Graptolites

In Silurian strata, one of the most important index fossils are graptolites, which have been globally utilized as a tool to carry out relative dating. As dating tools, the establishment of a standardized graptolites biozonation was developed to calibrate subsequent works.

5.2.1. Graptolite Preservation

In this study, the graptolite specimens were encountered in shale and siltstone, and show various degrees of the preservation (Fig. 29). In sandstone, specimens were absent, possibly because they were subjected to high hydrodynamic energy associated with the depositional setting of the sandstone, which destroyed the graptolites. The recoverable materials were preserved as complete body fossils and graptolites fragments which are truncated or bleached by erosion, weathering, or diagenesis of the rock where the graptolites deposited. All the specimens in this study were recovered as flattened rhabdosomes, techa, septa, and nemata, with might be subjected to the burial processes after the deposition of the clay size materials.

5.2.2. Graptolite Biozonation

Recoverable graptolite specimens from the samples, the Lower Silurian succession in the Old Qusaiba Village, Qasim Region are included in the L. convolutus biozone.

1. Undefined zone 1

   This zone is characterized by unrecovered graptolites specimens, which may due to low assemblages of the graptolites during the deposition of the rock record. This condition contrasts with the postulated study that the highest assemblages of the graptolites can be encountered in the offshore rock record. Based on the Zalaszewicz et al. (2007) study, this zone is assigned to the *L. convolutus* zone.

2. Convolutus biozone

   The *Lituigraptus convolutus* biozone, which was first established by Marr and Nichol (1888), is widely established and well calibrated (Williams et al., 2016). The beginning of this biozone is characterized by first occurrence of *Lituigraptus convolutus*.

   The interval, the succession from 1.8 meters to 8.5 mteres from the basal part of the section, is interpreted as the L. convolutus biozone, in agreement with Zalaszewicz et al. (2007) and Williams et al. (2016). This interval consists of a relatively high abundance of *Normalograptus scalaris* and *Pristiograptus regularis*. The convolutus biozone, in this succession, was defined by the occurrence of the *Neolagarograptus reckadsi*, *Pristiograptus renaudi*, and *Neolagarograptus tenuis* in sample Q9 (Fig.29), which was collected approximately 5 m from the bottom of the succession. Unlike the other successions in the United Kingdom, Wales, which is famous for the discovery of rich graptolite assemblages, this interval has a low abundance of graptolites, which can be explained due to its location close to the land.

3. Undefined zone 2

The second undefined zone in this study, ranging from 8.5 m upward and is characterized by the sparse presence of *Pristiograptus regularis* and some poorly preserved undefined graptolite specimens. This zonation is considered as undefined owing to the difficulties in recognizing poorly preserved (or absent) graptolites in a sand-dominated lithology. This interval may be classified as a *L. convolutus* biozone to *S. sedgwickii* (Zalaszewicz et al., 2007; Williams et al. 2016). Based on the other graptolites studies in different locations of Saudi Arabia, the L. convolutus biozone is overlain by *S. sedgwickii,* which is indicated by the presence of *Neolagarograptus tenuis* and the first occurrence of *Parapetalolithus altissiimus,* which can be correlated to the sedgwickii biozone in Libia (Štorch and Massa, 2006, Williams et al., 2016).

Figure 28: Representative species of recovered graptolite from section 1. A. *Normalograptus scalaris* (?); B. *Pristiograptus regularis;* C. *Pristiograptus renaudi;* D. *Normalograptus scalaris;* E. *Metaclimacograptus bohemicus;* F. *Pristiograptus variabilis;* G. *Metaclimacograptus hugesi;* H. *Neolagarograptus rickardsi;* I. *Normalograptus trifilis* (?); J. *Normalograptus ajjeri*.

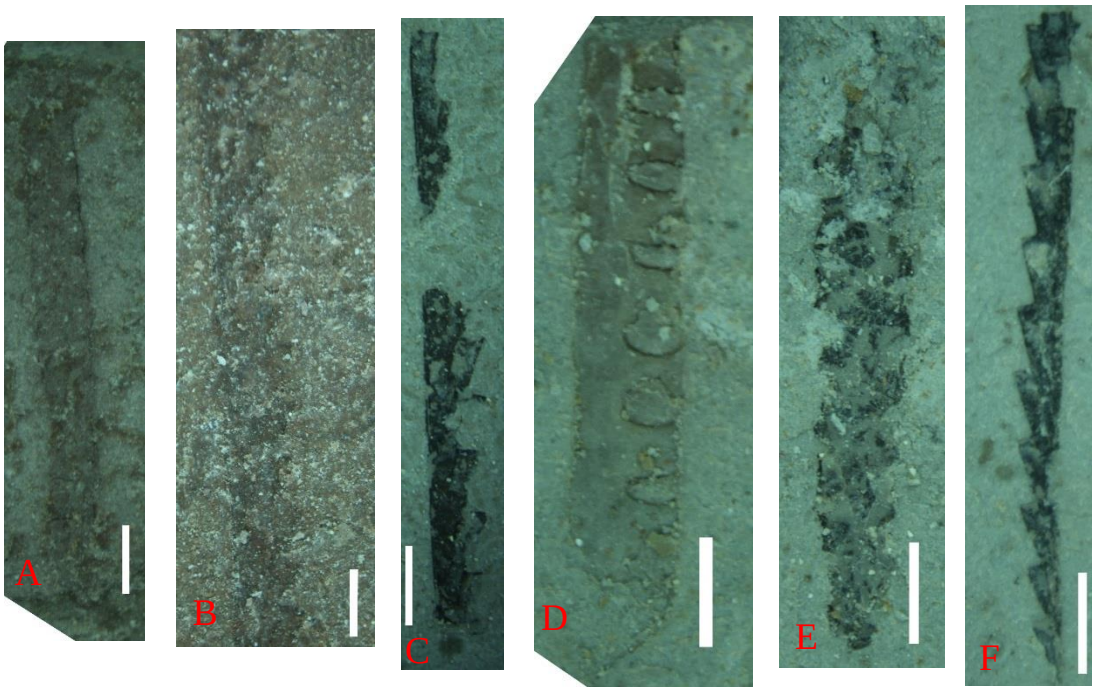

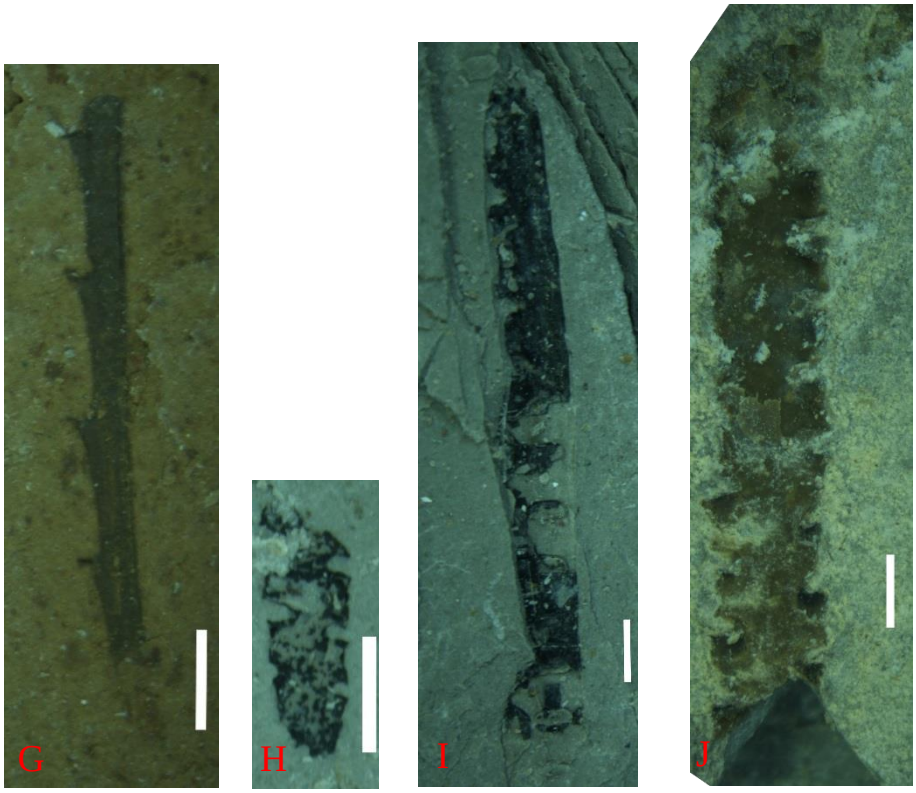
G
H
I
J

CHAPTER 6

GEOCHEMISTRY

6.1. Introduction

The focus of the geochemical investigation in this study is mainly on the mineralogical results acquired by XRD and major, minor, and trace elements plotting and trend obtained by XRF. All the elements recorded in this study were displayed in weight percent (wt%) for the major elements and part per million (ppm) for the trace metals. Microsoft Excel was utilized to generate graphs and plots of the elements.

6.2. XRD Results

The upper Qusaiba shale consists predominantly of quartz and clay minerals with potassium feldspar as a subordinate mineral, and calcite, dolomite, anhydrite, and gypsum rarely found (Fig. 29) (Table 3). However, the lowermost Sharawra Formation consists of alternating quartz arenite sandstone (Abbas, 2015) and claystone. The quartz content in the Qusaiba shale is between 36%-64% with an average value of 52.17%. This quartz dominant component is associated with strong detrital supply transported from terrestrial sources. The presence of the calcite, dolomite, anhydrite may represent secondary minerals origin, while the gypsum occurs as nodules.

Table 4: Mineral contents of the Qusaiba Shale from section 1.

Sample	Quartz	K Felds	Calcite	Dolomite	Gypsum	Anhydrite	T. Clay
	Mineral Content (wt %)						
Q0	60	15	1	0	0	0	24
Q1A	64	15	1	0	0	0	20
Q1B	56	16	1	1	0	0	26
Q1D	62	17	1	0	0	0	20
Q1E	48	15	3	2	0	3	29
Q1F	53	17	0	0	10	0	20
Q1G	48	18	2	0	3	1	28
Q2	51	22	2	0	0	2	23
Q3	58	18	1	0	0	2	21
Q4	49	22	2	0	0	0	27
Q5	57	18	1	0	0	0	24
Q6	47	16	1	0	0	0	36
Q7	49	14	2	0	0	0	35
Q8	55	19	1	1	0	0	24
Q9	54	16	1	0	0	0	29
Q10	51	11	1	1	0	0	37
Q11	59	15	2	0	0	0	24
Q12	53	15	1	0	0	0	31
Q13	55	14	1	0	0	0	30
Q14	51	17	0	0	0	0	32
Q15	49	17	1	0	0	0	33
Q16	45	9	1	0	0	0	45
Q17	43	18	1	1	0	0	37
Q18	36	14	0	0	1	1	48

Table 4: Statistical parameters of mineral contents in shale samples.

Mineral	Min	Max	Mean	StDev	Q1	Q2	Q3
	wt %						
Quartz	36.00	64.00	52.17	6.24	48.14	51.83	57.10
K Feldspar	9.17	22.00	51.83	2.81	15.00	16.00	17.88
Calcite	0.00	3.00	1.17	0.69	1.00	1.00	1.75
Dolomite	0.00	2.00	0.25	0.52	0.00	0.00	0.00
Gypsum	0.00	10.00	0.58	2.06	0.00	0.00	0.00
Anhydrite	0.00	3.00	0.38	0.52	14.58	16.38	18.00
T. Clay	20.00	48.00	29.29	7.40	24.00	28.50	34.50

Figure 29: Mineral distribution acquired from XRD in section 1.

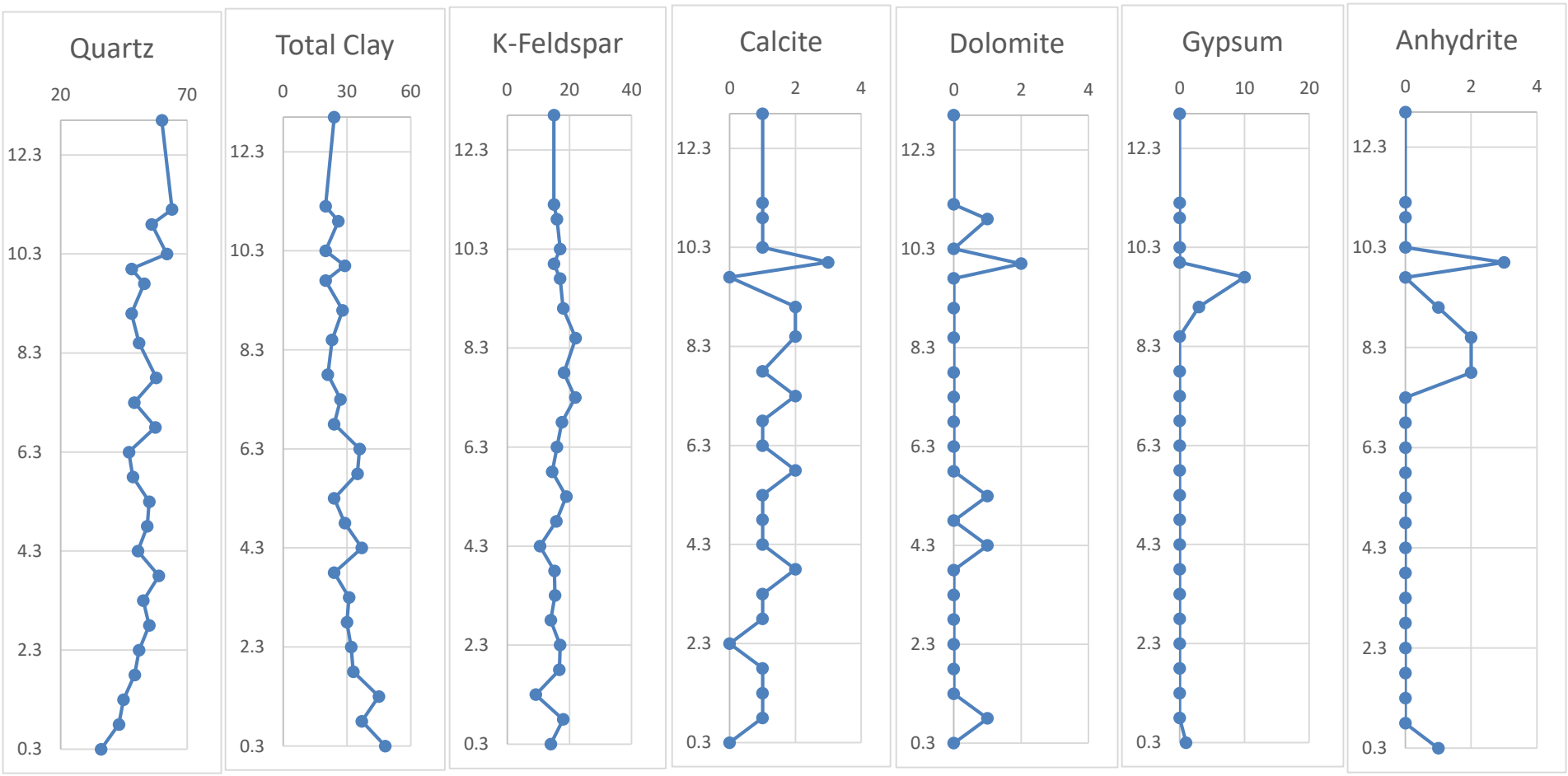

Table 5: Statistical parameters of clay contents in shale samples.

Sample	T. Clay	Kaolinite	Illite	Smectite
	Clay Contetnt (wt %)			
Q0	24	14	9	1
Q1A	20	11	7	2
Q1B	26	15	11	0
Q1D	20	11	9	0
Q1E	29	17	12	0
Q1F	20	19	1	0
Q1G	28	19	9	0
Q2	23	13	10	0
Q3	21	13	8	0
Q4	27	15	12	0
Q5	24	11	12	0
Q6	36	28	8	0
Q7	35	21	13	0
Q8	24	15	8	0
Q9	29	19	10	0
Q10	37	26	8	3
Q11	24	18	5	1
Q12	31	22	8	0
Q13	30	20	10	0
Q14	32	26	6	0
Q15	33	20	10	3
Q16	45	32	8	5
Q17	37	24	12	1
Q18	48	36	13	8

The clay mineral content in this shale is comprised predominantly of kaolinite and subordinate illite and smectite. The range of the total clay content varies from 21% to 48% (average 29.29). The trend of the total clay content in graphs shows increasing values in the bottom part of the studied succession. A significant rise in the value of the total clay content in the succession started from sample Q12 to sample Q18, which increases from 30% to 48% – the maximum value of the total clay content. Based on the clay mineral

compositions, kaolinite has a similar trend as the total clay content, while illite exhibits a fluctuating trend and smectite shows an abrupt change in the bottom part of the record.

Table 6: Statistical parameters of clay contents in shale samples.

Mineral	Min	Max	Mean	StDev	Q1	Q2	Q3
				wt %			
T. Clay	20.00	48.00	29.29	7.40	24.00	28.50	34.50
Kaolinite	9.17	36.24	19.36	6.54	14.14	18.62	23.86
Illite	1.33	13.45	9.20	2.69	8.01	9.11	11.51
Smectite	0.00	8.31	1.15	1.99	0.00	0.30	1.16

As minerals that are sensitive to changes in temperature, pressure, and climate, clay minerals can be utilized as a paleoclimate proxy (dd). In advance, investigation of the origin of clay minerals whether deposited in the basin as a product of weathering, detrital input, or authigenic processes is essential to be carried out.

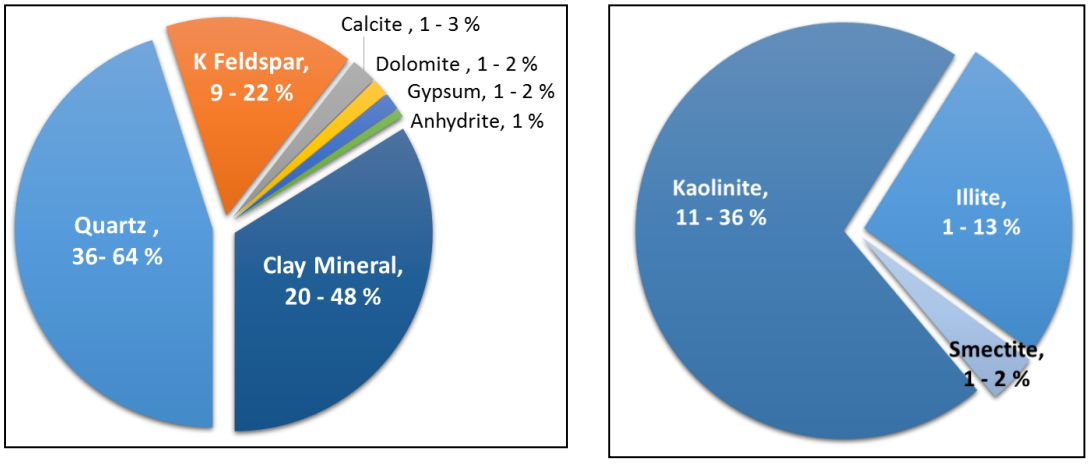

Figure 30: A. Mineral percentages obtained from XRD B. Clay minerals percentage obtained from XRD.

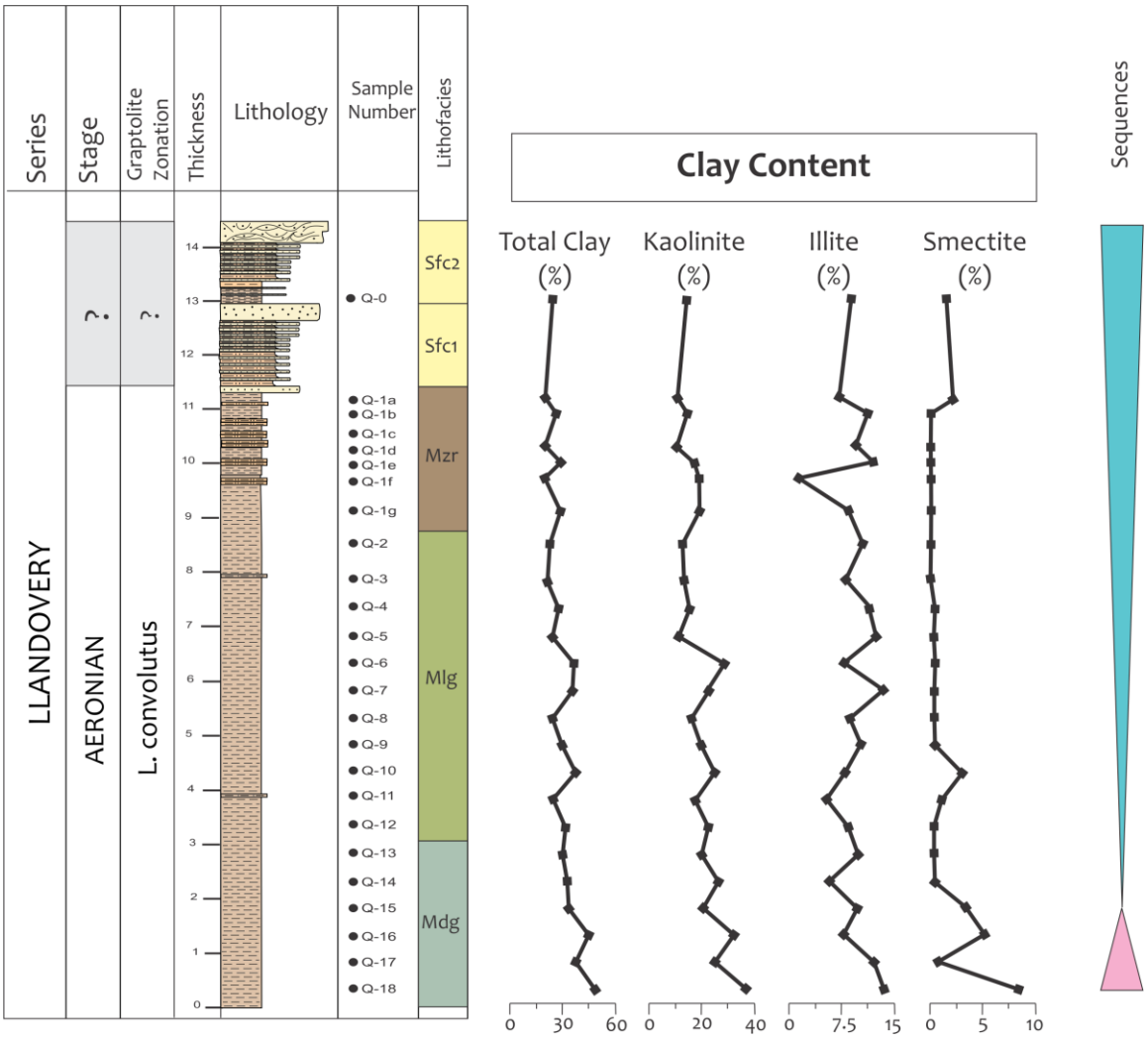

Figure 31: Clay content distribution of section 1.

6.3 XRF Results

Major and trace elements have been identified from the shale using XRF. These elements can be used to obtain mineral and chemical composition of the shale samples, which can be compared to the XRD in order to validate the analysis. Minerals and chemical composition also can be utilized as a tool to interpret the provenance of the rock, paleoenvironment, and construct chemostratigraphic correlation (e.g. Calvert and Pedersen, 1993; Jones and Manning, 1994; Jarvis et al., 1998; Brumsack, 2006; Algeo and Rowe, 2012, Creigi, 2016). The results of major elements are provided as an oxide, which means requires conversion to obtain an elemental substance. Conversely, trace elements acquired from XRF analysis are ready to be used.

6.3.1 Major Elements

The oxide of the major element attained from the XRF identification consist predominantly of SiO_2 and Al_2O_3 for about 45.02-56.13 wt% and 21.94-29.19 wt% respectively. Subsequently, Fe_2O_3, K_2O, MgO, SO_3, represent an oxide percentage more than 1 wt%, and TiO_2, P_2O_5, CaO have mean value less than 1 wt%. Compared with the results of the XRD analysis that have not shown iron minerals, Fe_2O_3 results from XRF, with a mean value of 8.97 wt% cannot be neglected.

Table 7: Statistical parameters of major elements obtain from XRD.

Major Elements	Min	Max	Mean	StDev	Q1	Q2	Q3
			wt %				
MgO	1.27	3.54	2.12	0.52	1.71	2.06	2.44
Al_2O_3	21.94	29.12	27.08	1.48	26.47	27.17	28.23
SiO_2	45.02	56.13	52.11	2.61	50.14	52.56	54.10
P_2O_5	0.50	0.77	0.58	0.07	0.53	0.57	0.60
SO_3	0.44	7.38	2.56	1.51	1.54	2.18	3.28
K_2O	3.96	5.68	4.71	0.47	4.37	4.65	5.03
CaO	0.14	1.57	0.33	0.30	0.17	0.21	0.42
Fe_2O_3	4.43	20.70	8.97	3.69	6.60	8.01	10.24
TiO_2	0.68	1.02	0.90	0.08	0.85	0.91	0.96

Figure 32: Major element oxide distribution obtained from XRF.

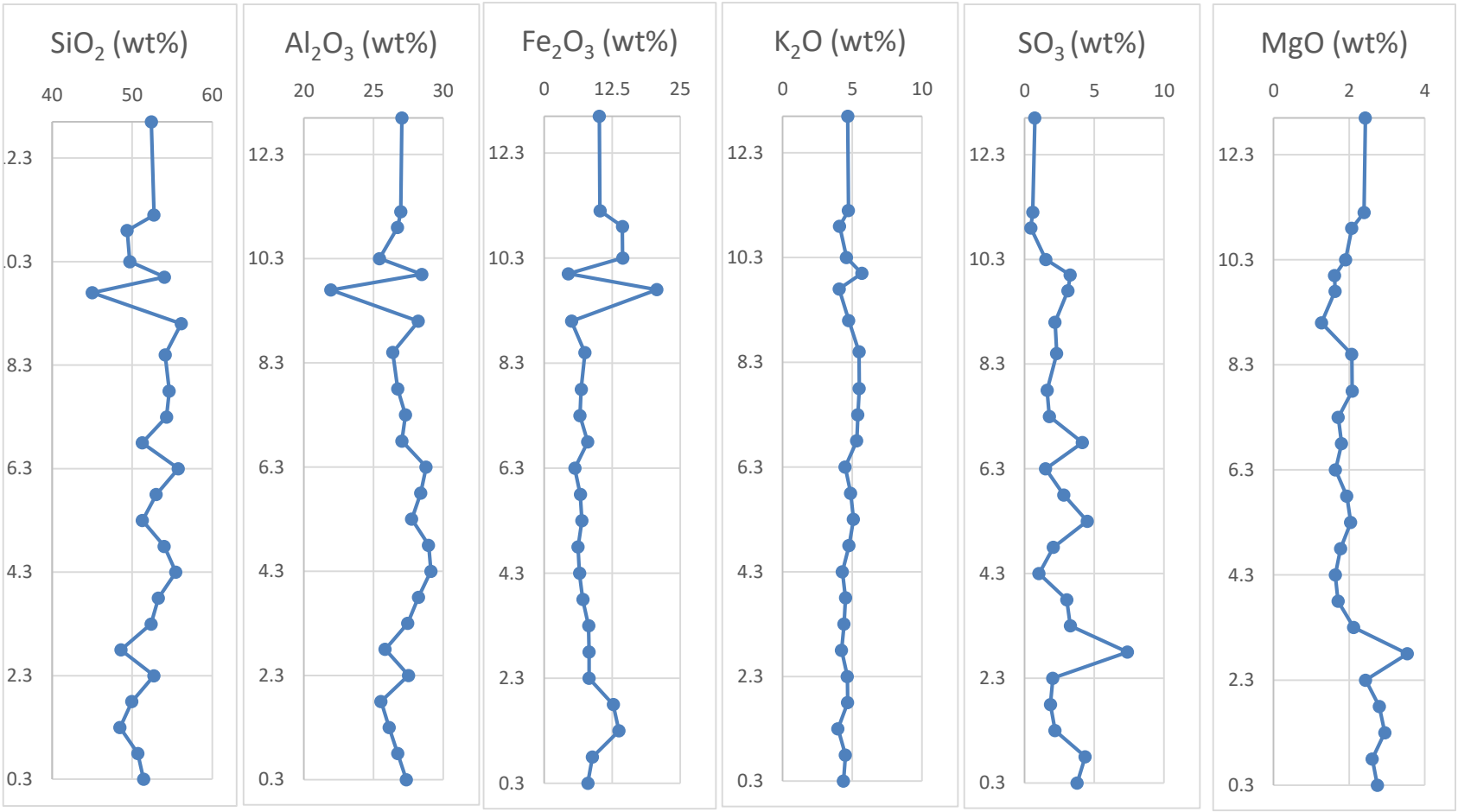

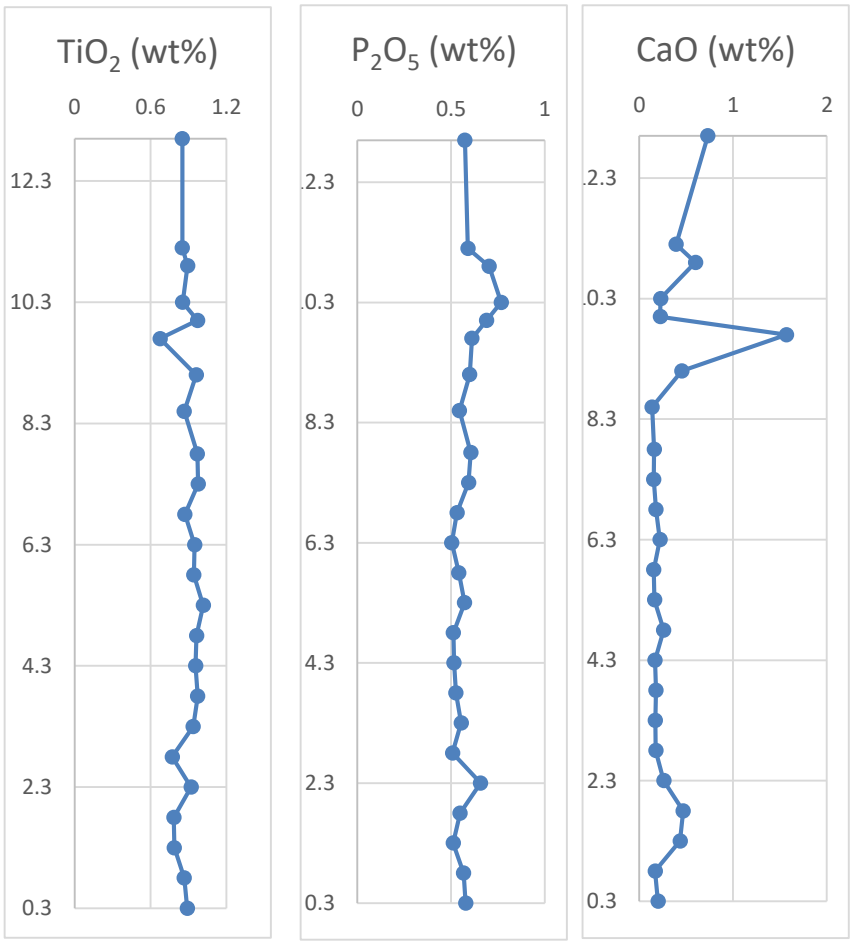
TiO2 (wt%)
0
0.6
1.2
12.3
10.3
8.3
6.3
4.3
2.3
0.3
P2O5 (wt%)
0
0.5
1
2.3
0.3
8.3
6.3
4.3
2.3
0.3
CaO (wt%)
0
1
2
2.3
0.3
8.3
6.3
4.3
2.3
0.3

6.3.2 Trace elements

Trace elements composition of the sample acquired from XRF, consist of 25 elements. In advance, this trace element is anlyzed to interpret the paleoenvironmental conditions during the Aeronian to the studied section.

Table 8 : Statistical parameters of trace elements.

Trace Elements	Min	Max	Mean	St.Dev	Q1	Q2	Q3
				ppm			
V	141.50	298.80	194.69	26.49	182.48	194.25	202.03
Cr	167.50	292.10	217.56	26.29	204.10	211.20	227.55
Mn	0.11	925.10	394.67	260.76	211.43	325.75	546.78
Co	140.90	626.50	296.96	112.69	221.23	268.60	343.25
Ni	48.10	255.20	92.71	42.37	69.35	79.00	104.03
Cu	49.80	157.60	96.10	22.62	77.25	98.95	98.95
Zn	83.00	552.20	192.64	90.92	142.98	173.45	205.65
Ga	28.50	56.40	48.92	5.64	46.30	49.40	52.30
Ge	0.40	3.80	1.84	1.10	1.03	1.65	2.80
As	0.00	14.50	2.58	3.44	0.00	1.10	5.13
Se	0.00	1.30	0.38	0.43	0.00	0.20	0.88
Br	0.50	7.70	2.44	1.60	1.30	1.75	3.30
Rb	160.00	349.70	253.79	34.93	231.43	259.10	270.85
Sr	66.50	596.00	150.05	120.21	80.90	110.75	156.55
Y	13.70	78.60	43.53	15.27	31.43	39.65	55.23
Zr	137.70	203.70	173.27	19.53	158.03	176.85	189.53
Nb	19.40	29.60	24.33	2.54	23.00	23.20	26.10
Mo	0.10	1.80	0.88	0.42	0.57	0.85	1.20
Ag	0.10	997.40	678.78	393.79	211.61	872.45	913.90
Cd	0.10	2.80	0.89	0.59	0.50	0.50	1.15
In	2.40	6.10	3.56	0.83	2.75	3.50	4.08
Sn	40.00	65.20	47.97	5.27	44.50	46.60	51.50
Sb	10.30	19.40	13.44	2.43	10.95	13.20	14.80
Ba	280.40	494.10	369.32	67.60	304.75	356.25	447.05
Pb	16.30	149.50	54.13	29.67	38.05	44.45	61.73

6.3.3 Cross Plot Analysis

In this section, cross plots of elemental concentrations were generated in order to understand the relationships between two elements. For the following figures, several cross plots, including Al against other major element and several trace metals were displayed. Plotting Al against other major and trace elements can support interpretation of the elemental relationships whether influenced by detrital input, or enrichment due to diagenesis processes, because Al has a high association to terrigenous origin and is low to immobile during diagenesis. Therefore, a positive coefficient of correlation between Al and other elements represents mainly terrigenous origin and those plotted elements are not related to paleoredox environments (Tribovillard et al., 2006). In addition, as a part of the clay minerals, Al is also associated to those minerals. Thus, a positive correlation between Al and plotted elements indicates elemental association of the clay minerals (Moran, 2013).

In the following cross plot analysis, the relationship between Al and other major elements (Si, K, Fe, Ca, Mg, Ti, Mn, S) in oxide form were examined. There are clearly demonstrated several strong positive correlations between Al, Ti and Si, and negative correlations with Fe and Ca. The conditions can be inferred that Al, Ti, and Si can be utilized as a detrital proxy, while Fe and Ca in this study can be interpreted as an authigenic element, which are not related to detrital influx. Hence, high detrital supply will perturb the generation of Fe and Ca. In other cases, cross plot graphs of Al against S and Mg show no correlation. Therefore, S and Mg are not parts of the detrital elements, which are transported from terrestrial sources and the generation of those elements is not influenced by sediment supply.

Figure 33: Crossplot analysis between Al_2O_3 and other oxides of the major elements.

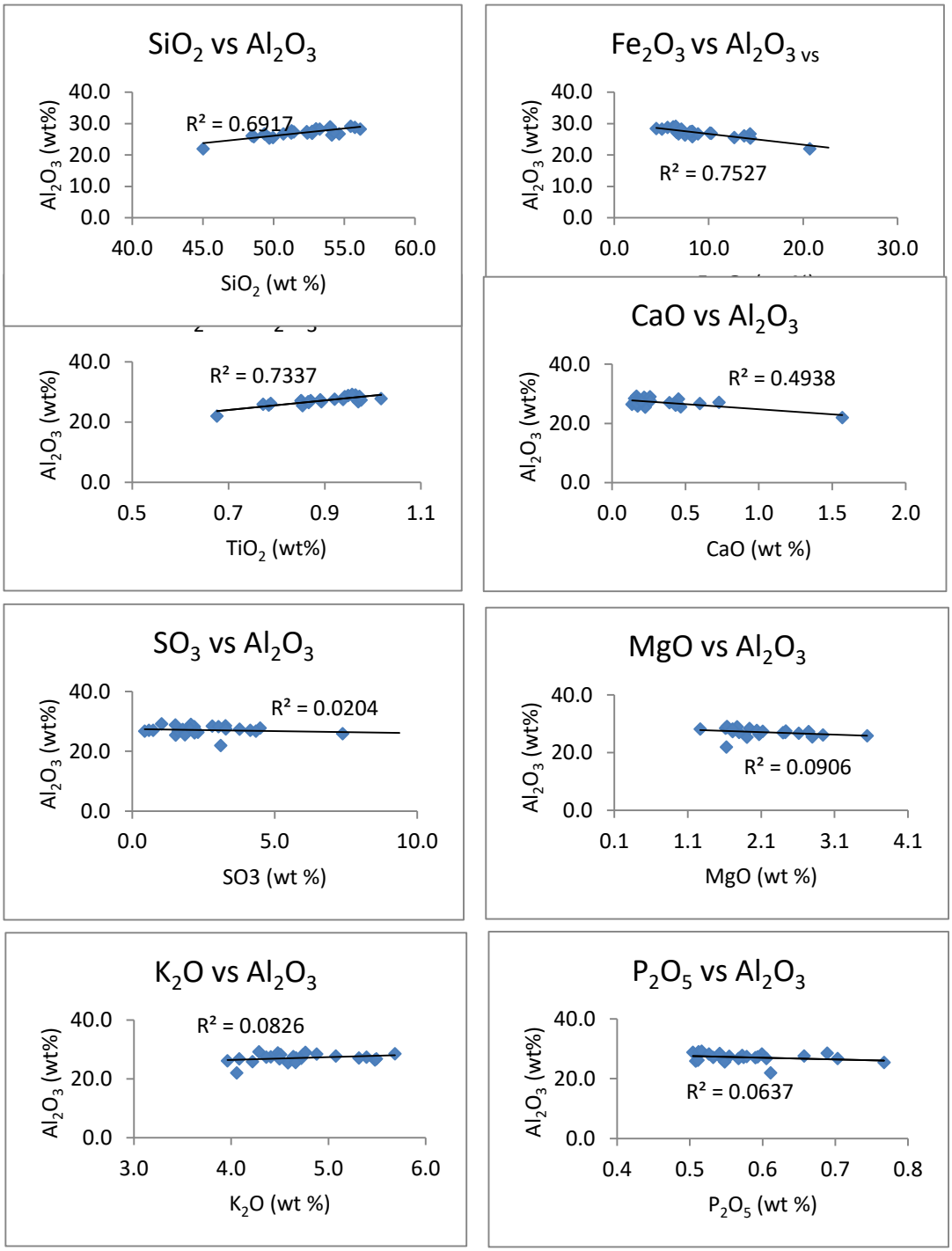

6.4 Environmental Proxies Analysis

Application of trace metal analysis in respect to interpret prevailing paleoenvironmental factors gained wide acceptance in the recent decade. The wide acceptance of this approach is inherent to the increasing studies about shale characterization. The advancement on the geochemistry analytical device is also supporting the development of elemental analysis approaches. Therefore, the elemental proxy analysis method can be a reliable tool for validating sedimentological and paleontological data.

The main purpose of this part is to infer paleoenvironmental variables of detrital flux, paleoredox, and paleoproductivity conditions, which are based on changes in the concentrations of specific elements.

6.4.1 Sediment flux proxy

Some elements are renowned to be utilized for inferring clastic influx in a particular environment (Sageman and Lyons, 2004; Ver Straeten et al., 2011, Reolid et al. 2012; Lash, 2017). This approach previously used quartz or silica content of sediment samples, whereas recently this approach has been challenged due to some bias whether the Si content in the sediment is coming from terrestrial origin or opaline skeletal products (Calvert and Pedersen, 2007; Lash, 2017). Therefore, immobile or less mobile elements such as Ti and Zr are used to validate or substitute the application of Si in determining sediment influx.

In this determination of the sediment influx component, quartz and total clay content acquired by XRD are paired with Ti/Al and Zr/Al elemental ratios obtained from XRF. The general trend of the detrital proxy exhibit declining trends of quartz, Ti/Al, Zr/Al, and

increase value of the total clay content to the facies Mdg (Fig. 34). Fluctuations in the values can be recognized from the all proxies except the Zr/Al ratio which shows a gradual and slight change toward the basal part (Fig. 34).

The lowest value of the detrital proxies in the basal part of the studied section coincides with the low abundance of foraminiferal assemblages in the Mldg lithofacies (Fig. 34).

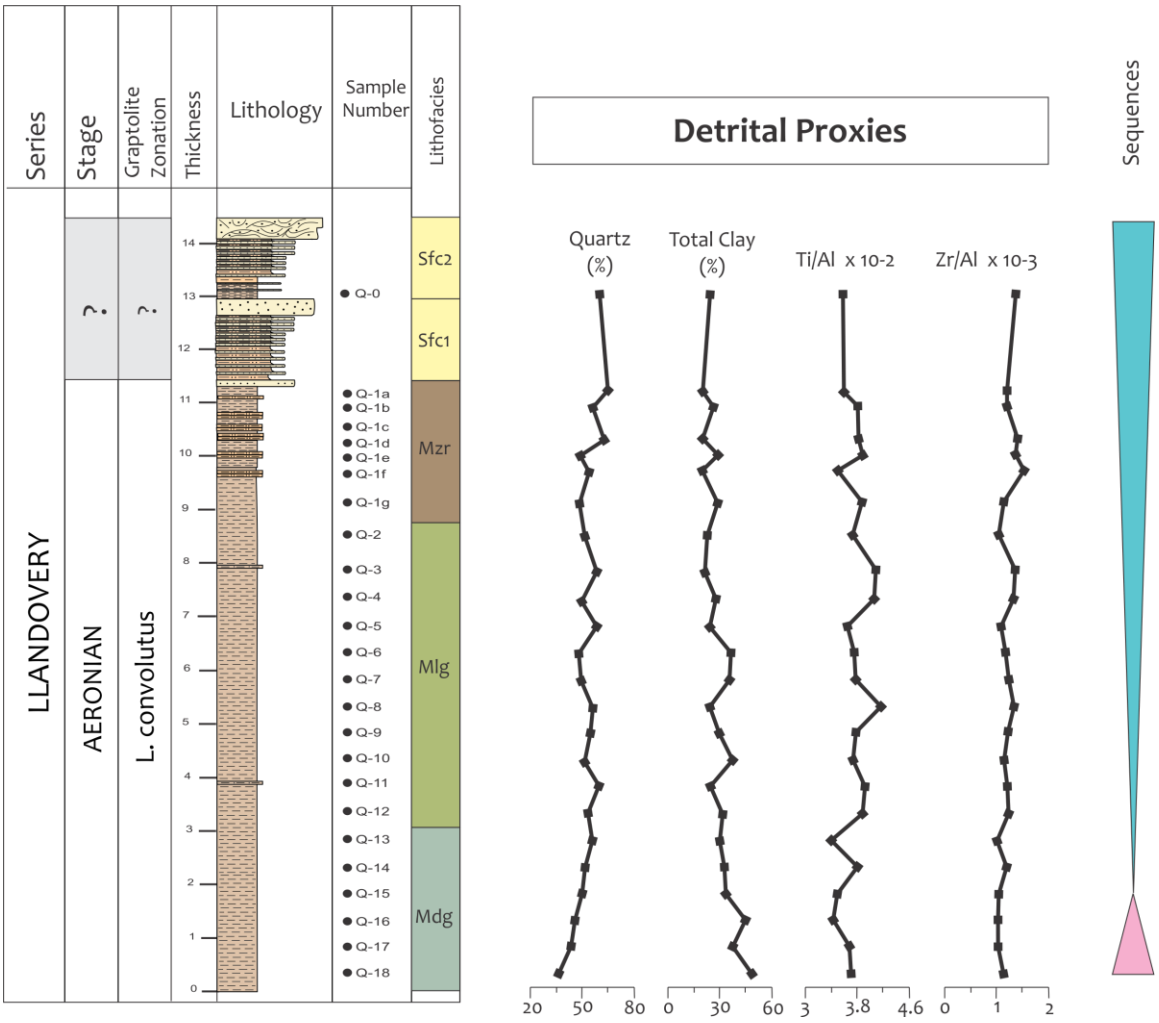

Figure 34: Detrital proxies distribution of section 1.

6.4.2 Paleoredox Proxy

Various methods which rely on the minerals such the degree of pyritization, measurement of pyrite framboids (e.g., Wignall et al. 2005; Bond and Wignall 2010; Liao et al. 2010; Wang et al. 2013; Wei et al. 2015); as well as trace metal analysis are carried out with an aim of determining the paleoredox conditions (Calvert and Pedersen, 1993; Tribovillard et al., 2006; Reolid et al., 2012; Lash, 2017). In this study, the redox sensitive trace element ratios V/Cr, Mo/Al, Co/Al, and Fe/Al have been selected since these trace elements are associated with the precipitation of sulphide minerals and organic matter in anoxic conditions.

The distribution of the analyzed trace metal ratios exhibits a major change of Co/Al, Fe/Al and a minor change of V/Cr at the base of facies Mdg (Fig. 35). Subsequently, within the facies Mlg, constant values of V/Cr, Co/Al, and Fe/Al are observed. However, Mo/Al ratio shows irregular fluctuations along the succession. A second major change in all analyzed elements is observed in the upper part of the Mzr lithofacies. This second major change coincides with the transition between a shale and sand dominated lithofacies (Fig. 35). The high dynamic value of some trace element ratio in facies Mzr coincides with the presence of the gypsum and anhydrite as secondary minerals in the mudstone, and may be related to the weathering and percolation of near surface water altering the shale.

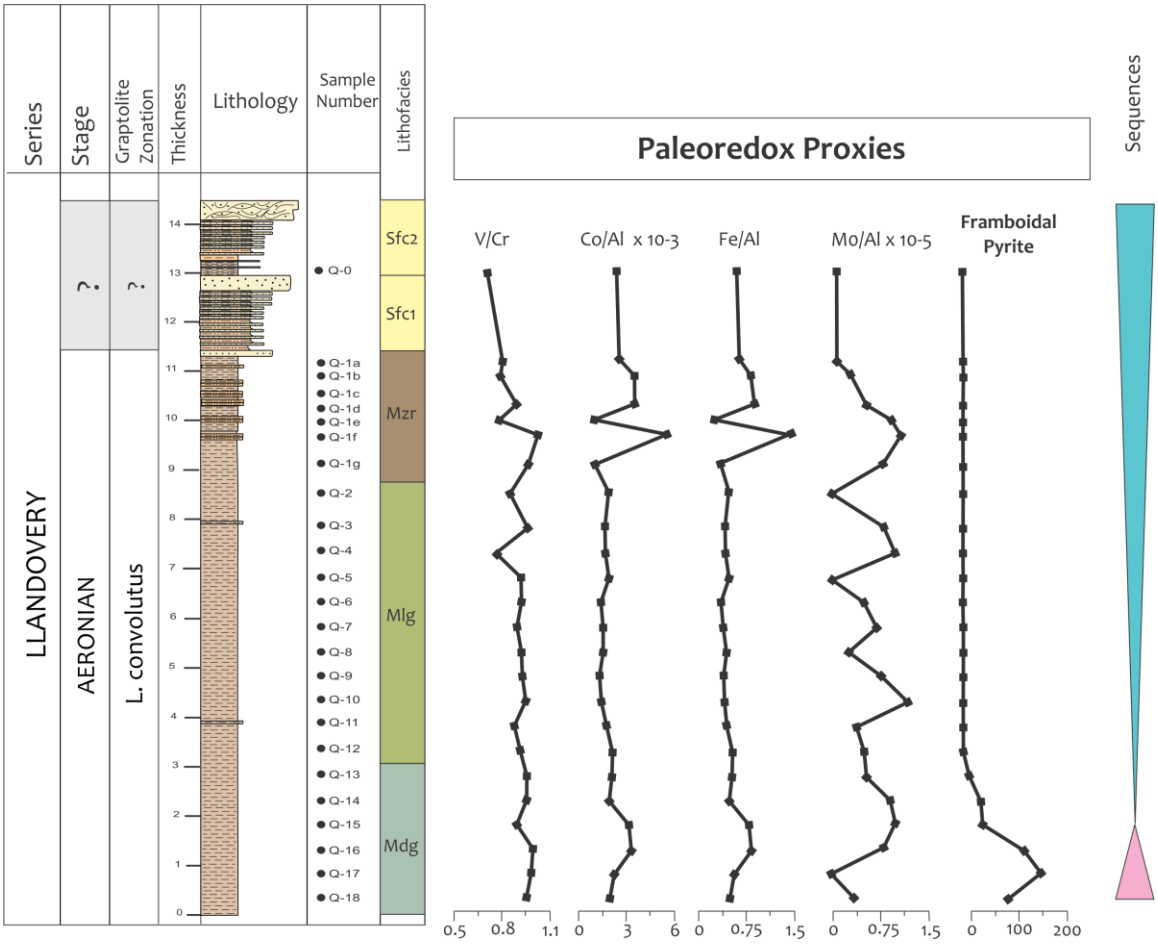

Figure 35: Paleoredox proxies distribution of section 1.

6.4.3 Paleoproductivity Proxies

Common elements used in analyzing the paleoproductivity of the ocean are phosphorus, barium, nickel, zinc, copper, and cadmium (Brumsack et al., 2006; Tribovillard, et al. 2006). In this study, phosphorus, barium, nickel, and zinc normalization with Al has been selected to interpret the paleoproductivity conditions. Phosphorus is a major constituent of the skeleton of organisms, an element in enzymes, DNA, and RNA, which means the P prevailing in the sediment originated from phytoplankton, skeletal remains, and fish bones,

and an enrichment in P content can be considered as a high productivity indicator in the marine environment (Tribovillard et al. 2006). Equivalent to the phosphorus, barite is also a constituent that constructs the skeleton of organisms, and also related to the phytoplankton (Whitfield, 2002; Tribovillard, et al. 2006). Therefore, Ba can be utilized as a proxy for paleoproductivity. In addition, zinc and nickel are organometallic materials, which have a role as a micro nutrient in an oxic environment. These elements can also be preserved in a reduced condition as pyrite organic matter or sulphide mineral associations. The stratigraphic distribution of paleoproductivity proxies shows relatively high P/Ti and Ba/Al values in facies Mdg, followed by relatively constant values in facies Mlg, until the elemental ratios clearly change with the highest values as well as the highest amplitude fluctuations in the Mzr lithofacies (Fig. 36). However, Ni/Al and Zn/Al values exhibit two enrichments in the transition between Mdg and Mlg as well as highest values in the transition between the sand and shale dominated lithology (Fig. 36). At the facies Mdg these elemental ratios also underwent slight enrichment compared with the average value of the middle part (Fig. 36). Thus, based on the stratigraphic distribution of the analyzed elemental ratio, the highest paleoproductivity occurred during the deposition of the Mdg lithofacies and the deposition of the middle to upper part of the Mzr lithofacies respectively.

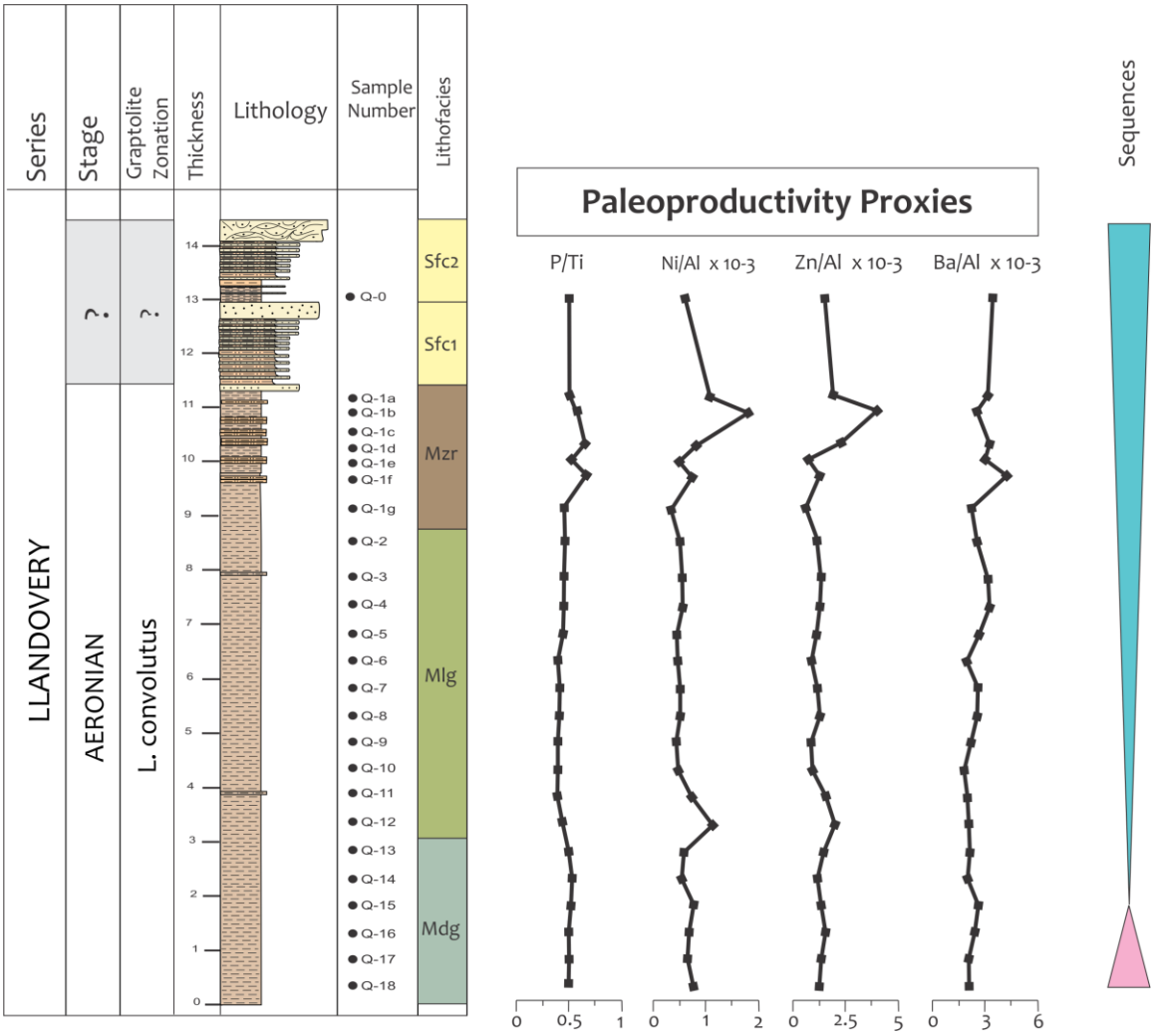

Figure 36: Paleoprodctivity proxies distribution of section 1.

6.5 Framboidal pyrite

Framboidal pyrite consists of homogenous equidimensional microcrystals of iron sulfide (pyrite), which is packed densely into a single spheroidal or subspheroidal form (Wilkin et al. 1996; Ohfuji and Rickard 2005). They are generated due to the interaction between Iron minerals and sulfate reducing bacteria (SRB) surrounding the sediment-water interface. Framboidal pyrites can be discovered also in marine cold-seeps within methane derived carbonates (Peckmann and Thiel 2004; Merinero et al. 2017). They are also associated with other morphologies, such as sunflower and euhedral pyrite (Large et al. 1999; Merinero et al. 2009; Cavalazzi et al. 2012; Wang et al. 2013; Gallego-Torres et al. 2015).

The diameter of authigenic framboidal pyrite ranges generally from 5 to 20 mm, and the size of the component microcrystals is usually less than 2 mm, although framboids up to 250 mm have been reported (Ohfuji and Rickard 2005). Based on the work of Wilkin et al. (1996), the size distribution of small framboidal pyrite has been used to infer the palaeo-oxygenation conditions (e.g., Wignall et al. 2005; Bond and Wignall 2010; Liao et al. 2010; Wang et al. 2013; Guan et al. 2014; Tian et al. 2014; Takahashi et al. 2015; Wei et al. 2015).

Framboidal pyrites were recovered from the basal part of the studies succession (facies Mdg) (Fig.37). The recovered framboidal pyrite represents a large diameter size, >65 μm with rounded to angular framboid form. The occurrence of framboidal pyrite in this succession coincides with enriched values of iron oxide from the XRF data. The presence of the larger framboidal pyrite may indicate a dysoxic environment.

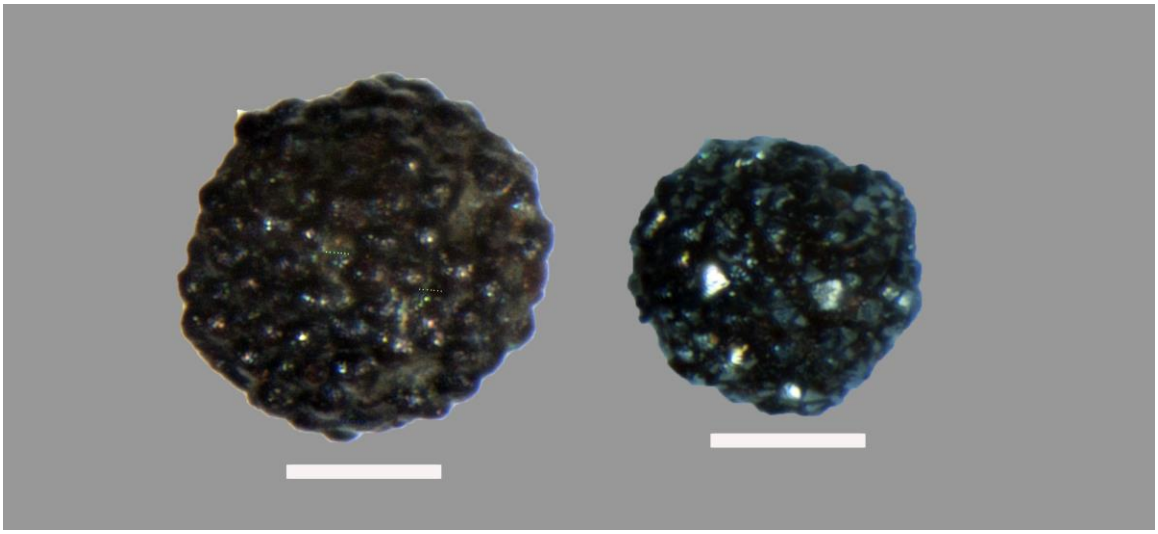

Figure 37: Two representatives of ramboidal pyrite recovered from the bottom part of section 1. Scale bars are 100 µm.

6.6 Paleoecology and Paleoenvironmental Reconstruction

The transgressive event during the Early Aeronian was witnessed both globally and across the northern epicontinental shelves of the Gondwana paleocontinent (Loydell, 1998; Johnson 2006; Luning, et al 2000; Cantrel et al., 2014; Creigi, 2016; Hayton et al., 2017). Rising sea level that occurred during the Aeronian in the study area lead to the deposition of pelagic material in an offshore environment below the storm wave base (Laboun, 2009; Hayton et al., 2017) (Fig. 38). This environment was indicated by tranquil water energy, characterized by low quartz, Ti/Al, and relatively low Zr/Al and high clay mineral contents (Figs. 34 and 38). Relatively high oceanic paleoproductivity is observed in this environment, which is specified by relatively high P/Ti, Ni/Al, Zn/Al, and Ba/Al (Fig. 36). On the contrary, such conditions were not favorable for the blooming of foraminifera. The high productivity with low number of the foraminifera in this section, coincides with higher values of V/Cr, Co/Al, and can be associated with low oxygen bottom waters (Fig. 35).

Thus, this environment may be considered as dysoxic. The inferred dysoxic conditions are also supported by the abundance of large framboidal pyrite with a diameter >65 μm (Fig. 37). To some extent, the dysoxic conditions in this environment may have undergone periodic alternations with oxic conditions. Such conditions resulting in some intercalation of dark gray mudstone in the rock record and indicated by fluctuating foraminiferal richness.

Oxic conditions, which are likely due to increasing terrigenous influx, increasing quartz, Ti/Al, and decreasing clay mineral content, in the environment in the further shallower offshore, is interpreted for the light gray mudstone overlain the basal lithofacies. This oxic interval is characterized by decreasing values of the V/Cr, Co/Al, and Fe/Al, ratios. Such conditions lead to the blooming of foraminifera which are characterized by the dominant flattened form of epifauna species constructed of fine grained siliceous material. The presence of a few infaunal taxa reveal that the oxygen penetrated into a few centimeters beneath the sediment water interface. In this interval, the diversity indices show fluctuating diversity and species richness. Decreasing numbers of foraminifera is most likely associated with the increased detrital influx, since the paleoproductivity indicators represent almost constant values. It means that increasing terrigenous supply may disrupt the foraminiferal habitat, even though the food source remains constant. On the other hand, the highest diversity and species richness is more likely attributed to the food supply. In this succession, the highest diversity and species richness is located at 3,5m (sample Q12) from the base of the succession (Figs. 21-22) which coincides with high Ni/Al and Zn/Al values (Fig. 36).

During the regressive event of the deposition of alternating greenish gray mudstone and reddish silt to fine grained sandstone, to some extent, foraminifera are absent. The interval is indicated by the presence of nodular gypsum, and highest values of redox (V/Cr, Co/Al, and Fe/Al) and all paleoproductivity proxies. The barren interval may as a result of the deposition of the secondary gypsum in a reduced environment. Therefore, associated minerals such as calcite, dolomite, anhydrite and elements such as Ba, Zn, Ni, P, are enriched.

In the uppermost part of the section, two regressive cycles are evidenced by the deposition of the sand dominated facies (Laboun, 2009; Abbas et al., 2017; Hayton et al., 2017). This environment represents an oxic environment with high detrital influx and relatively low foraminiferal abundance compared with the offshore environment. Foraminiferal assemblages, which contain a high proportion of specimens with a coarsely agglutinated wall surface, are only recovered from the muddy part. The occurrence of a rough wall surface represents the available substrate to life and material to construct their wall.

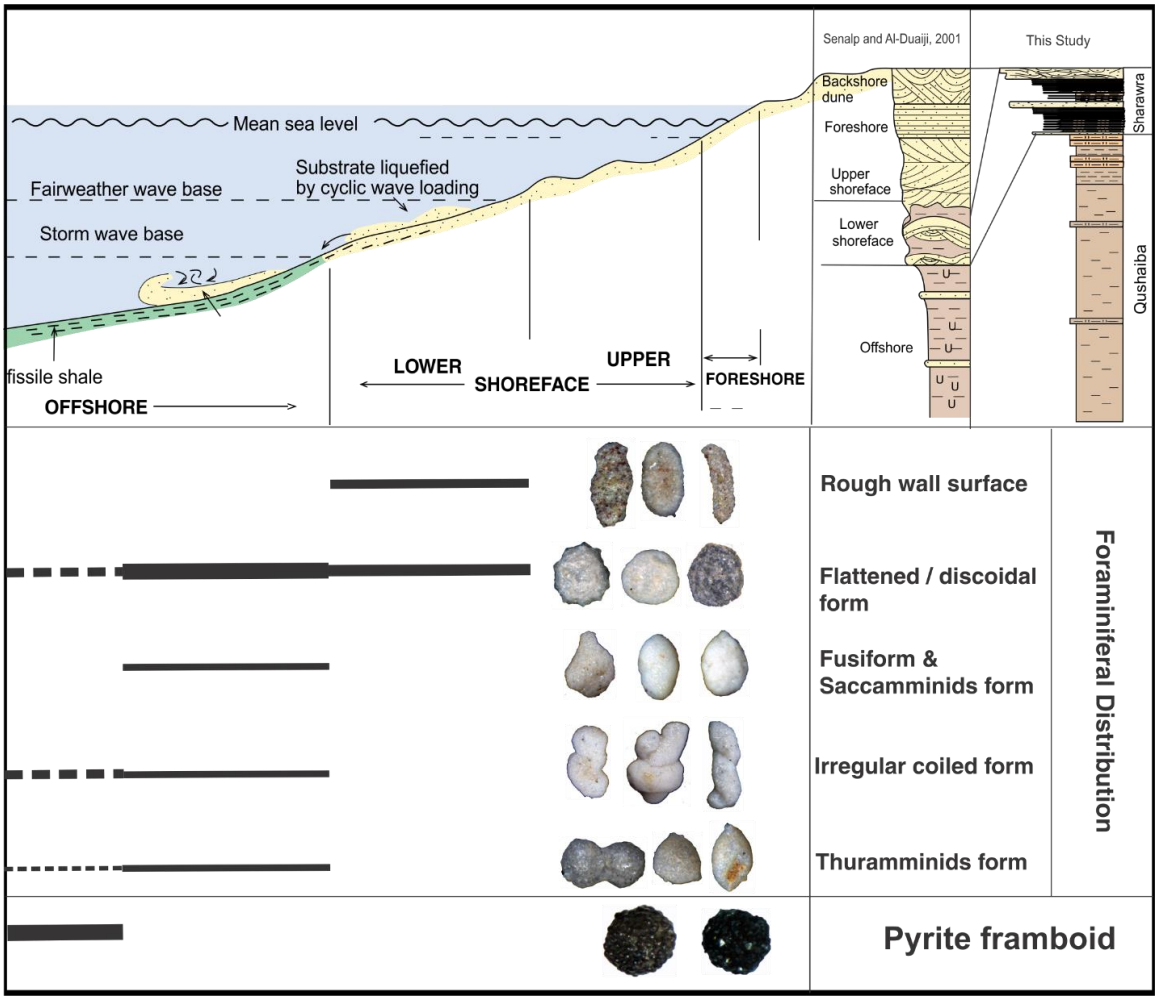

Figure 38: Paeloenvironmental model of the Aeronian Qusaiba Formation in the Qasim Region, based on sedimentology, foraminiferal biofacies, and framboidal pyrite contents. Sedimentary depositional model was modified after Senalp and Al Duaji (2001).

CHAPTER 7

CONCLUSIONS AND RECOMMENDATIONS

7.1 Conclusions

The Early Silurian foraminiferal assemblages documented from the Qusaiba Formation in the Old Qusaiba Town, Qasim Region, Saudi Arabia, represent the first recovered Silurian foraminifera from the Middle East as well as from a clastic setting on the Gondwanan paleocontinent. The recovered assemblage consists of 24 genera, 77 species, and are mostly dominated by monochambered forms which constitue >95% of the total specimens. Compared with the Silurian foraminifera studied across the globe, the Silurian foraminifera in this study potentially become the most diverse recovered foraminiferal ever recorded.

For the purpose of paleoenvironmental reconstruction, foraminiferal assemblages were classified into three morphogroups and five subgroups or morphotypes. The foraminiferal assemblages are comprised predominantly of forms with an epifaunal life habit. Analysis of the morphogroups alone cannot reveal the paleoenvironment, therefore, a wall texture classification has been carried out. Based on the wall texture, the Aeronian foraminifera can be classified into three groups, which are (1) rough, (2) thuramminids, and (3) smooth fine-grained wall texture. Rough wall textures characterize the lower shoreface environment, which is prone to high hydrodynamic energy. Meanwhile, the thuramminids wall texture is mostly found in a tranquil environment in the offshore, and fine smooth-grained wall texture distributed throughout all the different environments.

In compliment to the foraminiferal analysis, elemental composition acquired by geochemical identification had been carried out. Elemental analysis was performed for the interpretation of paleoredox, paleoproductivity, and detrital supply conditions. Those elements are V, Cr, Co, Fe, Mn, Mo as a redox proxy; P, Ni, Zn, Ba as a productivity proxy; and Ti, Zr, quartz, and clay minerals representing terrigenous influx. In addition, large size framboidal pyrite, which is > 65μm also applied for the paleo-oxygenation interpretation.

The paleoenvironment of the Lower Silurian gray-warm shale unit of the middle to upper Qusaiba Foramtion at the Old Qusaiba Village, Qasim Region, has been successfully reconstructed by applying integrated sedimentological, geochemical and foraminiferal analysis. Based on the graptolite content, the Lower Silurian succession is considered as Aeronian in age, belonging to the Lituograptus convolutus zone. The succession can be interpreted as deposited in dysoxic conditions at the base of the studied section, which was deposited in a deeper offshore environment, in oxic conditions of the shallower offshore environment in the middle part, and oxic conditions during the regressive event of the lower shoreface environment in the sand dominated uppermost part.

7.1 Recommendations for further study

Additional studies are required to be done in the future to overcome the limitations of this study. Therefore, the following recommendations are:

1. Conducting TOC, Th, U, analysis in compliment to the foraminiferal and elemental analysis for paleoenvironmental interpretation purposes.
2. Extending the foraminiferal investigation to both outcrops and the subsurface with the purpose of studying the known ranges of Ammobaculites-type forms and developing well-established a Silurian foraminiferal biozonation in Saudi Arabia.
3. Applying the foraminiferal biofacies for the purpose of biosteering after the Silurian foraminiferal biozonation has been established in Saudi Arabia.

REFERENCES

Abbas, M.A., Kaminski, M.A. & Dogan, A.U. 2017. Source, origin, and facies distribution of the Silurian Sharawra Formation, the Old Qusaiba Village, Central Saudi Arabia. *Journal of African Earth Sciences*, 130, 48–59.

Aldridge, R.J., Dorning, K.J., Hill, P.J., Richardson, J.B. & Siveter, D.J. 1979. Microfossil distribution in the Silurian of Britain and Ireland. In: Harris, A.L., Holland, C.H. & Leake, B.L. (Eds), *The Caledonides of the British Isles.* Scottish Academic Press, Edinburgh, for the Geological Society of London. pp. 433-438.

Algeo, T.J. & Rowe, H. 2012. Paleoceanographic applications of trace-metal concentration data. *Chemical Geology*, *324–325*, 6–18.

Abu-Ali, M.A., Franz, U.A., Shen, J., Monnier, F., Mahmoud, M.D., & Chambers, T.M. 1991. Hydrocarbon generation and migration in the Paleozoic sequence of Saudi Arabia. *Conference Proceedings of the Society of Petroleum Engineers 7th Middle East Oil Show*, 345–356.

Abu-Ali, M.A., Rudkiewicz, J.L.L., McGillivray, J.G. & Behar, F. 1999. Paleozoic petroleum system of central Saudi Arabia. *GeoArabia*, 4, 321–336.

Abu-Ali, M. & Littke, R., 2005, Paleozoic petroleum systems of Saudi Arabia: a basin modeling approach, *GeoArabia*, 10, 131-168.

Al-Hajri, S. & Paris, F. 1998. Age and palaeoenvironment of the Sharawra Member (Silurian of North-Eastern Saudi Arabia). *Geobios*, 31, 3–12.

Al-Laboun, A.A., 1986. Stratigraphy and hydrocarbon potential of the Paleozoic succession of both the Widyan and Tabuk basins, Arabia. In Halbouty, M. (Ed.), Future Petroleum Provinces of the World, American Association of Petroleum Geologists Memoir No. 50, pp. 373–394.

Al-Laboun, A.A., 1987. Unayzah Formation: a new Permo-Carboniferous unit in Arabia. *The American Association of Petroleum Geologists Bulletin*, 71, 29–38.

Al-Laboun, A. 2009. Tectonostratigraphy of the exposed Silurian deposits in Saudi Arabia. *Arabian Journal of Geosciences*, 2, 119–131.

Alsharhan, A.S. & A.E. M. Nairn, 1997, Sedimentary Basins and petroleum geology of the Middle East: Elsevier Science B.V., Amsterdam, 843 pp.

Aoudeh, S., Al-Hajri, S., 1995. Regional distribution and chronostratigraphy of the Qusaiba Member of the Qalibah Formation in the Nafud Basin, Northwestern Saudi Arabia. The Middle East Petroleum Geosciences 1. *Gulf PetroLink*, 143–154.

Bahafzallah, A., Jux, U. & Omara, S., 1981. Stratigraphy and facies of the Devonian Jauf Formation, Saudi Arabia. *Neues Jahrbuch für Geologie und Paläontologie, Monatschefte*, 1, 1-18.

Bell, K. N., Cockle, P., & Mawson, R. 2000. Agglutinated foraminifera (Silurian and Early Devonian) from borenore and Windellama, New South Wales. *Western Australian Museum Records, Supplement*, 58, 1–20.

Bernhard, J.M., 1986. Characteristic assemblages and morphologies of benthic foraminifera fromanoxic, organic-rich deposits: Jurassic through Holocene. *Journal of*

Foraminiferal Research, 16, 207–215.

Bond, D.P., & Wignall, P.B. 2010. Pyrite framboid study of marine Permian– Triassic boundary sections: a complex anoxic event and its relationship to contemporaneous mass extinction. *Geological Society of America Bulletin*, 122, 1265–1279.

Bosak, T., Lahr, D. J. G., Pruss, S. B., Macdonald, F. A., Dalton, L., & Matys, E. D. 2011. Agglutinated tests in post-Sturtian cap carbonates of Namibia and Mongolia. *Earth & Planetary Science Letters*, 308, 27–40.

Brady, H. B. 1879. Notes on the reticularian Rhizopoda of the "Challenger" expedition. 1. On new and little known arenaceous types. *Quarterly Journal of Microscopical Science*, 19, 20–63.

Brumsack, H. 2006. The trace metal content of recent organic carbon-rich sediments : Implications for Cretaceous black shale formation, *Palaeogeography, Palaeoclimatology, Palaeoecology, 232*, 344–361.

Bykova, E. V. 1961. Caradocian foraminifera of eastern Kazakhstan. *Izvestiia Akademii Nauk Kazakhskoj SSR*, 1–119.

Cantrell, D.L., Nicholson, P.G., Hughes, G.W., Miller,M.A., Buhlar, A.G., AbdelBagi, S.T., Norton, A.K., 2014. Tethyan petroleum systems of Saudi Arabia. In: Marlow, L., Kendall, C., Yose, L. (Eds.), Petroleum Systems of the Tethyan Region. American Association of Petroleum Geologists Memoir, 106, pp. 613 - 639.

Calvert, S.E., Pedersen, T.F., 1993. Geochemistry of recent oxic and anoxic marine sediments: implications for the geological record. Marine Geology 113, 67–88.

Cavalazzi, B., Barbieri, R., Cady, S.L., George, A.D., Gennaro, S., Westall, F., Lui, A., Canteri, R., Rossi, A.P., Ori, G.G., & Taj-Eddine, K. (2012) Iron- framboids in the hydrocarbon-related Middle Devonian Hollard Mound of the Anti-Atlas mountain range in Morocco: Evidence of potential microbial biosignatures. Sedimentary Geology, 263-264, 183–193.

Cetean, C. G., Bâlc, R., Kaminski, M. A., & Filipescu, S. 2011. Integrated biostratigraphy and palaeoenvironments of an upper Santonian - upper Campanian succession from the southern part of the Eastern Carpathians, Romania. *Cretaceous Research*, *32*, 575–590.

Cole, G. A., 1994, Graptolite-chitinozoan reflectance and its relationship to other geochemical maturity indicators in the Silurian Qusaiba Shale, Saudi Arabia. *Energy and Fuels*, 8, 1443–1459.

Cole, G. A. 1994a, Organic geochemistry of the Paleozoic petroleum system of Saudi Arabia, *Energy and Fuels*, 8, 1425–1442.

Cole, G. A., H. I. Halpern, & S. M. Aoudeh, 1994b, The relationships between iron-sulfur-carbon and gamma-ray response, Silurian basal Qusaiba Shale, northern Saudi Arabia, *Saudi Aramco Journal of Technology*, 9–19.

Conkin, J. E. 1961. Mississippian smaller foraminifera of Kentucky, southern Indiana, northern Tennessee, and southcentral Ohio. *Bulletins of American Paleontology*, 43, 131–368.

Conkin, J. E. & Conkin, B. M. 1964. Devonian Foraminifera: Part 1, The Louisiana

Limestone of Missouri and Illinois. *Bulletins of American Paleontology,* 47, 53–105.

Conkin, J. E., Conkin, B. M., & Pike, J. W. 1965. Mississippian foraminifera of the United States. Part 2 – The Hannibal Formation of northeastern Missouri and western Illinois. *Micropaleontology*, 11, 335–359.

Conkin, J. E., Conkin, B. M., & Canis, W. F. 1968. Mississippian foraminifera of the United States. Part 3 – The limestones of the Chouteau Group in Missouri and Illinois. *Micropaleontology*, 14, 133–178.

Conkin, J. E. & Conkin, B. M. 1981. Early Mississippian (Kinderhookian) smaller Foraminifera from the McCraney Limestone of Missouri and Illinois. University of Louisville. 15, 14.

Conkin, J. E. & Conkin, B. M. 1982. North American Paleozoic agglutinate foraminifera. In: Buzas, M. A., & Sen Gupta, B. K., *Foraminifera, notes for a short course*. University of Tennessee Department of Geological Sciences Studies in Geology, 6, 177–191.

Corliss, B.H., 1985. Microhabitats of benthic foraminifera within deep-sea sediments. *Nature*, 314, 435-438.

Corliss, B.H., & Chen, C. 1988. Morphotype patterns of Norwegian Sea deep-sea benthic foraminifera and ecological implications. *Geology*, 16, 716-719.

Crespin, I. 1958. *Permian Foraminifera of Australia. Bureau of Mineral Resources, Geology and Geophysics Bulletin*, 48, 1–207.

Crespin, I. 1961. Upper Devonian foraminifera from Western Australia. *Palaeontology*, 3, 397–409.

Culver, S. J. 1991. Early Cambrian Foraminifera fiom West Mica. *Science*, 254, 689–691.

Craigie, N.W. 2016. Chemostratigraphy of the Silurian Qusaiba Member, Eastern Saudi Arabia. *Journal of African Earth Sciences*, 113, 12-34.

Dixon, M., and Haig, D. W. 2004. Foraminifera and Their Habitats Within a Cool-Water Carbonate Succession Following Glaciation, Early Permian (Sakmarian), Western Australia. The Journal of Foraminiferal Research, 34(4), 308–324.

du Châtelet, E. A., Bout-Roumazeilles, V., Coccioni, R., Frontalini, F., Guillot, F., Kaminski, M. A., ... & Ventalon, S. 2013. Environmental control on shell structure and composition of agglutinated foraminifera along a proximal–distal transect in the Marmara Sea. *Marine Geology*, *335*, 114-128.

Dunn, P. H., Journal, S., May, N., & Dunn, P. H. 1942. Silurian foraminifera of the Mississippi Basin. *Journal of Paleontology*, 16, 317–342.

Dunnington, H.V., R. Wetzel, D.M. Morton, & R.C. Van Bellen, 1959, Iraq: Lexique Stratigraphique International, v. 3, Asie, fascicle 10a, *Centre National de la Recherche Scientique*, pp 1-133.

Eisenack, A. 1938. Neue Mikrofossilien des baltischen Silurs. I. *Palaeontologische Zeitschrift*, 19, 217–243.

Eisenack, A. 1954. Foraminiferen aus dem baltischen Silur. *Senckenbergiana Lethaea*, 35, 51–72.

Eisenack, A. 1969. Einige ordovizische und silurische Foraminiferen des baltischen Gebietes. *Palaontologische Zeitschrift*, 43, 199–204.

El-Khayal, A.A. 1987. Silurian graptolites from the Qusayba Shale (Llandovery) of central Saudi Arabia. *Bulletin of the Geological Society of Denmark*, 35, 125-133.

Føyn, S. & Glaessner, M. F. 1979. *Platysolenites*, other animal fossils, and the Precambrian–Cambrian transition in Norway. *Norsk Geologisk Tidsskrift*, 59, 25–46

Gagnier, P. Y., Blieck, A., Emig, C. C., Sempere, T., Vachard, D., & Vanguestaine, M. 1996. New paleontological and geological data on the Ordovician and Silurian of Bolivia. *Journal of South American Earth Sciences*, 9, 329–347.

Gallego-Torres, D., Reolid, M., Nieto-Moreno, V., and Martínez-Casado, F.J. 2015. Pyrite framboid size distribution as a record for relative variations in sedimentation rate: An example on the Toarcian Oceanic Anoxic Event in Southiberian Palaeomargin. *Sedimentary Geology*, 330, 59–73.

Gamero-Diaz, H., Miller, C. K., & Lewis, R. 2013. sCore: a mineralogy based classification scheme for organic mudstones. In *SPE Annual Technical Conference and Exhibition*. Society of Petroleum Engineers.

Gaucher, C. & Sprechmann, P. 1999. Upper Vendian skeletal fauna of the Arroyo de Soldado Group, Uruguay. *Beringeria* 23, 55–91.

Golonka, J., Krobicki, M., Pajak, J., Van Giang, N., & Zuchiewicz, W. 2006. Global plate tectonics and paleogeography of Southeast Asia. Kraków: Arkadia Publishers, Faculty of Geology, Geophysics and Environmental Protection, AGH University of Science & Technology, pp. 128.

Gnoli, M. & Serpagli, E. 1984. An unusually preserved foraminiferal association from the Upper Silurian – Lower Devonian beds in southwestern Sardinia. *Bolletino della*

Societá Paleontologica Italiana, 23, 211–220.

Grubbs, D. M. 1939. Fauna of the Niagaran nodules of the Chicago Area. Journal of Paleontology, 13(6), 543–560.

Gutschick, R. C. 1962. Arenaceous foraminifera from oncolites in the Mississippian Sappington Formation of Montana. *Journal of Paleontology*, 36, 1291–1304.

Gutschick, R. C. & Treckman, J. F. 1959. Arenaceous Foraminifera from the Rockford limestone of northern Indiana. *Journal of Paleontology*, 33, 229–250.

Gutschick, R. C., Weiner, J. L., & Young, L. 1961. Lower Mississippian arenaceous Foraminifera from Oklahoma, Texas, and Montana. *Journal of Paleontology*, 35, 1193–1221.

Haig, D., and Mory, A. J. 2016. Middle Permian (Roadian) Foraminifera from mudstone facies of the type Baker Formation, Southern Carnarvon Basin, Western Australia. Journal of the Royal Society of Western Australia, 99(2), 61-75.

Hayton, S., Rees, A.J. & Vecoli, M. 2017. A punctuated late Ordovician and early Silurian deglaciation and transgression: Evidence from the subsurface of northern Saudi Arabia. *American Association of Petroleum Geologists Bulletin*, 101, 863–886.

Helal, A.H. 1964: On the Occurrence of Lower Paleozoic Rock in the Tabuk Area, Saudi Arabia. *Neues Jahrbuch fur Geologie und Palaontologie Monatshefte*, 7, 391–414.

Hemleben, C., Mühlen, D., Olsson, R. K., & Berggren, W. A. 1991. Surface texture and the first occurrence of spines in planktonic foraminifera from the early Tertiary. *Geologisches Jahrbuch, 128*, 117-146.

Hemleben, C., & Olsson, R. K. 2006. Wall textures of Eocene planktonic foraminifera. *Atlas of Eocene Planktonic Foraminifera*, 47-66.

Holcová, K. 2002. Silurian and Devonian foraminifers and other acid-resistant microfossils from the Barrandian area. *Acta Musei Nationalis Pragae, Series B, Historia Naturalis*, 58, 83–140.

Holcová, K., & Slavík, L. 2013. The morphogroups of small agglutinated foraminifera from the Devonian carbonate complex of the Prague Synform, (Barrandian area, Czech Republic). *Palaeogeography, Palaeoclimatology, Palaeoecology*, *386*, 210–224.

İnan, S., Goodarzi, F., Schmidt Mumm, A., Arouri, K., Qathami, S., Ardakani, O.H., Inan, T., & Tuwailib, A.A., 2016. The Silurian Qusaiba Hot Shales of Saudi Arabia: An Integrated Assessment of Thermal Maturity. *International Journal of Coal Geology*, 159, 107–115.

İnan, S., Hakami, A., & Abu Ali, M. 2017. A Petroleum System and Basin Modeling Study of Northwest and East-Central Saudi Arabia: Effect of Burial History and Adjacent Rock Lithology on the Gas Potential of the Silurian Qusaiba Shales, in Mahdi A. AbuAli, Isabelle Moretti, and Hege M. Nordgard Bolas, eds., Petroleum Systems Analysis—Case Studies: *AAPG Memoir* 114, p. 1–35.

Ireland, H. A. 1966. Silurian arenaceous Foraminifera from subsurface strata of northeastern Kansas. *Micropaleontology*, 12, 215–234.

Ireland, H. A. 1956. Upper Pennsylvanian Arenaceous Foraminifera from Kansas. *Journal of Paleontology*, 30, 831–864.

Janjou, D., Halawani, M.A., Al-Muallem, M.S., Brosse, J.M., Becq- Giraudon, J.F., Dagain, J., Genna, A., Razin, P., Roobol, M.J., Shorbaji, H., Wyns, R., 1996a. Geologic map of the Tabuk quadrangle, sheet 28B, Kingdom of Saudi Arabia, Saudi Arabian Deputy Ministry for Mineral Resources. Jeddah, Geoscience Map GM-137.

Janjou, D., Halawani, M.A., Al-Muallem, M.S., Robelin, C., Brosse, J.-M., Courbouleix, S., Dagain, J., Genna, A., Razin, P., Roobol, M.J., Shorbaji, H., Wyns, R., 1996b. Geologic map of the Al Qalibah quadrangle, sheet 28C, Kingdome of Saudi Arabia (with text): Saudi Arabian Deputy Ministry for Mineral Resources. Jeddah, Geoscience Map GM-135.

Jarvis, I., Moreton, J., & Gerard, M. 1998. Chemostratigraphy of madeira abyssal plain miocene-pleistocene turbidites, site 950. *Proceedings of the Ocean Drilling Program: Scientific Results, 157*, 535-558.

Johnson, M. E. 2006. Relationship of Silurian sea-level fluctuations to oceanic episodes and events. *GFF*, *128,* 115–121.

Jones, R.W., and Charnock, M.A. 1985. “Morphogroups” of agglutinated foraminifera. Their life positions and feeding habits and potential applicability in (paleo) ecological studies. *Revue de Paleobiologie*, 4, 311-320.

Jones, B., & Manning, D. A. C. 1994. Comparison of geochemical indices used for the interpretation of palaeoredox conditions in ancient mudstones. *Chemical Geology, 111,* 111-129.

Jones, P.J. & T.E. Stump 1999. Depositional and Tectonic Setting of the Lower Silurian Hydrocarbon Source Rock Facies, Central Saudi Arabia. *American Association of Petroleum Geologists Bulletin,* 83, 314-332.

Kaminski, M.A., Kuhnt, W., 1995. Tubular agglutinated foraminifera as indicators of organic carbon flux. In: Kaminski, M.A., Geroch, S., Gasinski, M.A. (Eds.), Proceedings of the Fourth International Workshop on Agglutinated Foraminifera: Grzybowski Foundation Special Publication, 3, 141–144.

Kaminski, M.A., Gradstein, F.M. 2005. Atlas of Paleogene Cosmopolitan Deep-Water Agglutinated Foraminifera. Grzybowski Foundation Special Publication, 10,. 574+vii pp.

Kaminski, M.A., Silye, L., Kender, S., 2005. Miocene deep-water agglutinated Foraminifera from ODP Hole 909c: implications for the paleoceanography of the Fram Strait Area, Greenland Sea. *Micropaleontology,* 51, 373–403.

Kaminski, M. A., 2014. The year 2010 classification of the agglutinated foraminifera. *Micropaleontology,* 61, 89–108.

Kaminski, M. A. & Perdana, P. 2017a. Early Silurian Foraminifera from Saudi Arabia. In: Sotak et al. (eds), Tenth International Workshop on Agglutinated Foraminifera – Abstracts. Grzybowski Foundation Special Publication, 23, 51–52.

Kaminski, M. A. & Perdana, P. 2017b. New Foraminifera from the Lower Silurian Qusaiba Shale Formation of Saudi Arabia. *Micropaleontology,* 62, 59–66.

Kaminski, M. A., Henderson, A. S., Cetean, C. G., & Waskowska-Oliwa, A. 2009. A new family of agglutinated foraminifera: the Ammolagenidae n.fam., and the evolution of multichambered tests. *Micropaleontology*, 55, 487–494.

Kaminski, M. A., Setoyama, E., & Cetean, C. G. 2010. The Phanerozoic diversity of Agglutinated Foraminifera: Origination and Extinction rates. *Acta Paleontologia Polonica*, 55, 529–539.

Kaminski, M. A. 2014. The year 2010 classification of the agglutinated foraminifera. *Micropaleontology*, *60*, 89–108.

Kaminski, M. A., Ferretti, A., Messori, F., Papazzoni, C. A., & Sevastopulo, G. 2016. Silurian agglutinated foraminifera from the Dingle Peninsula, Ireland. *Bollettino degli Societa Paleontologica Italiana*, 55, 111–122.

Kender, S., Kaminski, M.A., Jones, R.W., 2008. Early to middle Miocene foraminifera from the deep-sea Congo Fan, offshore Angola. *Micropaleontology*, 54, 477–568.

Kircher, J. M. & Brasier, M. D. 1989. Cambrian to Devonian. In: Jenkins, G. D. & Murray, J. W. (eds), *Stratigraphical Atlas of Fossil Foraminifera, second edition.* British Micropalaeontological Society Series, 21–31.

Kuhnt, W., Moullade, M. & Kaminski, M.A., 1996, Ecological structuring and evolution of deep sea agglutinated foraminifera—a review. *Revue de Micropaléontologie*, 39, 271-281.

Konert, G., Afifi, A.M. & Al-Hajri, S.A., H. Droste, 2001, Paleozoic Stratigraphy and Hydrocarbon Habitat of the Arabian Plate. *Geoarabia*, 6, 407-442.

Lash, G. G. 2017. A multiproxy analysis of the Frasnian-Famennian transition in western.

Palaeogeography, Palaeoclimatology, Palaeoecology, *473*, 108–122.

Le Herisse, A., H. Al-Tayyar, & J. G. L. A. van der Eem, 1995, Stratigraphic and paleogeographic significance of Silurian acritarchs from Saudi Arabia, in B. Owens, H. A. Al-Tayyar, and J. G. L. A. van der Eem, eds., The Paleozoic palyno-stratigraphy of the Kingdom of Saudi Arabia. *Review of Paleobotany and Palynology*, 89, 49–74.

Le Hérissé, A., Molyneux, S.G. & Miller, M.A., 2015, Late Ordovician to early Silurian acritarchs from the Qusaiba-1 shallow core hole, central Saudi Arabia. *Review of Palaeobotany and Palynology*, 212, 22-59.

Lewan, M.D., & Maynard, J.B. 1982. Factors controlling enrichment of vanadium and nickel in the bitumen of organic sedimentary rocks. *Geochimica et Cosmochimica Acta*, 46, 2547-60.

Loeblich, A. R. and Tappan, H. 1957. Eleven New Genera of Foraminifera. Bulletin United States National Museum. 215: 223-232.Loeblich, A.R. & Tappan, H. 1987. Foraminiferal Genera and their Classification. 970 pp + 847 pl. Van Nostrand Reinhold, New York.

Loeblich, A.R. and Tappan, H. 1989. Implications of wall composition and structure in agglutinated foraminifera. *Journal of Paleontology*, 63, 769–777.

Loeblich, A.R. and Tappan, H. 1992. Present status of foraminiferal classification. In: Takayanagi, Y. & Saito, T., Eds., Studies in benthic foraminifera, 93–102. Tokyo: Tokai University Press.

Loeblich, A.R. and Tappan, H. 1994. Foraminifera of the Sahul Shelf and Timor Sea. Washington, DC: Cushman Foundation for Foraminiferal Research Special Publication 31, pp. 661.

Loydell, D. K. 1998. Early Silurian sea-level changes. *Geological Magazine*, 447–471.

Lüning, S., Craig, J., Loydell, D.K., Štorch, P. & Fitches, B., 2000. Lower Silurian hot shales' in North Africa and Arabia: regional distribution and depositional model. *Earth-Science Reviews*, 49, 121-200.

Mahmoud, M. D., D. Vaslet, & M. I. Husseini, 1992, The Lower Silurian Qalibah Formation of Saudi Arabia: an important hydrocarbon source rock: *American Association of Petroleum Geologists Bulletin*, 76, 1491–1506.

Malec, J. 1992. Arenaceous Foraminifera from Lower-Middle Devonian Boundary Beds of western part of the Góry Świętokrzyskie Mts. *Annales Societatis Geologorum Poloniae*, 62, 269–287.

McClellan, W. A. 1966. Arenaceous foraminifera from the Waldron Shale (Niagaran) of southeast Indiana. *Bulletins of American Paleontology*, 50, 447–518.

McClellan, W. A. 1973 Siluro-Devonian microfaunal biostratigraphy in Nevada. *Bulletins of American Paleontology*, 62, 235–375.

McClure, H.A., 1988. Chitinozoan and acritarch assemblages, stratigraphy and bio-geography of the Early Palaeozoic of Northwest Arabia. *Review of Palaeobotany and Palynology*, 56, 41–60.

McGillivray, J.G. & Al-Husseini, M.I., 1992. The Paleozoic Petroleum Geology of Central Saudi Arabia. *American Association of Petroleum Geologists Bulletin*, 76, 1473-1490.

Melvin, J., 2015. Lithostratigraphy and depositional history of Upper Ordovician and low-ermost Silurian sediments recovered from the Qusaiba-1 shallow core hole, Qasimregion, central Saudi Arabia. *Review of Palaeobotany and Palynology*, 212, 3–21.

Merinero, R., Lunar, R., Somoza, L., Díaz-del-Río, V., & Martínez-Frías, J. 2009. Nucleation, growth and oxidation of framboidal pyrite associated with hydrocarbon-derived submarine chimneys: lessons learned from the Gulf of Cadiz. *European Journal of Mineralogy*, 21, 947–961.

Merinero, R., Cárdenes, V., Lunar, R., Boone, M. N., & Cnudde, V. 2017. Representative size distributions of framboidal, euhedral, and sunflower pyrite from high-resolution X-ray tomography and scanning electron microscopy analyses. *American Mineralogist, 102*, 620–631.

Mikhalevich, V. I. 2004. On the heterogeneity of the former Textulariina (Foram- inifera). In: Bubik, M. & Kaminski, M. A. Eds., Proceedings of the Sixth International Workshop on Agglutinated Foraminifera, 317–349. Kraków: Grzybowski Foundation. Special Publication, 8.

Miller, M., Melvin, J., 2005. Significant new biostratigraphic horizons in the Qusaiba Member of the Silurian Qalibah Formation of central Saudi Arabia, and their sedimentological expression in a sequence stratigraphic context. *GeoArabia* 10, 49–92.

Morais, L., Fairchild, T. R., Lahr, D.J.G., Rudnitzki, I. D., Schopf, J. W., Garcia, A. K., Kudryavtsev, A. B., & Romero, G. R. 2017. Carbonaceous and siliceous Neoproterozoic vase-shaped microfossils (Urucom Formation, Brazil) and the question of early protistan biomineralization. *Journal of Paleontology*, 91, 393–406.

Moreman, W. L. 1930. Arenaceous Foraminifera from Ordovician and Silurian Limestones of Oklahoma. *Journal of Paleontology*, 4, 42–59.

Moreman, W. L. 1933. Arenaceous Foraminifera from the Lower Paleozoic Rocks of Oklahoma. Journal of Paleontology. 7(4), 393-397.

Moreman, W. L. 1935. Arenaceous Foraminifera from the Lower Paleozoic Rocks of Oklahoma. *Journal of Paleontology*, 7, 393–397.

Mound, M. C. 1968. Arenaceous Foraminiferida and zonation of the Silurian rocks of northern Indiana. Department of Natural Resources, Geological Survey. Bulletin Indiana Geological Survey., Bloomington, 38, 1–126.

Murray, J.W., Alve, E., & Jones, B.W. 2011. A new look at modern agglutinated benthic foraminiferal morphogroups: their value in palaeoecological interpretation. *Palaeogeography, Palaeoclimatology, Palaeoecology*, 309, 229-241.

Nagy, J. 1992. Environmental significance of foraminiferal morphogroups in Jurassic North Sea deltas. *Palaeogeography, Palaeoclimatology, Palaeoecology*, 95, 111-134.

Nagy, J., Gradstein, F.M., Kaminski, M.A., & Holbourn, A.E., 1995. Foraminiferal morphogroups, palaeoenvironments and new taxa from Jurassic to Cretaceous strata of Thakkhola, Nepal. In: Kaminski, M.A., Geroch, S., Gasiński, M.A. (Eds.),

Proceedings of the Fourth International Workshop on Agglutinated Foraminifera. Grzybowski Foundation Special Publication, v.3, 181–209.

Nagy, J., Reolid, M., & Rodríguez-Tovar, F. J. 2009. Foraminiferal morphogroups in dysoxic shelf deposits from the Jurassic of Spitsbergen. *Polar Research*, 28, 214-221.

Nestell, G. P., Pour, M. G., Jahangir, H., Tolmacheva, T. Y., Popov, L. E., Hunt, A., & Chakrabarty, P. (2016). First Middle Ordovician (Darriwilian) Foraminifers from the Alborz Mountains, northern Iran. *Micropaleontology*, 62(6), 415–427.

Ohfuji, H., & Rickard, D. 2005. Experimental syntheses of framboids—a review. *Earth Science Reviews*, 71, 147–170.

Olempska, E., & Olempska, E. 1983. The uppermost Devonian foraminifers. of the Świętokrzyskie (Holy Cross) Mts., Poland. *Acta Palaeontologica Polonica*, 28(3–4), 393–416.

Olsson, R.K., Hemleben, C., Berggren, W. A., Liu, C. 1992. Wall texture classification of planktonic foraminifera genera in the Lower Danian. *Journal of Foraminiferal Research*, *22*, 195–213.

Paris, F., Verniers, J., Al-Hajri, S., & Al-Tayyar, H., 1995. Biostratigraphy and palaeogeographic affinities of early Silurian chitinozoans fromSaudi Arabia. *Review of Palaeobotany and Palynology*, 89, 75–90.

Paris, F.,Miller, M., Al-Hajri, S., Zalasiewicz, J., & Williams, M., 2008. Aeronian and Telychian Chitinozoans from Central Saudi Arabia. IPC, Bonn, pp. 215.

Paris, F., Verniers, J., Miller, M., Al-Hajri, S., Melvin, J., Wellman, C., 2015. Late Ordovician– earliest Silurian chitinozoans fromthe Qusaiba-1 core hole, (North Central Saudi Ara- bia) and relation to the Hirnantian glaciation. *Review of Palaeobotany and Palynology,* 212, 60–84.

Peckmann, J., & Thiel, V. 2004. Carbon cycling at ancient methane seeps. *Chemical Geology*, 205, 443–467.

Plummer, H. J. 1945. Smaller Foraminifera in the Marble Falls, Smithwick, and lower Strawn strata around the Llano uplift in Texas. *Bulletin University of Texas Bureau of Economic Geology and Technology,* 4401, 209–271.

Powers, R. W., 1968, Lexique stratigraphique international, Asie, Fasc. 10.B1, Saudi Arabia: *Centre National de la Recherche Scientifique*, 3, 177.

Powers, R. W., L. F. Ramirez, C. D. Redmond, & E. L. Elberg, Jr., 1966, Geology of the Arabian Peninsula: U.S. Geological Survey, Professional Paper 560D, pp. 1–147.

Raiswell, R, Buckley, F, Berner, R.A., & Anderson T.F. 1988. Degree of pyritization of iron as a paleoenvironmental indicator of bottom-water oxygenation. *Journal of Sedimentary Petrology*, 58, 812-19.

Reolid, M., Rodríguez-Tovar, F.J., Nagy, J., Olóriz, F. 2008a. Benthic foraminiferal morphogroups of mid to outer shelf environments of the Late Jurassic (Prebetic Zone, southern Spain): characterization of biofacies and environmental significance. *Palaeogeography Palaeoclimatology Palaeoecology*, 261, 280–299.

Reolid, M., Nagy, J., Rodríguez-Tovar, F. J., & Olóriz, F. 2008b. Foraminiferal Assemblages as Palaeoenvironmental Bioindicators in Late Jurassic Epicontinental Platforms: Relation with Trophic Conditions. *Acta Palaeontologica Polonica*, 53, 705–722

Reolid, M., Rodríguez-Tovar, F.J., Marok, A. & Sebane, A., 2012. The Toarcian oceanic anoxic event in the Western Saharan Atlas, Algeria (North African paleomargin): Role of anoxia and productivity. *Geological Society of America Bulletin*, 124, 1646-1664.s

Reolid, M., Chakiri, S., & Bejjaji, Z. 2013. Adaptative strategies of the Toarcian benthic foraminiferal assemblages from the Middle Atlas (Morocco): Palaeoecological implications. *Journal of African Earth Sciences*, 84, 1-12.

Said, R. and R.A. Eissa. 1969. Some microfossils from Upper Paleozoic rocks of western coastal plain of Gulf of Suez region, Egypt. Proceedings of the 3rd African Micropaleontology Colloquium, Cairo, 1, 337-383.

Schmidt Mumm, A. & İnan. S. 2016. Raman Spectroscopic determination of Organic Maturity using Graptolites. *International Journal of Coal Geology*, *162*, 96-107.

Scott, D. B., Medioli, F., & Braund, R. 2003. Foraminifera from the Cambrian of Nova Scotia: The oldest multichambered foraminifera. *Micropaleontology*, 49, 109–126.

Senalp, M., & Al-Duaiji, A. A. 2001. Qasim formation: Ordovician storm-and tide-dominated shallow-marine siliciclastic sequences, Central Saudi Arabia. *GeoArabia*, *6*(2), 233–268.

Setoyama, E. 2012. Late Cretaceous Foraminifera from the northern proto Atlantic – Arctic Seaway: Biostratigraphy, Palaeoenvironment, Palaeobiogeography. PhD Thesis, Instytut Nauk Geologicznych Polskiej Akademii Nauk.

Setoyama, E., Radmacher, W., Kaminski, M.A., & Tyszka, J. 2013. Foraminiferal and palynological biostratigraphy and biofacies from a Santonian–Campanian submarine fan system in the Vøring Basin (offshore Norway). *Marine and Petroleum Geology*, 43, 396-408.

Sharland, P.R., Archer, R., Casey, D.M., Davies, R.B., Hall, S.H., Heward, A.P., Horbury, A., & Simmons, M.D. 2001. Arabian plate sequence stratigraphy. GeoArabia Special Publication, 2, pp. 370.

Steemans, P., Higgs, K., & Wellman, C.H., 2000. Cryptospores and trilete spores from the Llandovery, NYYM-2 borehole, Saudi Arabia. In: Al-Hajri, S., Owens, B. (Eds.), Stratigraphic palynology of the Palaeozoic of Saudi Arabia. GeoArabia Special Publication 1, pp. 92–115.

Stewart, G. A., Priddy, R. R., Stewart, G. A., & Priddy, R. R. 1941. Arenaceous Foraminifera from the Niagaran Rocks of Ohio and Indiana, *Journal of Paleontology*, 15, 366–375.

Štorch, P., & Massa, D. 2006. Middle Llandovery (Aaeronian) graptolites of the Western Murzuq Basin and Al Qarqaf Arch Region, South-West Libya. *Palaeontology*, 49, 83–112.

Takahashi, S., Yamasaki, S.I., Ogawa, K., Kaiho, K. & Tsuchiya, N. 2015. Redox conditions in the end-Early Triassic Panthalassa. *Palaeogeography, Palaeoclimatology, Palaeoecology*, 432, 15–28.

Tribovillard, N., Algeo, T., Lyons, T., & Riboulleau, A., 2006, Trace metals as palaeoredox and palaeoproductivity proxies: An update. *Chemical Geology*, 232, 12–32.

Tyszka, J., 1994. Response of Middle Jurassic benthic foraminiferal morphogroups to dysoxic/anoxic conditions in the Pieniny Klippen Basin, Polish Carpathians. *Palaeogeography, Palaeoclimatology, Palaeoecology*,110, 55–81.

Tyszka, J., & Kaminski, M.A., 1995. Factors controlling the distribution of agglutinated foraminifera in Aalenian–Bajocian dysoxic facies (Pieniny Klippen Belt, Poland). In: Kaminski, M.A., Geroch, S., Gasiński, M.A. (Eds.), Proceedings of the Fourth International Workshop on Agglutinated Foraminifera. Grzybowski Foundation Special Publication, 3, 271–291

Vaslet, D., 1987. The Paleozoic (pre–Late Permian) of central Arabia and correlations with neighboring regions: Ministry of Petroleum and Mineral Resources, Technical Record BRGM-TR-07-2, p. 161.

Vaslet, D., Kellogg, K. S., Berthiaux, A., LeStrat, P., & Vincent, P. L. 1987. Explanatory notes to the geologic map of the Baq'a Quadrangle, sheet 27F, Kingdom of Saudi Arabia: Ministry of Petroleum and Mineral Resources, p. 45.

Ver Straeten, C.A., Brett, C.E., & Sageman, B.B., 2011. Mudrock sequence stratigraphy: a multi-proxy (sedimentological, paleobiological and geochemical) approach,

Devonian Appalachian Basin. *Palaeogeography Palaeoclimatology Palaeoecology*, 304, 21–53.

Wang, P., Huang, Y., Wang, C., Feng, Z., & Huang, Q. 2013 Pyrite morphology in the first member of the Late Cretaceous Qingshankou formation, Songliao Basin, northeast China. *Palaeogeography, Palaeoclimatology, Palaeoecology*, 385, 125–136.

Wei, H., Algeo, T.J., Yu, H., Wang, J., Guo, C., & Shi, G. 2015 Episodic euxinia in the Changhsingian (late Permian) of South China: Evidence from framboidal pyrite and geochemical data. *Sedimentary Geology*, 319, 78–97.

Wignall, P.B., & Myers, K.J., 1988, Interpreting the benthic oxygen levels in mudrocks: A new approach. *Geology*, 16, 452–455.

Wignall, P.B., Newton, R., & Brookfield, M.E. 2005 Pyrite framboid evidence for oxygen-poor deposition during the Permian–Triassic crisis in Kashmir. *Palaeogeography, Palaeoclimatology, Palaeoecology*, 216, 183–188.

Wilkin, R.T., Barnes, H.L., & Brantley, S.L. 1996. The size distribution of framboidal pyrite in modern sediments: an indicator of redox conditions. *Geochimica et Cosmochimica Acta*, 60, 3897–3912.

Williams, M., Zalasiewicz, J., Boukhamsin, H., & Cesari, C. 2016. Early Silurian (Llandovery) graptolite assemblages of Saudi Arabia: Biozonation, palaeoenvironmental significance and biogeography. *Geological Quarterly*, 60 (1), 3–25.

Yilmaz, I.O., Altiner, D., Tekin, U.K., Tuysuz, O., Ocakoglu , F., & Acikalin, S., 2010, Cenomanian–Turonian oceanic anoxic event (OAE2) in the Sakarya Zone, northwestern Turkey: Sedimentological, cyclostratigraphic, and geochemical records: *Cretaceous Research*, 31, 207–226.

Zalasiewicz, J., Williams, M., Miller, M., Page, A., & Blackett, E., 2007. Early Silurian (Llandovery) graptolites from Central Saudi Arabia: first documented record of Telychian faunas from the Arabian Peninsula. *GeoArabia* 12, 15–36.

APPENDICES

A. Systematic Palaeontology

The higher systematics of the agglutinated foraminifera utilized in this study are taken from the updated classification of Kaminski (2014), while the taxonomy of agglutinated foraminiferal species is based to a large extent on the classic papers of Moreman (1930, 1935), Ireland (1939), Grubbs (1939), Stewart and Priddy (1941), and Dunn (1942), as well as the taxonomic monographs of Conkin (1961), McClellan (1966), Loeblich and Tappan (1987), and Holcová (2002). New taxa from the Qusaiba shale were described by Kaminski and Perdana (2017b).

Class FORAMINIFERA d'Orbigny, 1826
Order ASTRORHIZIDA Lankester, 1885
Suborder ASTRORHIZINA Lankester, 1885
Family RHABDAMMINIDAE Brady, 1884
Genus *Rhabdammina* M. Sars in Carpenter, 1869

Rhabdammina trifurcata Moreman, 1933
Fig. 6A.
1933 *Rhabdammina trifurcata* sp.nov.; Moreman 1933: 394, pl. 47: 1 2.
Material.—Five specimens from three samples.
Remarks.—Some of our specimens exhibit different diameter size of the arms, which sometimes possesses one arm, and two smaller identical arms.
Stratigraphic range.—Upper Ordovician to Silurian.
Geographic distribution.—This species was first recovered from Oklahoma USA (Moreman 1933), and also has been reported from the Silurian succession in New South Wales, Australia (Bell et al. 2000).

Family BATHYSIPHONIDAE Avnimelech, 1952
Genus *Bathysiphon* Sars, 1872
Type species. Bathysiphon filiformis G.O. & M. Sars, 1872

Bathysiphon sp. 1

Fig. 6B, C.

Type horizon: Qusaiba shale early Silurian (Aeronian).

Type locality: Old Qusaiba Town, Qasim Region Saudi Arabia.

Material.— 26 specimens from eight samples.

Dimensions.—Length: 156.3 to 212.5 μm, width: 43.75 to 187.5 μm

Description.—Tubular monothalamous, with slightly smaller diameter at the initial stage and constant toward the end. Apertures located at both ends. Wall composed of fine silica particles.

Remarks.—All of our specimens show truncation of the test due to preservation processes that affect the fragile test.

Bathysiphon sp. 2

Fig. 6D.

Type horizon: Early Silurian (Aeronian), Qusaiba Formation.

Type locality: Old Qusaiba Village, Qasim Region, Saudi Arabia.

Material.— A single specimen.

Dimensions.— 430 μm in length and 218.75 μm in width

Description.— Test free, elongate, monothalamous form, unchanging in diameter. Aperture most probably at both ends; wall thick, made of fine quartz grains.

Remarks.— Our specimen is broken, due to poor degree of preservation. This form is rare in the middle part of the succession.

Bathysiphon sp. 3

Fig. 6E, F.

Type horizon: Early Silurian (Aeronian), Qusaiba Formation.

Type locality: Old Qusaiba Village, Qasim Region, Saudi Arabia.

Material.—Nine specimens from five samples.

Dimensions.—156.3 to 656.3μm 120 to 218.74 μm in width

Description.—Test free, tubular unbranching form, with constant diameter, aperture most probably situated at both ends of the tube; wall thin, composed of finely agglutinated materials, may have a mottled surface.

Remarks.—Specimens are broken, due to the fragile nature of the *Bathysiphon* body. Individual test vary in size.

Family HIPPOCREPINELLIDAE Loeblich and Tappan, 1984

Genus *Amphitremoida,* Eisenack, 1938

Type species. Amphitremoida citroniforma Eisenack, 1938

Amphitremoida citroniforma Eisenack, 1954

Fig. 6G–I.

1954 *Amphitremoida citroniforma* sp. nov.; Eisenack 1954: 55, pl. 3: 14–16; pl. 4: 12–13.

Material.—242 specimens from 13 samples.

Remarks.—Some of our specimens compare well to the description of Eisenack (1954), and others a have depression lateral to the length of the test. *Amphithremoida citroniforma* is one of the most common foraminifera recoverable from the middle part of our succession.

Stratigraphic range.—Upper Ordovician to Silurian.

Geographic distribution.—This species was first recovered from the Samland Peninsula, East Prussia (Eisenack 1938) and the description was updated utilizing samples from the Lyckholm Formation, Estonia (Eisenack 1954).

Amphitremoida eisenacki Conkin and Conkin, 1964

Figs. 6J–M.

1964 *Amphitremoida eisenacki* sp. nov; Conkin and Conkin 1964: 7, pl. 12: 8–l 0.

Material.— 22 specimens two sample..

Remarks: Compare to the specimens described by Conkin and Conkin (1964) from the Devonian of Louisiana, these specimens have a wider test in the middle stage of the chamber. Some species exhibit a truncation in the aperture end, slightly compressed. Wall composed of medium to coarse particles.

Stratigraphic range: Aeronian (Silurian) to Devonian

Geographic distribution: This species was first described by Conkin and Conkin (1964) from the Lousiana (USA).

Amphitremoida sp. 1

Fig. 6O–P.

Type horizon: Qusaiba shale early Silurian (Aeronian).

Type locality: Old Qusaiba Town, Qasim Region, Saudi Arabia.

Material.—22 specimens four samples.

Dimensions.—150 to 212.5 μm in length 106.25 to 125 μm in width.

Description.—Test free, fusiform to slightly discoidal, flattened, comprised of a single chamber with two rounded tube apertures situated at the opposite ends of the test. Apertures are slightly produced and surrounded by a low collar. Test wall composed of rough siliceous grains, colour pale rusty white.

Remarks.—The features distinguishing this species from *Amphitremoida eisenacki* Conkin and Conkin, 1964, are the more compressed test shape with distinctly rounded apertures. It differs from *Thurammina forstei* Dunn, 1942 in its more flattened form, with a thick wall and medium grain size of the agglutinated particles.

Amphitremoida sp. 2

Fig. 6Q1, 6Q2.

Type horizon: Qusaiba shale early Silurian (Aeronian).

Type locality: Old Qusaiba Town, Qasim Region Saudi Arabia.

Material.— A single specimen.

Dimensions.—Length: 309.2 μm, width: 125 μm.

Description. — Elongated, slender monothalamous, slightly tapering at both ends; test somewhat bent at the center, possessing two apertures situated at each end of the tapering part. Wall agglutinated of fine siliceous particles, surface smooth.

Remarks.—This species is close to *Bathysiphon* and *Stegnammina* in shape. It differs in having two apertures.

Amphitremoida sp. 3

Fig 6N.

Type horizon: Early Silurian (Aeronian), Qusaiba Formation.

Type locality: Old Qusaiba Village, Qasim Region, Saudi Arabia.

Material.—17 specimens from three samples.

Dimensions.—length: 280.94 to 350 μm, width: 125 to 150 μm.

Description.—Test free, fusiform, compressed laterally, possessing two apertures located at both ends, wall thin, made up of medium to coarse quartz grains with a rough surface.

Remarks.—This species differs from the other *Amphetremoida* species in possessing an almost perfectly fusiform shape, which is symmetrical with respect to the axial line. Moreover, this species also exhibits lateral compression.

Suborder SACCAMMININA Lankester 1885

Family STEGNAMMINIDAE Moreman 1930

Genus *Blastammina* Eisenack, 1932

Type species. Blastammina polymorpha Eisenack, 1932

Blastammina vulgaris Bykova, 1961

Figs. 6R–T.

1961 *Blastammina vulgaris* sp. nov; Bykova 1961: 21–22, pl 1: 1–5.

Material.— Four specimens from one sample.

Remarks.— These specimens do not have a visible aperture, and most closely resemble *Blastammina vulgaris* described by Bykova (1961).

Stratigraphic range.— Ordovician (Caradocian) (Bykova 1961) to Silurian (Aeronian) (this study).

Geographic distribution. — First described from the Caradocian of north Kazakhstan by Bykova (1961).

Genus *Ceratammina* Ireland, 1939

Type species. Ceratammina cornucopia Ireland, 1939

Ceratammina cornucopia Ireland, 1939

Figs. 7A, B.

1939 *Ceratammina cornucopia* sp. nov; Ireland 1939: pl. A: 31–32.

Material.—Eight specimens from seven samples.

Remarks.—Our specimens closely agree with the holotype described by Ireland (1939).

Stratigraphic range.—The known stratigraphic interval is Silurian to Devonian.

Geographic distribution.—This species is reported from North America and Saudi Arabia.

Ceratammina sp. 1

Fig 7C.

Type horizon: Qusaiba shale early Silurian (Aeronian).

Type locality: Old Qusaiba Town, Qasim Region, Saudi Arabia.

Material.—One specimen.

Dimensions.—300 μm in length and 212 μm in width.

Description.—Test free, monothalamous, chamber size increasing gradually at the initial end, and abruptly broader and crooked at about 1/3 the length to the end of the chamber; aperture not recognized; wall made of fine agglutinated grains.

Remarks.—Our specimen is placed in the genus *Ceratammina* in accordance to its shape, which best resembles *Ceratammina cornucopia*, but it differs in having an abrupt bend and in the larger size of the later stage.

Ceratammina sp. 2

Figs. 7D, E.

Type horizon: Early Silurian (Aeronian), Qusaiba Formation.

Type locality: Old Qusaiba Village, Qasim Region, Saudi Arabia.

Material.—Three specimens from three samples.

Dimensions.— Specimens range from 350 µm to 687.5 µm in length, and 175 µm to 350 µm in diameter across the tubular chamber.

Description. — Test free, elongated, with undivided chamber, uniform test size, somewhat bent, exhibiting a nipple like shape in the early portion of the test. Aperture terminal. Wall constructed of medium to coarse siliceous particles.

Remarks. — This species is similar to *Ceratammina cornucopia*, which differs in having a nipple like shape in the early portion.

Genus *Raibosammina* Moreman, 1930

Type species. Raibosammina mica Moreman, 1930

Raibosammina aspera Moreman, 1930

Fig 7F.

1930 *Raibosammina aspera* sp. nov.; Moreman 1930; 50, pl. 6: 13–15.

Material.—Two specimens from two samples.

Remarks.—Our specimens compare well to the holotype illustrated by Moreman (1930), but have a smoother wall surface.

Stratigraphic range.—Late Ordovician (Moreman 1930) to Silurian (this study).

Geographic distribution.—This species is reported from North America and Saudi Arabia.

Genus *Stegnammina* Moreman, 1930

Type species. Stegnammina cylindrica Moreman, 1930

Stegnammia contorta McClellan, 1966

Fig. 7G, H.

1966 *Stegnammia contorta* sp. nov.; McClellan 1966: 476, pl. 36: 17a, b; pl. 40: 17a, b.

Material.—52 specimens from ten samples.

Remarks.—Our specimens conform well with the McClellan (1966) species.

Stratigraphic range.—Silurian.

Geographic distribution.—This species was first described from Indiana (USA) (McClellan 1966).

Stegnammina elongata Ireland, 1939

Fig. 7I–K.

1939 *Stegnammina elongata* sp. nov.; Ireland 1939: 194, gr. A: 17

Material.—113 specimens from 12 samples.

Remarks.—The Ireland (1939) specimen is identical to ours. Some specimens are somewhat curved.

Stratigraphic range.— Silurian (Aeronian) to Devonian.

Geographic distribution.—This species was first reported from Oklahoma (USA) (Ireland 1939).

Stegnammina sp. 1

Fig. 7L–N.

Type horizon: Qusaiba shale early Silurian (Aeronian).

Type locality: Old Qusaiba Town, Qasim Region Saudi Arabia.

Material.—34 specimens from five samples.

Dimensions.—212.5 to 625 μm in length and 93.75 to 125 μm in width.

Description.—Test free, unilocular, tubular form with constant dimensions, slightly bent at the later stage. Test slightly compressed, aperture not visible, test wall constructed of medium to coarse silica particles.

Remarks.—These specimens resemble *Stegnammina contorta* Moreman, but differ in having a compressed test.

Stegnammina sp. 2

Fig. 7O.

Type horizon: Qusaiba shale early Silurian (Aeronian).

Type locality: Old Qusaiba Town, Qasim Region Saudi Arabia.

Material.—One specimen.

Dimensions.—337.5 μm in length and 187.5 μm in width.

Description.—Test free, rhomboid in outline, monothalamous, laterally compressed; aperture not visible; wall agglutinated, constructed by fine quartz particles.
Remarks.—This specimen is placed into *Stegnammina* because of its shape and the lack of a distinct aperture, which distinguishes it from the single aperture observed in *Saccammina* and *Lagenammna.*

Stegnammina sp. 3
Fig. 7P.
Type horizon: Early Silurian (Aeronian), Qusaiba Formation.
Type locality: Old Qusaiba Village, Qasim Region, Saudi Arabia.
Material.—31 specimens from six samples
Dimensions.—281.25 to 500 μm in length and 156.25 to 250 μm in width.
Description.—Test free, elongate monothalamous form, chamber constant to tapering at both ends; no aperture present, constructed of fine grain silica materials.
Remarks. —The distinguishing features of this species compared with other species of *Stegnammina* is the ratio between the length and width of the test of about 2:1.

Stegnammina sp. 4
Fig. 7Q.
Type horizon: Early Silurian (Aeronian), Qusaiba Formation.
Type locality: Old Qusaiba Village, Qasim Region, Saudi Arabia.
Material.—130 specimens from six samples.
Dimensions.—162.5 to 400 μm in length and 93.75 to 118.75 μm in width.
Description.—Test free, elongated, monothalamous, slightly flattened, somewhat tapering on one side, showing depressions in center of the test parallel to the long axis, apparently thicker at the periphery of the test; no aperture visible; agglutinated wall of medium to coarse materials with a rough surface.
Remarks.—This species is probably a member of the genus *Stegnammina* due to its elongated shape and the absence of an aperture, and its characteristic flattened test.

Genus *Thuramminoides* Plummer, 1945

Type species. *Thuramminoides sphaeroidalis* Plummer, 1945

Thuramminoides sphaeroidalis Plummer, 1945

Fig. 8A, B, E.

1945 *Thuramminoides sphaeroidalis* sp. nov.; Plummer 1945: 218, pl. 15: 4–10.

1961 *Thuramminoides sphaeroidalis* Plummer, 1945; Conkin 1961: 243, pl. 17: 1–10; pl. 18: 1–4.

2002 *Thuramminoides sphaeroidalis* Plummer, 1945; Holcová 2002: 89, pl. 1: 1, 2, 4, 6; pl. 2: 6, 8, 14; pl. 3: 14; pl. 7: 1; pl. 8: 12–15; pl. 9: 1, 15–16; pl. 10: 7; pl. 12: 3; pl. 13: 5; pl. 14: 8–11.

Material.—873 specimens from 19 samples.

Remarks.—Conkin (1961) transferred the genus *Thuramminoides* from the Saccamminidae to the Astrorhizidae because it possesses a labyrinthic internal structure. In this study we follow the classification of Kaminski (2014), who placed the genus in the Stegnammininae.

In this study, *Thuramminoides sphaeroidalis* is the second most abundant taxon, which is commonly distributed in almost all samples.

Stratigraphic range.— Lower Cambrian (Culver 1991) to Permian (Conkin et al. 1968).

Geographic distribution. — This species has been widely reorted from West Africa (Culver 1991), North America (Conkin 1961; Conkin, et al. 1968), Europe (Holcová 2002), and Australia (Bell et al. 2000; Dixon and Haig, 2004).

Thuramminoides plummerae Kaminski and Perdana, 2017

Fig. 8C, F.

Thuramminoides plummerae sp.nov.; Kaminski and Perdana, 2017b: 62, pl. 1, 17–18.

pars. 1945 *Thuramminoides sphaeroidalis* sp. nov.; Plummer, 1945: 218, pl. 15: 8.

Type horizon: Early Silurian (Aeronian), Qusaiba Formation.

Type locality: Old Qusaiba Village, Qasim Region, Saudi Arabia.

Material.—27 specimens from four samples.

Dimensions.—Specimens range from 187.5 µm to 600 µm in diameter.

Description.—Test free, spheroidal and strongly compressed, bearing several protuberances at the edge of its periphery. The protuberances exhibit a rounded terminal short tube-like opening.

Remarks.—These specimens are similar to one of the paratypes of *Thuramminoides sphaeroidalis* Plummer, 1945, which is here assigned to a different species due to the distinctive protuberances at the margin of the test.

Thuramminoides sp. 1*?*

Fig. 8D.

Type horizon: Qusaiba shale early Silurian (Aeronian).

Type locality: Old Qusaiba Town, Qasim Region Saudi Arabia.

Material.—214 specimens from six samples.

Dimensions.—162.5 to 275 μm in length and 55 to 93 μm in width.

Description.—Test free, unilocular ellipsoidal form, with a flattened test depressed in the center and thickened at the peripheral side. Aperture is not visible. Wall constructed of medium to coarse grains.

Remarks.—This species classified into the genus of *Thuramminoides* due to the flattened, depressed in the center and thickening of the periphery. It differs from *Thuramminoides sphaeroidalis* in having an ellipsoid test shape. Diagnostic feature of this species is the ratio of the width and length of the test about 1:3.

Family HEMISPHAERAMMINIDAE Loeblich and Tappan, 1961, emend Mikhalevich, 1995

Genus *Hemisphaerammina* Loeblich and Tappan, 1957

Type species. Hemisphaerammina batalleri Loeblich and Tappan, 1957

Hemisphaerammina casteri McClellan, 1966

Fig. 8N.

1966 *Hemisphaerammina casteri* sp. nov.; McClellan 1966: 486, pl. 38:1a, b; pl. 42: 1a, b.

Materials.—Three specimens from one sample.

Remarks.—Our specimens conform well to the specimens reported by McClellan (1966).

Stratigraphic range.—Silurian.

Geographic distribution.—This species was first reported from Indiana (USA).

Hemisphaerammina sp. 1

Fig. 8G–K.

Type horizon: Qusaiba shale early Silurian (Aeronian).

Type locality: Old Qusaiba Town, Qasim Region, Saudi Arabia.

Material.—18 specimens from 11 samples.

Dimensions.—112.5 to 237.5 µm in diameter.

Description.—Monothalamous, planconvex shape, aperture not visible; wall thin, constructed of fine to medium grains.

Remarks.—Compared with *Hemisphaerammina cecillalickeri* Conkin and Conkin, 1981, our specimens have thinner wall and more planconvex form. In addition, some of our specimens have a flange.

Hemmisphaerammina sp. 2

Fig. 8L.

Type horizon: Qusaiba shale early Silurian (Aeronian).

Type locality: Old Qusaiba Town, Qasim Region, Saudi Arabia.

Materials.—One specimen.

Dimensions.—150 µm in length and 100 µm in width.

Description.—Test attached, monothalamous, planconvex form, somewhat acute at the edges of the chamber, no aperture apparent, wall constructed of fine to medium particles.

Remarks: Compared with *Hemisphaerammina batalleri* Loeblich and Tappan, 1957 and *Hemisphaerammina casteri* McClellan, 1966, our specimen is more hemispherical in outline and acute at the edges.

Hemisphaerammina sp. 3

Fig. 8M.

Type horizon: Qusaiba shale, early Silurian (Aeronian).

Type locality: Old Qusaiba Town, Qasim Region, Saudi Arabia.

Material.—One specimen.

Dimensions.—206 µm in length and 125 µm in width.

Description.—Test attached, plano-convex form, chamber constricted at the center that separate the blunt smaller from the bigger slightly tapering one. No distinct aperture. Wall thin, made of fine to medium siliceous particles.

Remarks.—Our specimen almost resembles *Sorosphaera bicella* described by Dunn (1942), but it does not have exactly two separated chambers, that make this specimen classified as *Hemisphaerammina*.

Family SACCAMMINIDAE Brady, 1884

Genus *Lagenammina* Rhumbler, 1911

Type species. Lagenammina laguncula Rhumbler, 1911

Lagenammina aff. *cumberlandiae* (Conkin, 1961)

Fig. 9A, B.

1961 *Proteonina cumberlandiae* sp. nov.; Conkin 1961: 248, pl. 19: 1-3; pl. 26: 4,5; :2,3.

1966 *Lagenammina cumberlandiae* (Conkin), 1961; McClellan 1966: 477, pl. 36: 19; pl. 40: 19.

1982 *Lagenammina cumberlandiae* (Conkin), 1961; Mabillar and Aldridge 1982: 132, pl.1: 11.

Material.—Three specimens from one sample.

Remarks.—Our specimens have a shorter neck, are more compressed, coarser wall texture compared with the holotype of *Lagenammina cumberlandiae* described by Conkin (1961).

Stratigraphic range.—Silurian to Carboniferous (Mississippian).

Geographic distribution.—This species was first reported from the New Providence Formation of Kentucky, southern Indiana, and Ohio (USA) (Conkin 1961). McClellan

(1966) and Mabillar and Aldridge (1982) also described Silurian *Lagenammina cumberlandiae* from Indiana and the Wenlock area, Shropshire England respectively.

Lagenammina ligula (Gutschick, Weiner, and Young, 1961)

Fig. 9C, D.

1961 *Saccammina ligula* sp. nov.; Gutschick, Weiner, and Young 1961: 1207, pl. 150: 3,6,8,11.

Material.—22 specimens from seven samples.

Remarks.—We follow McClellan (1966), who regarded that *Lagenammina* differs from *Saccammina* in having a pyriform shape and a neck. Compared with the specimens of Gutschick et al. (1961), some of our specimens have an ovoid to ellipsoid form, are laterally compressed, and possess a rough surface.

Stratigraphic range.—Silurian to Carboniferous (Mississippian).

Geographic distribution.—This species was reported previously from Oklahoma (Pontotoc County), northern Indiana (Rockford), and Texas (Chappel), USA.

Lagenammina silnica Malec, 1992

Fig. 9E.

1992 *Lagenammina silnica* sp. nov.; Malec 1992: 280–281, pl. 1: 1, 4; pl. 2: 1-3; pl. 3: 5, 8.

Material.—24 specimens from nine samples.

Remarks.—Our specimens conform well to the description of Malec (1992).

Stratigraphic range.—Early Silurian (Aeronian) (this study) to uppermost lower Devonian.

Geographic distribution.—This species was first described from the Dabrowa borehole in southeastern Poland.

Lagenammina sp. 1

Fig. 9F.

Type horizon: Qusaiba shale early Silurian (Aeronian).

Type locality: Old Qusaiba Town, Qasim Region, Saudi Arabia.

Material.—20 specimens from four samples.

Dimensions.—375 to 562.5 µm in length and 125 to 200 µm in width.

Description.—Test free, elongate, single undivided chamber. Initial stage of this chamber wider and slightly tapering toward the aperture end. The center part of the test is depressed and shows some perforations. Aperture terminal, situated at the open end of the tube. Wall thin, composed of fine siliceous materials.

Remarks.—This species is similar to the younger species *Saccammina scutella* Malec, 1992 and *Lagenammina cumberlandiae*, but has distinct differences in having a depressed center and perforations of the center part. Moreover, this species has a smoother test constructed of fine grained material.

Lagenammina sp. 2

Fig. 9I.

Type horizon: Qusaiba shale early Silurian (Aeronian).

Type locality: Old Qusaiba Town, Qasim Region, Saudi Arabia.

Materials.—Two specimens.

Dimensions.—200 to 218 µm in length and 175 to 187.5 µm in width.

Description.—Test free, monothalamous, spherical in shape with short neck where aperture terminal situated, test slightly compressed, composed of medium to coarse quartz particles.

Remarks.—Our specimen has finer wall material compared with the holotype and paratype of *Lagenammina ampulacea* Crespin, 1961 from the Devonian. Moreover, it has more compressed chamber.

Lagenammina sp. 3

Fig. 9K, L.

Type horizon: Qusaiba shale early Silurian (Aeronian).

Type locality: Old Qusaiba Town, Qasim Region, Saudi Arabia.

Material.—Two specimens.

Dimensions.—400 to 487 µm in length and 212.5 to 350 µm in width.

Description.—Test free, nearly elongated monothalamous, laterally compressed, with the terminal aperture situated at the end of the short neck, composed of fine siliceous particles.

Remarks.—These specimens are placed into the genus *Lagenammina* because they possess an aperture at the end of short circular neck.

Genus *Saccammina* Carpenter, 1869

Type species. Saccammina sphaerica Brady, 1871

Saccammina aspera Stewart and Priddy, 1941

Fig. 9G, H.

1941 *Saccammina aspera* sp. nov.; Stewart and Priddy 1941: 372, pl. 54: 13.

Materials.—43 specimens from nine samples.

Remarks.—The distinctive feature of this species is short circular aperture at the open end of the chamber. In addition, our specimens have a smoother wall compared to the Steward and Priddy (1941) specimens from Ohio and Indiana (USA).

Stratigraphic range.—Silurian.

Saccammina sp. 1

Fig. 9J.

Type horizon: Qusaiba shale early Silurian (Aeronian).

Type locality: Old Qusaiba Town, Qasim Region, Saudi Arabia.

Materials.—12 specimens in two samples.

Dimensions.—214 to 412 μm in diameter.

Description.—Test free, spherical single chambered form, shows lateral compression that makes the test flattened, aperture terminal at the end of short neck. Wall composed of medium to coarse siliceous grains.

Remarks.—This species is close to *Saccammina moremani* (Ireland 1939), a Silurian taxon from the Hunton Formation limestone, but differs in having a smaller and tubular aperture neck.

Genus *Saccamminita* Kaminski and Perdana, 2017

Type species: Saccamminita galinae Kaminski and Perdana, 2017

Saccamminita galinae Kaminski and Perdana, 2017

Figs. 10A–D.

2017 *Saccamminita galinae* sp.nov.; Kaminski and Perdana, 2017b: 62, pl. 1: 1–3.

Type horizon: Early Silurian (Aeronian), uppermost part of the Qusaiba Formation.

Type locality: Old Qusaiba Village, Qasim Region, Saudi Arabia.

Material.—Three specimens from one sample.

Dimensions.—Specimens range from 312.5 µm to 375 µm in length, and 112.5 µm to 156.25 µm in diameter across the tubular chamber.

Description.—Test free, elongated, with a uniform undivided elongated chamber, laterally compressed, tapering slightly at both ends. Width to length ratio is approximately 1:3, with maximum width approximately in the central part of the test. Wall agglutinated of fine quartz grains. A single short apertural neck at one end of the test.

Remarks.—The shape of the test resembles *Amphitremoida simehkuhensis* Nestell and Ghobadi Pour (in press) from the Ordovician of Iran, but it differs in possessing only a single aperture.

Genus *Thurammina* Brady, 1879

Type species. Thurammina papillata Brady, 1879

Thurammina arcuata Moreman, 1930

Fig. 10E.

1930 *Thurammina arcuata* sp. nov.; Moreman 1930: 54, pl. 6: 2, 3.

2002 *Thurammina arcuata* Moreman, 1930; Holcová 2002: 96, pl. 16: 11.

Materials.—Ten specimens in five samples.

Remarks.—Our specimens conform well to holotype illustrated by Moreman (1930), and specimens described by Holcová (2002).

Stratigraphic range.—Silurian.

Geographic distribution.—First reported from the Chimney Hill Limestone, Oklahoma, USA (Moreman 1930), and from the Barrandian area of the Czech Republic (Holcová 2002).

Thurammina holcovae Kaminski and Perdana, 2017

Fig. 10F.

2017 *Thurammina holcovae* sp.nov.; Kaminski and Perdana 2017b: 62, pl. 1: 14.

2002 *Thurammina triradiata* Gutschick and Treckman, 1959; Holcová 2002: 97, text-fig. 15g, pl. 4: 3, pl. 16: 4.

Type horizon: Early Silurian (Aeronian), uppermost part of the Qusaiba Formation. Holcová (2002) reported the species from the Lower Devonian (Lochlovian to Pragian) of the Czech Republic.

Type locality: Old Qusaiba Village, Qasim Region, Saudi Arabia.

Material.—Seven specimens from five samples.

Dimensions.—Specimens range from 156 µm to 200 µm in diameter.

Description.—Test free, rounded-triangular in outline, with three tapering neck-like projections situated at the corners of the triangle. Apertures circular, at the end of the projections. Wall finely agglutinated, translucent, with medium-size grains.

Remarks.—These specimens differ from *Thurammina triradiata* Gutschick and Treckman 1959, emended by Conkin et al. (1968) in their more triangular outline, and having apertures situated at the apex of the triangle. Our specimens are most similar to the Lower Devonian (Pragian) specimen illustrated by Holocová (2002) as *Thurammina triradiata*. Holcová's specimen has an inflated chamber, with short tubes serving as apertures located at each corner.

Thurammina papillata Brady, 1879

Fig. 10G.

1879 *Thurammina papillata* sp. nov.; Brady 1879: 45, pl. 6: 4–8.

2002 *Thurammina papillata* Brady, 1879; Holcová 2002: 96, pl. 16: 11.

Material.—33 specimens from eleven samples.

Remarks.—Our specimens compare well with the specimens illustrated by Holcová (2002). However, our specimens have fewer protuberances and are more compressed.
Stratigraphic range.—Silurian to Recent.
Geographic distribution.—Barrandian area, Czech Republic (Holcová 2002) and Saudi Arabia (this study).

Thurammina pentagona Kaminski and Perdana, 2017
Figs. 10H–J.
2017 *Thurammina pentagona* sp.nov.; Kaminski and Perdana 2017b: 62, pl. 1: 8–9.
Type horizon: Early Silurian (Aeronian), uppermost part of the Qusaiba Formation.
Type locality: Old Qusaiba Village, Qasim Region, Saudi Arabia.
Material.—Five specimens from three samples.
Dimensions.—Specimens range from 175 µm to 250 µm in diameter.
Description.—Test free, rounded-pentagonal in outline, slightly inflated, with five small neck-like projections situated at the corners of the pentagon. Apertures circular, at the end of the projections. Wall finely agglutinated, translucent, with fine to medium-size grains.
Remarks.—Our species most closely resembles *Thurammina hexagona* Dunn, which differs in having an extra aperture located at the periphery of the test and its hexagonal rather than pentagonal outline.

Thurammina (?) sp. 1
Fig. 10K.
Type horizon: Qusaiba shale early Silurian (Aeronian).
Type locality: Old Qusaiba Town, Qasim Region, Saudi Arabia.
Material.—One specimen.
Dimensions.—Length: 212.5 µm, width: 187.5 µm.
Description.—Test free, single chamber, somewhat triangular in outline, with three neck like projections, wall composed of fine to medium siliceous grains.

Remarks.—This specimen most probably belongs to the genus *Thurammina* in regard to its shape and neck-like projections. The outline of this specimen more or less resembles *Thurammina holcovae*, but has a thicker, more compressed wall.

Family PSAMMOSPHAERIDAE Haeckel, 1894

Genus *Psammosphaera* Schulze, 1875

Type species. Psammosphaera fusca Schulze, 1875

Psammosphaera cava Moreman, 1930

Fig. 10N.

1930 *Psammosphaera cava* sp. nov.; Moreman 1930: 48, pl. 6: 12.

1966 *Psammosphaera cava* Moreman, 1930; Ireland 1966: 225, pl. 1: 16.

1999 *Psammosphaera cava* Moreman, 1930; Watkins, Walsh and Kuglitsch 1999: 543, fig. 5: 8-9.

2016 *Psammosphaera cava* Moreman, 1930; Kaminski et al. 2016: 118, pl. 1: 9–12.

Material.—299 specimens from 22 samples.

Remarks.—Our specimens are conformed well with those described by Ireland (1939). However, our specimens have smaller test diameter of about 110–120 µm.

Stratigraphic range.—Upper Ordovician (Mound 1968) to Early Carboniferous (Conkin and Conkin 1982).

Geographic distribution.—First described from the Silurian of Oklahoma (USA) by Moreman (1930); it has also been reported from the Silurian of England (Mabillard and Aldridge 1982), Ireland (Kaminski et al. 2016), Sardinia (Gnoli and Serpagli 1984), Australia (Bell et al. 2000) and Lower-Middle Devonian of the Czech Republic (Holcova 2004), and the Upper Devonian of central Poland (Olempska 1983).

Psammosphaera sp. 1

Fig. 10O.

Type horizon: Early Silurian (Aeronian), Qusaiba Formation.

Type locality: Old Qusaiba Village, Qasim Region, Saudi Arabia.

Materials.—34 specimens from two samples.

Descriptions.—Test free, nearly fusiform single chamber, no aperture visible, the ratio between width and length about ½, exhibits a smooth wall composed of fine siliceous particles, white in colour.

Remarks.—These specimens are similar to *Amphitremoida huffmani* (Conkin and Conkin 1964), but lack apertures at both ends.

Psammosphaera (?) sp. 2

Fig. 10L.

Type horizon: Early Silurian (Aeronian), Qusaiba Formation.

Type locality: Old Qusaiba Village, Qasim Region, Saudi Arabia.

Material.— 3426 specimens from 23 samples.

Dimension.—93.8 to 375 μm in diameter.

Description.—Test free, discoidal, monothalamous; apparently depressed in the center, and thicker peripheral side; no distinct aperture; wall thin, translucent, composed of fine siliceous grains.

Remarks.—This species differs from *Psammosphaera* in having a discoidal form, and from *Thuramminoides* in possessing a thin, translucent wall. This species is the most common foraminiferal species recovered from the whole section.

Psammosphaera (?) sp. 3

Fig. 10M.

Material.—Nine specimens from four samples.

Dimension.—112.5 to 375 μm in diameter.

Description.—Test free, triangular to sub-triangular in outline, monothalamous, having triangular flange, aperture not visible; wall thin, translucent, constructed of minute siliceous particles.

Remarks.—This species differs from *Psammosphaera*? sp. 2, in having a triangular outline.

Type Level.—Early Silurian (Aeronian), Qusaiba Formation.

Type Locality.—Old Qusaiba Village, Qasim Region, Saudi Arabia.

Genus Sorosphaera Brady, 1879

Type species. Sorosphaera confusa Brady, 1879

Sorosphaera bicella Dunn, 1942

Fig. 10P.

1942 *Sorophaera bicella* sp. nov.; Dunn 1942: 325, pl. 42: 11–18.

1966 *Sorophaera bicella* Dunn, 1942; McClellan 1966: 472, pl. 37: 3–9; pl. 41: 7–9.

Materials.—Three specimens from three samples.

Remarks.—Our specimens conform well to the specimen of Dunn (1942).

Stratigraphic range.—Silurian.

Geographic distribution.—This species was first described from the southwest section of the town of Joliet, Illinois (USA) (Dunn 1942).

Sorosphaera tricella Moreman, 1930

Fig. 10Q.

1930 *Sorosphaera tricella* sp. nov.; Moreman 1930: 49, pl. 5: 12, 14.

1966 *Sorophaera tricella* Moreman, 1930; McClellan 1966: 472, pl. 37: 10; pl. 41: 10.

Material.—One specimen.

Remarks.—Our specimen compares well to specimens described by Moreman (1930), but it differs in having a heterogenous chambers with unparalleled arrangement.

Stratigraphic range.—Silurian.

Geographic distribution.—The holotype of this species was described by Moreman (1930) from the Chimney Hill Limestone, Arbuckle Mountain region, Oklahoma, USA.

Family LACUSTRINELLIDAE Mikhalevich, 1995

Genus *Webbinelloidea* G.A. Stewart and Lampe, 1947

Type species. Webbinelloidea similis G.A. Stewart and Lampe, 1947

Webbinelloidea sp. 1

Figs. 11A, B.

Type horizon: Early Silurian (Aeronian), Qusaiba Formation.

Type locality: Old Qusaiba Village, Qasim Region, Saudi Arabia.

Material.—Two specimens from single sample.

Dimensions.—150 to 175 µm in length and 93 µm in width.

Description.—Test attaches to another object, monothalamous, half ovoid form, aperture absent, wall surface smooth, consisting of fine-medium silica grains.

Remarks.—Our specimens are identical to the younger representative *Webbinella cretacea* Hofker, 1949 from the Cretaceous. It is probable that our specimens are the ancestor of that species.

Order AMMODISCIDA Mikhalevich, 1980

Suborder HIPPOCREPININA Saidova, 1981

Family HIPPOCREPINIDAE Rhumbler, 1895

Genus *Kechenotiske* Loeblich and Tappan, 1984

Type species. *Hyperamminoides expansus* Plummer, 1945

Kechenotiske cf. *expansa* (Plummer, 1945)

Figs. 11C, D.

1945 *Hyperamminoides expanus* sp. nov.; Plummer 1945: 223–224, pl. 16: 1–6.

2016 *Kechenotiske expansa* (Plummer), 1945; Haig and Mory 2016: 71, figs. 5v, w.

Material.—Two specimens from one sample.

Remarks.—Our specimens are mostly identical to *Kechenotiske expansa*, illustrated by Haig and Mory (2016). However, our specimens proloculus are missing because only broken specimens were recovered from our samples.

Stratigraphic range.—The previous stratigraphic interval this species was reported as Upper Carboniferous to Permian. This report revises its stratigraphic range as Lower Silurian to Permian.

Geographic distribution.—This species was first reported from the Smithwick Formation, Algerita, Texas, USA (Plummer 1945), and was also discovered in the Bulgadoo Shale, Baker Formation (Crespin 1958; Haig and Mory 2016) of Western Australia.

Family HYPERAMMINIDAE, Eimer and Fickert 1899

Genus *Hyperammina* Brady, 1878

Type species. Hyperammina elongata Brady, 1878

Hyperammina sinuosa Kaminski and Perdana, 2017

Figs. 11E–G.

Hyperammina sinuosa sp.nov.; Kaminski and Perdana, 2017b: 62, pl. 1, 4–6.

Type horizon: Early Silurian (Aeronian), uppermost part of the Qusaiba Formation.

Type locality: Old Qusaiba Village, Qasim Region, Saudi Arabia.

Material.—Four specimens from one sample.

Dimensions.—Specimens range from 275 µm to 437 µm in length, and 100 µm to 112 µm in diameter across the tubular chamber.

Description.—Test free, elongated, with a rounded proloculus and an undivided short bent or sinuous tubular second chamber. Proloculus may be slightly wider than the tubular chamber. Aperture terminal, situated at the open end of the tube. Wall thin, constructed of medium to coarse siliceous particles.

Remarks.—The species is characterized by its globular proloculus, which is visible in immersion, and its short tubular chamber which may be bent or slightly sinuous. The specimens are laterally compressed. Our species differs from the Ordovician species *Hyperammina minuta* Moreman in possessing a thinner more coarsely agglutinated wall and short tubular section.

Hyperammina sp. 1

Fig. 11H.

Type horizon: Qusaiba shale early Silurian (Aeronian).

Type locality: Old Qusaiba Town, Qasim Region, Saudi Arabia.

Material.—One specimen

Dimensions.—437.5 µm in length and 125 µm in width, 162.5 µm in diameter of the proloculus.

Description.—Test free, elongated, with oval and large proloculus followed by slightly tapering second chamber, test slightly compressed, and has a medium to coarse grain wall texture.

Remarks.—Our specimen shows truncation at the end of the apertural side, and can be compared to the *Hyperammina hastata* Saurin, 1960, which represents a larger second chamber and coarser grained wall.

Hyperammina sp. 2

Fig 11I.

Type horizon: Early Silurian (Aeronian), Qusaiba Formation.

Type locality: Old Qusaiba Village, Qasim Region, Saudi Arabia.

Material.—A single specimen.

Dimensions.—350 µm in length and 63 µm in width, 75 µm in diameter of the proloculus

Description.—Test free, elongated, slightly curved in its 1/3 proximal, then straight up to its distal part, which underwent an enlargement in size, constituting one subglobular proloculus. Aperture terminal, situated at the distal end. Wall constructed of fine-medium quartz particles.

Remarks.—Our specimens closely resemble the modern species *Hyperammina spiculifera* Lacroix, 1928 in their shape and outline. On the contrary, wall construction by spicules, which is the special feature of *Hyperammina spiculifera*, is absent. The large difference occurrence in stratigraphic interval may suggest that this specimen is the ancestor of *H. spiculifera*.

Suborder AMMODISCINA Mikhalevich, 1980

Family AMMODISCIDAE Reuss, 1862

Genus *Ammovertella* Cushman, 1928

Type species. Ammodiscus (Psammophis) inversus Schellwien, 1898

Ammovertella sp. 1

Fig. 11J.

Type horizon: Qusaiba shale early Silurian (Aeronian).

Type locality: Old Qusaiba Town, Qasim Region, Saudi Arabia.

Material.— One specimen.

Dimensions.—612 μm in length, 450 μm in width, and 163 μm in diameter of the proloculus.

Description: Test attached, proloculus not visible because of adherent to the discoidal material, second chamber compressed, and closely bended, back and forth toward the vertical plan. Aperture not visible due to preservation, wall composed of fine to medium particles.

Remarks.—This species is very rare in the Qusaiba samples.

Ammovertella sp. 2

Fig. 11K.

Type horizon: Qusaiba shale early Silurian (Aeronian).

Type locality: Old Qusaiba Town, Qasim Region, Saudi Arabia.

Material.—Two specimens in one sample.

Dimensions.—218 μm in length and 150 μm in width.

Description.—Test attached, consisting of a proloculus, and tubular second chamber winding half enclosing the proloculus in the lateral plane, proloculus and second chamber separated by a constriction. Tubular chamber increasing in diameter gradually toward the distal end.

Remarks.—These specimens are classified as *Ammovertella* due to the fact that they are winding laterally in single plane. These specimens were recovered from the middle part of the shale succession.

Ammovertella sp. 3

Fig. 11L.

Type horizon: Qusaiba shale early Silurian (Aeronian).

Type locality: Old Qusaiba Town, Qasim Region Saudi Arabia.

Material.—12 specimens from five samples.

Dimensions.—Length 310 μm, diameter 110 μm.

Description.—Test attached, tubothalamous with a spherical proloculus, continued by a tubular second chamber winding sinuously in one plane, proloculus and second chamber have constant size. Aperture located at the open end. Test constructed of fine to medium quartz materials.

Remarks.—These broken specimens were recovered from the shale in the middle of the succession.

Ammovertella sp. 4

Fig. 11M.

Type horizon: Early Silurian (Aeronian), Qusaiba Formation.

Type locality: Old Qusaiba Village, Qasim Region, Saudi Arabia.

Material.— A single specimen.

Dimensions.—Proloculus: 312 μm, in length and 210 μm in width, second chamber: 150 μm in length and 87 μm, in width.

Description.—Test attached, consisting of a large compressed fusiform proloculus followed by an undivided tubular second chamber, bent and attached. The ratio between second chamber and the proloculus diameter is about 2:5. Wall smooth, made of agglutinated materials.

Remarks.—This specimen resembles *Lagenammina* in outline. On the contrary, the bent second chamber in single a plane is different from the neck of *Lagenammina*, which is the feature of *Ammovertella*.

Genus *Tolypammina* Rhumbler, 1895

Type species. Hyperammina vagans Brady, 1879

Tolypammina aihemerensis Said and Eissa, 1969

Figs. 11N., 12A.

1969 *Tolypammina aihemerensis* sp. nov.; Said and Eissa 1969: 359, pl. 3: 8–11.

Material.—23 specimens from five samples.

Remarks.—Proloculus and aperture in our specimens cannot be recognized since they were broken as a result of taphonomic processes. Nevertheless, we consider these

specimens as *Tolypammina aihemerensis* due to the uncoiled twisting and the presence of some constrictions on the second chamber.

Stratigraphic range.—The occurrence of this species in Qusaiba revises the known range of this species as Aeronian (Silurian) to Pennsylvanian (Carboniferous).

Geographic distribution. — Said and Eissa (1969) first described this species from shales in Egypt.

Tolypammina cf. *bulbosa* (Gutschick and Treckman, 1959) emend. Conkin and Conkin, 1964.

Fig. 12B.

1959 *Ammovertella bulbosa* sp. nov.; (Gutschick and Treckman 1959): 247, pl. 37: 6–7.

1964 *Tolypammina bulbosa* (Gutschick and Treckman, 1959); Conkin and Conkin 1964: 92, pl. 13, figs. 12–17,

2002 *Tolypammina bulbosa* Conkin and Conkin, 1964; Holcová 2002: 106, pl. 17: 11–12.

Material.—Twelve specimens from five samples.

Remarks.—Our specimens are broken, and no proloculus can be identified. Our specimens are closes to the specimens illustrated by Holcová (2002) in Fig 17 figure 11, but these specimens have a constant size of the second chamber.

Stratigraphic range.— Early Silurian (this study) to Devonian (Conkin and Conkin, 1964; Holcová 2002)

Geographic distribution. — This species was reported from Lousiana (USA) (Conkin and Conkin, 1964), Barandian Area Czech Republic (Holcová 2002), and Qasim Region (Saudi Arabia) (this study).

Tolypammina howchini (Ludbrook, 1967)

1967 *Ammovertella howchini* sp. nov.; Ludbrook 1967: 80, pl. 4: 6–8.

Figa. 12C–F.

Material.— 79 specimens from 14 samples.

Remarks.—Based on the *Tolypammina* and *Ammovertella* definition proposed by Conkin (1961), we transfer the *Ammovertella howchini* Ludbrook, 1967 to the genus *Tolypammina*. We also place all the tolypamminids that have a second chamber winding zigzag irregularly in this species.

Stratigraphic range.—Stratigraphic interval of this species is from Silurian to Permian.

Geographic distribution.—This species is only reported from South Australia and Saudi Arabia.

Tolypammina aff. *jackobchapelensis* Conkin, 1961

Figs. 12G, H.

1961 *Tolypammina jackobchapelensis* sp. nov.; Conkin 1961: 303, pl. 22: 16–21, pl. 27: 5.

Material.—18 specimens from seven samples.

Remarks.—Our specimens differ from typical *Tolypammina jackobchaepensis* in having larger oval proloculus. The winding mode is not apparent as a result of truncation.

Stratigraphic range.—Stratigraphic interval of this species is from Silurian (Aeronian) to Carboniferous (Mississippian).

Geographic distribution.—This species is only reported from North America and Saudi Arabia.

Tolypammina aff. *serpens* Ireland, 1956

Fig. 12I.

1956 *Tolypammina serpens* sp. nov.; Ireland 1956: 851, tf. 5:. 3–5

Material.—Two specimens from two samples.

Remarks.—Compared with the holotype of Ireland (1956), our specimens do not display intense coiling surrounding the proloculus.

Stratigraphic range.—Silurian (Aeronian) to Carboniferous (Pennsylvanian).

Geographic distribution.—Ireland (1956) first described this species from the upper Pennsylvanian Topeka, Burlingame, Wakarusa, Reading, and Dover Limestones of Kansas, USA.

Tolypammina tornella (Ireland, 1956)

Figs. 12J, 13A–C, E.

1956 *Ammovertella tornella* sp. nov.; Ireland 1956: 855, tf. 5: 16–19.

2002 *Tolypammina* aff. *tornella* Ireland; Holcová; 105, pl. 4: 11.

Material.—42 specimens from 12 samples.

Remarks.—Our specimens have a poor degree of preservation, which show a more open coil around other objects than the holotype described by Ireland (1956), and in Holcová's specimens. We also agree with the special characteristics of *Tolypammina* in contrast to *Ammovertella*, which does not wind back and forth in the same plane (Conkin and Conkin 1964).

Stratigraphic range.—Our finding of this species in the Lower Silurian (Aeronian), extends its known range from the Aeronian to the Carboniferous (Pennsylvanian).

Geographic distribution.—This species has been previously reported from the Topeka Limestone in eastern Kansas (USA) (Ireland 1956), and from the Barrandian Area of the Czech Republic (Holcová 2002).

Tolypammina cf. *tortuosa,* Dunn, 1942

Fig. 13D.

1942 *Tolypammina tortuosa* sp. nov.; Dunn 1942: 341, pl. 44: 19–21, 32.

2002 *Tolypammina* cf. *tortuosa* Holcová; 105, pl. 8: 7, 8.

Material.—Six specimens from two samples.

Remarks.—Our specimens closely resemble those from the Holcová collection (Fig 8, fig.7), but the preservation of our specimens is poor, and the proloculus and winding second chamber are not clearly visible.

Stratigraphic range.—Silurian to Devonian.

Geographic distribution.—First reported from the Mississippi Basin (Dunn 1942), and subsequently from the Barrandian area of the Czech Republic (Holcová 2002).

Tolypammina sp. 1

Figs. 13F–H.

Type horizon: Qusaiba shale early Silurian (Aeronian).

Type locality: Old Qusaiba Town, Qasim Region, Saudi Arabia.

Material.—Nine specimens from six samples.

Dimensions.—Proloculus: 150 μm in diameter; second chamber: 205 μm in length and 150 μm in width.

Description.—Test consisting of a large spherical, free proloculus followed by a slightly straight second chamber. The diameter of the proloculus and diameter of the tubular second chamber exhibit the same length; there is no indication of intense winding of the second chamber. Wall composed of fine to medium quartz grains.

Remarks.—This specimen has some similarity to *Tolypammina* sp.m illustrated by Holcová (2002), but the similar diameter size of the proloculus and the second chamber makes our specimen distinct. It also resembles the genus *Hyperammina*. However, because of the slightly twisted part between the proloculus and the initial stage of the second chamber, this species is better assigned to the genus *Tolypammina*.

Tolypammina sp. 2

Fig. 13I.

Type horizon: Qusaiba shale early Silurian (Aeronian).

Type locality: Old Qusaiba Town, Qasim Region, Saudi Arabia.

Material.—Eight specimens from three samples.

Dimensions.—275 to 350 μm in length and 75 to 112 μm in width.

Description.—Test attached, proloculus not visible due to poor preservation, slightly straight gradually increasing second chamber, and decreasing diameter ended with tapering at the distal apertural part; aperture circular, wall fine to medium quartz grains.

Remarks.—Our specimens are most likely a species of the genus *Tolypammina*, which are characterized by their attached test and tubothalamid form.

Tolypammina sp. 3

Figs. 14A-F, 15A, B.

Type horizon: Qusaiba shale early Silurian (Aeronian).

Type locality: Old Qusaiba Town, Qasim Region, Saudi Arabia.

Material.—12 specimens from four samples.

Dimensions.—Proloculus: 163 to 363 μm in diameter; 395 to 875 μm in length and 240 to 463 μm in width.

Description.—Test attached, consisting of a spherical to ovoid proloculus, and a tubular second chamber stacking and crossing previous bends of the chamber haphazardly; second chamber tubular compressed to flattened. Aperture not apparent due to poor preservation. Composed of fine to medium quartz grains.

Remarks.—Some specimens show no proloculus, and their aperture is not preserved. The specimens also represent the largest foraminifera that have been recovered from the Qusaiba shale in this study.

Tolypammina sp. 4

Fig. 15C.

Material.—10 specimens from four samples.

Dimensions.—Proloculus: 100 to 150 μm in diameter; second chamber: to 200 to 275 μm in length and 100 to 150 μm in width.

Description.—Test attached, comprised of a spherical to hemispherical proloculus with constant size of the tubular second chamber. The second chamber is attached to an unrecognized object; aperture probably at the open end, composed of fine grained silica.

Remarks.—This species is similar to *Tolypammina* sp.1, but it has an object attached to the tubular second chamber.

Tolypammina sp. 5

Fig. 15D.

Type horizon: Early Silurian (Aeronian), Qusaiba Formation.

Type locality: Old Qusaiba Village, Qasim Region, Saudi Arabia.

Material.—Three specimens from three samples.

Dimensions.—325 to 345 μm in length and 112 to 125 μm in width.

Description.—Test attached, consisting of a similar diameter of proloculus and an undivided tubular second chamber, which attach or embrace parallel to another second chamber individual or object; wall constructed of fine to medium grained silica.

Remarks.—The aperture cannot be recognized due to the broken test.

Tolypammina sp. 6

Fig. 15E.

Type horizon: Early Silurian (Aeronian), Qusaiba Formation.

Type locality: Old Qusaiba Village, Qasim Region, Saudi Arabia.

Material.—Two specimens from single sample.

Dimensions.—393 to 587 μm in length and 240 to 350 μm in width; proloculus: 187 to 200 in length and 112 to 125 μm in width.

Description.—Test attached, consisting of a rounded proloculus and an undivided tubular second chamber, which winds back and forth in the initial stage. The winding mode in the later stage is not visible due to the poor preservation. Aperture terminal. Wall smooth, composed of fine grain siliceous particles.

Remarks.—The specimens are poorly preserved; therefore, the winding mode of the second chamber is difficult to recognize.

Genus *Turritellella* Rhumbler 1905

Turritellella sp. 1

Figs. 15F, G.

Type horizon: Early Silurian (Aeronian), Qusaiba Formation.

Type locality: Old Qusaiba Village, Qasim Region, Saudi Arabia.

Material.—Six specimens from four samples.

Dimension.—280 to 320 μm in length and 90 to 110 μm in width.

Description—Test free, with open coiling in the vertical direction, compressed, proloculus and aperture not apparent due to the preservation, wall agglutinated of fine siliceous grains.

Remarks.—These specimens are placed into *Turritellella* due to their vertical coiling mode.

Order LITUOLIDA Lankester, 1885
Suborder LITUOLINA Lankester, 1885
Superfamily LITUOLOIDEA de Blainville, 1827
Family LITUOLIDAE de Blainville, 1827
Family LITUOLIDAE de Blainville, 1827
Genus *Ammobaculites* Cushman, 1910
Type species: Spirolina agglutinans d'Orbigny, 1846

Ammobaculites qusaibaensis Kaminski and Perdana, 2017
Figs. 16A–C.
Ammobaculites qusaibaensis sp. nov.; Kaminski and Perdana, 2017b: 62, pl. 1, 11–12.
Material.—Three specimens from two samples.
Dimensions.—Specimens range from 218.75 µm to 350 µm in length, and 93.5 µm to 156.25 µm in diameter across the tubular chamber.
Description.—Test free, small, elongated, early portion close coiled, comprised of only four visible chambers, separated by straight radial sutures, with a depressed umbilicus; later uncoiling and rectilinear, rounded in cross-section, comprised of three irregular, inflated chambers. Sutures in uniserial portion depressed. Wall medium to coarsely agglutinated. Aperture terminal, rounded, at the end of a broad neck.
Remarks.—A small, somewhat irregular *Ammobaculites* species with few chambers. Compared with the Early Devonian specimen illustrated by Holcová (2002), our specimens have a smaller coiled portion and somewhat more inflated uniserial chambers. Holcová's specimen of "*Ammobaculites* sp. 1" has five chambers in the uniserial part, and the aperture is shifted toward the dorsal margin of the test as in the genus *Ammomarginulina*. The specimen illustrated by Holcová (2002) as *Ammobaculites* aff. *leptos* Gutschick and Treckman, 1959 has a uniserial portion that is much narrower than the coiled portion.
Our finding of typical specimens of *Ammobaculites* in the Qusaiba Formation of Saudi

Arabia pushes back the known stratigraphic range of the genus from the late early Devonian (Dalejan Třebotov Limestone of the Czech Republic) to the Early Silurian (Aeronian).

Type Level.—Early Silurian (Aeronian), uppermost part of the Qusaiba Formation.

Type Locality.—Old Qusaiba Village, Qasim Region, Saudi Arabia.

Genus *Simobaculites* Loeblich and Tappan 1984

Type species. Ammobaculites cuyleri Tappan, 1940

Simobaculites sp. 1

Figs. 16D–F.

Type horizon: Early Silurian (Aeronian), uppermost part of the Qusaiba Formation.

Type locality: Old Qusaiba Village, Qasim Region, Saudi Arabia.

Material.—Three specimens.

Dimensions.—Specimens range from 237.5 µm to 575 µm in length, and 112.5 µm to 200 µm in diameter across the tubular chamber.

Description.—Test free, coiled in the early stage, uncoiling tangentially and straight in the final uniserial portion. The initial coil is comprised of six to seven irregular rounded chambers in the final whorl, separated by straight depressed radial sutures, with a distinct coil suture and depressed umbilicus. Uncoiled portion consists of three irregular chambers, broader than high, rounded to ellipsoidal in cross section, separated by depressed sutures. Wall consists of fine siliceous material. Aperture terminal, with an ellipsoidal shape.

Remarks.—Our specimens bear superficial resemblance with the early Mississippian species *Ammobaculites leptos* Gutschick and Treckman, 1959, which was regarded by Loeblich and Tappan to be the oldest known representative of the genus. However, the *Ammobaculites leptos* type specimens possess an undivided early portion and a later portion consisting of pseudochambers – these features are clearly visible in fig 3 of Gutschick and Treckman (1959). They therefore do not belong in the genus *Ammobaculites*, which has true (overlapping) chambers. Our specimens from the Qusaiba Shale appear to have clearly defined sutures in the uncoiled part and therefore

true chambers, even though these are somewhat irregular. Our finding revises the known stratigraphic range of the genus, which was previously reported to range upward from the upper Pennsylvanian (Loeblich and Tappan 1987).

Family PLACOPSILINIDAE Rhumbler, 1913

Genus Stacheia Brady, 1876

Type species. Stacheia pupoides Brady, 1876

Stacheia trepeilopsiformis Conkin, 1961

1961 *Stacheia trepeilopsiformis* sp. nov.; Conkin 1961: 341, pl. 25: 6,7; 39

Fig. 16G.

Materials.—Three specimens from two samples.

Remarks.—Our specimen in agreement with the holotype illustrated by Conkin (1961), which has an adherent test, nearly uniserial, consisting of three segments.

Stratigraphic range.—As the finding of this species will extend backward the previously recorded stratigraphic range of *Stacheia trepeilopsiformis* to the Early Silurian (Aeronian).

Geographic distribution.—The first *Stacheia trepeilopsiformis* was recovered from the Mississippian New Providence Formation, Kentucky (USA).

Stacheia sp. 1

Figs. 16H, I.

Type horizon: Qusaiba shale early Silurian (Aeronian).

Type locality: Old Qusaiba Town, Qasim Region, Saudi Arabia.

Material.—Two specimens from single sample.

Dimensions.—225 to 387 in μm in length and 150 to 236 μm in width.

Description.—Test adherent, with tapering early portion, and abruptly increasing size, consist of nearly uniserial, which is segmented into two parts that resemble a chamber. The shape of the segmentations is discoidal, *Thuramminoides sphaeroidalis* like, with a thick flange and slightly depressed center part. Wall fine agglutinated.

Remarks.—This specimen is placed into the genus *Stacheia* due to its adherent test, and nearly uniserial segments.

B. Plate Explanations.

Fig. 6. Photomicrographs of agglutinated foraminifera from the Lower Silurian Qusaiba Formation. Scale bars = 100μm.

A. *Rhabdammina trifurcata* Moreman, 1933

B–C. *Bathysiphon* sp. 1

D. *Bathysiphon* sp. 2

E–F. *Bathysiphon* sp. 3

G–I. *Amphitremoida citroniforma* Eisenack, 1954

J–M. *Amphitremoida eisenacki* Conkin and Conkin, 1964

N. *Amphitremoida* sp. 3

O–P. *Amphitremoida* sp. 1

Q. *Amphitremoida* sp. 2

R–T. *Blastammina vulgaris* Bykova, 1961

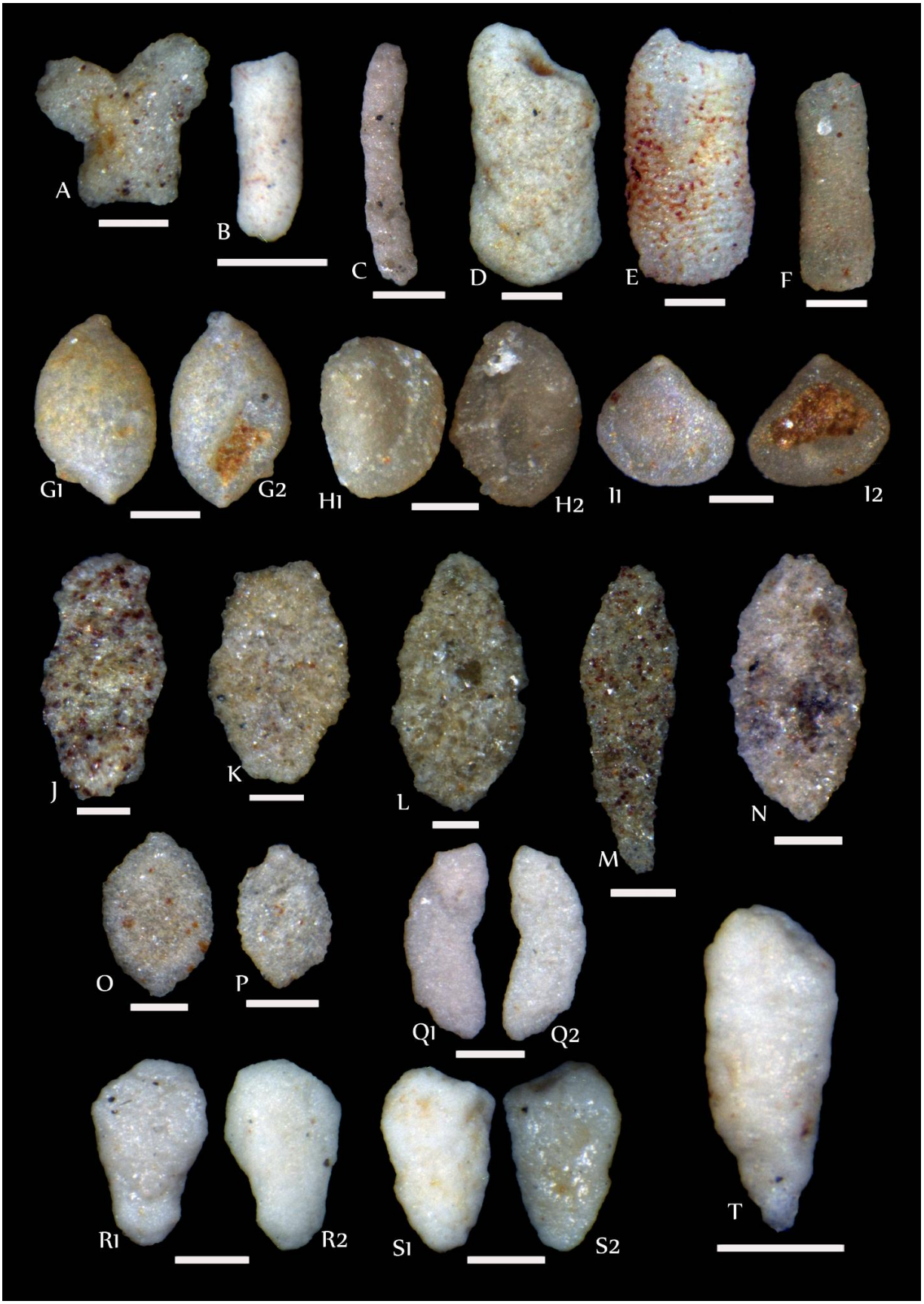
A
B
C
D
E
F
G1
G2
H1
H2
I1
I2
J
K
L
M
N
O
P
Q1
Q2
R1
R2
S1
S2
T

Fig. 7. Photomicrographs of agglutinated foraminifera from the Lower Silurian Qusaiba Formation. Scale bars = 100μm.

A–B. *Ceratammina cornucopia* Ireland, 1939

C. *Ceratammina* sp. 1

D–E. *Ceratammina* sp. 2

F. *Raibosammina aspera* Moreman, 1930

G–H. *Stegnammia contorta* McClellan, 1966

I–K. *Stegnammina elongata* Ireland, 1939

L–N. *Stegnammina* sp. 1

O. *Stegnammina* sp. 2

P. *Stegnammina* sp. 3

Q. *Stegnammina* sp. 4

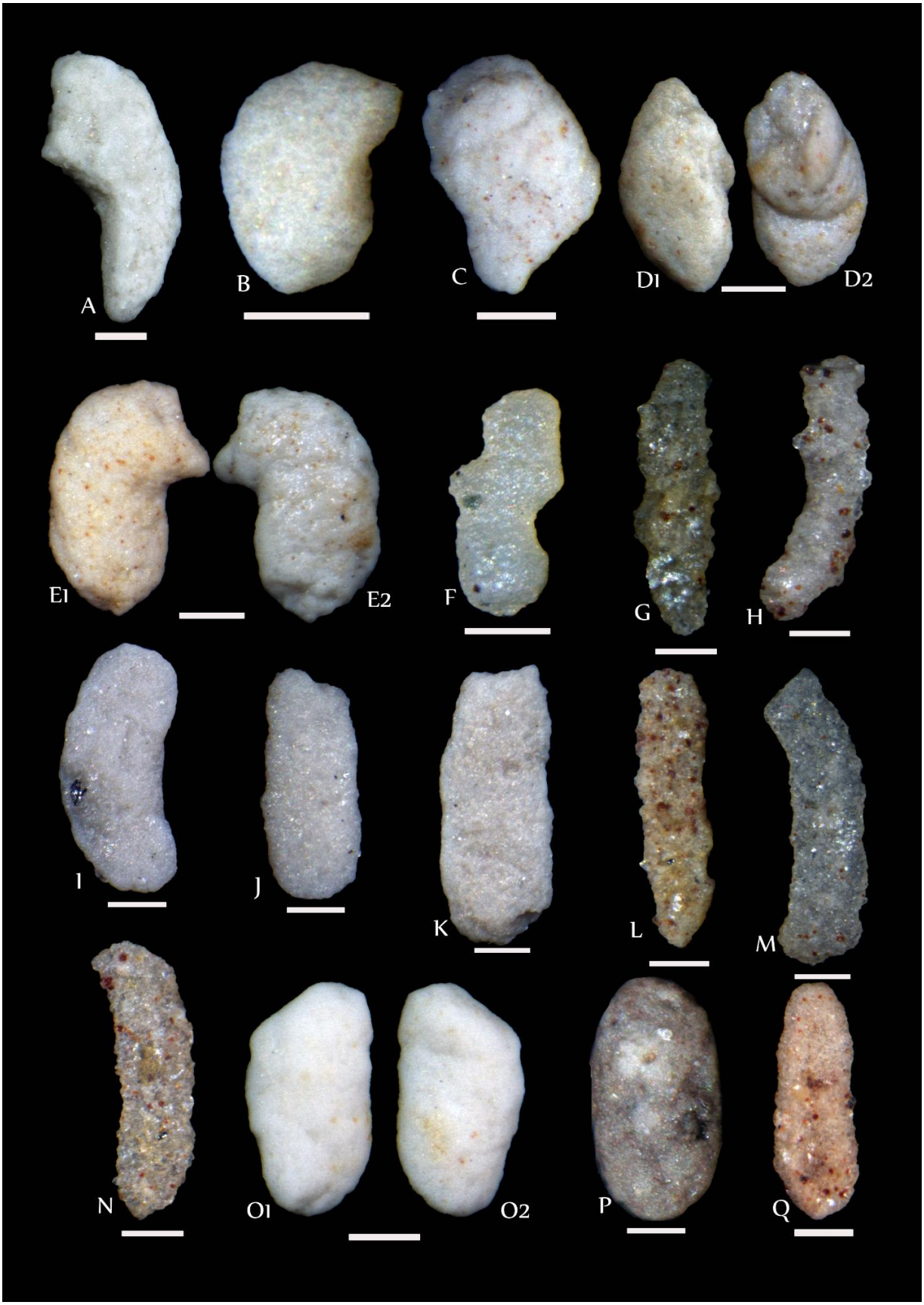
A
B
C
D1
D2
E1
E2
F
G
H
I
J
K
L
M
N
O1
O2
P
Q

Fig. 8. Photomicrographs of agglutinated foraminifera from the Lower Silurian Qusaiba Formation. Scale bars = 100μm.

A, B, E. *Thuramminoides sphaeroidalis* Plummer, 1945

C, F. *Thuramminoides plummerae* Kaminski and Perdana, 2017

D. *Thuramminoides* sp. 1

G–K. *Hemisphaerammina* sp. 1

L. *Hemisphaerammina* sp. 2

M. *Hemisphaerammina* sp. 3

N. *Hemisphaerammina casteri* McClellan, 1966

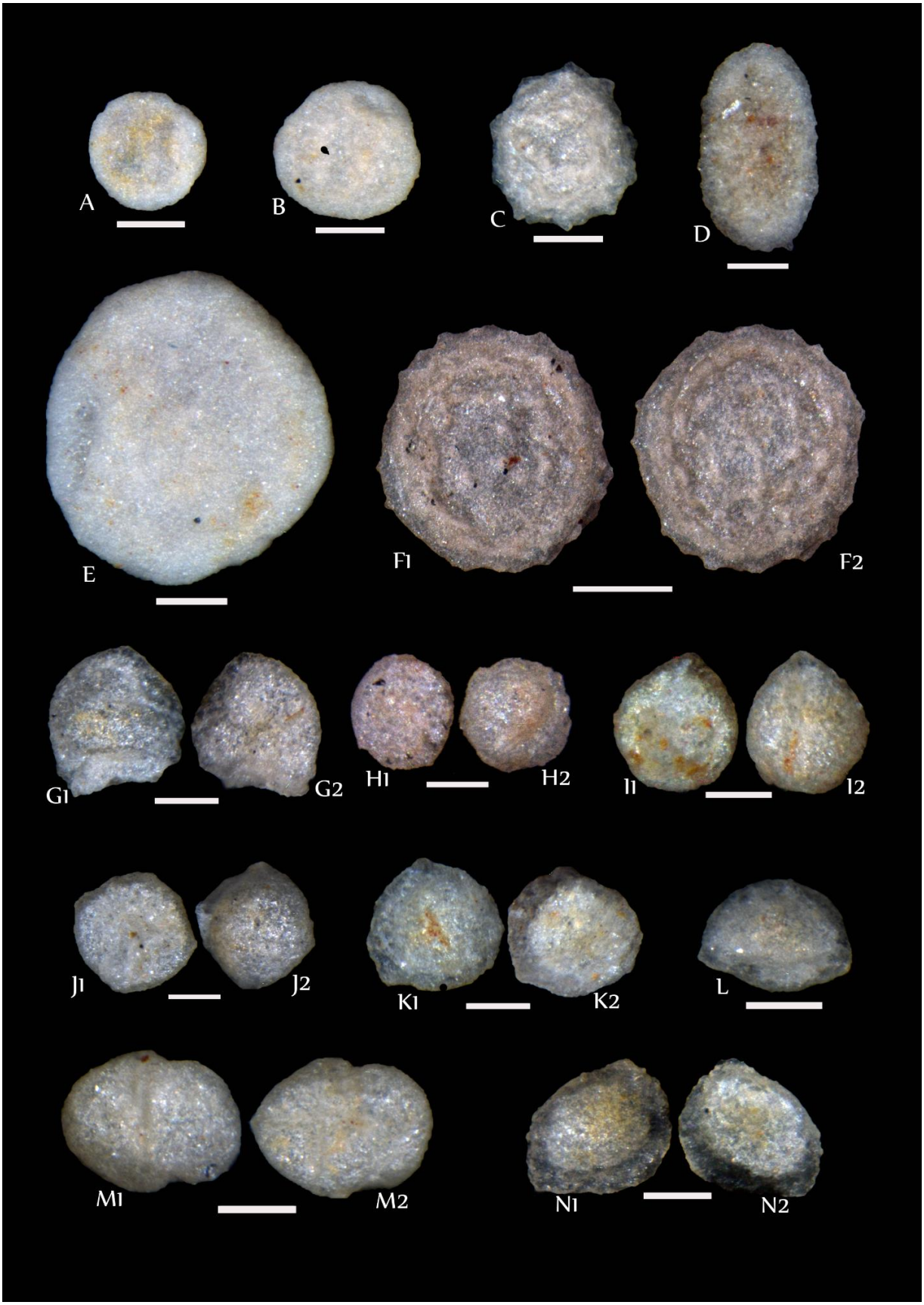
A
B
C
D
E
F1
F2
G1
G2
H1
H2
I1
I2
J1
J2
K1
K2
L
M1
M2
N1
N2

Fig. 9. Photomicrographs of agglutinated foraminifera from the Lower Silurian Qusaiba Formation. Scale bars = 100μm.

A, B. *Lagenammina* aff. *cumberlandiae* (Conkin, 1961)

C, D. *Lagenammina ligula* (Gutschick, Weiner, and Young, 1961)

E. *Lagenammina silnica* Malec, 1992

F. *Lagenammina* sp. 1

G, H. *Saccammina aspera* Stewart and Priddy, 1941

I. *Lagenammina* sp. 2

J. *Saccammina* sp. 1

K, L. *Lagenammina* sp. 3

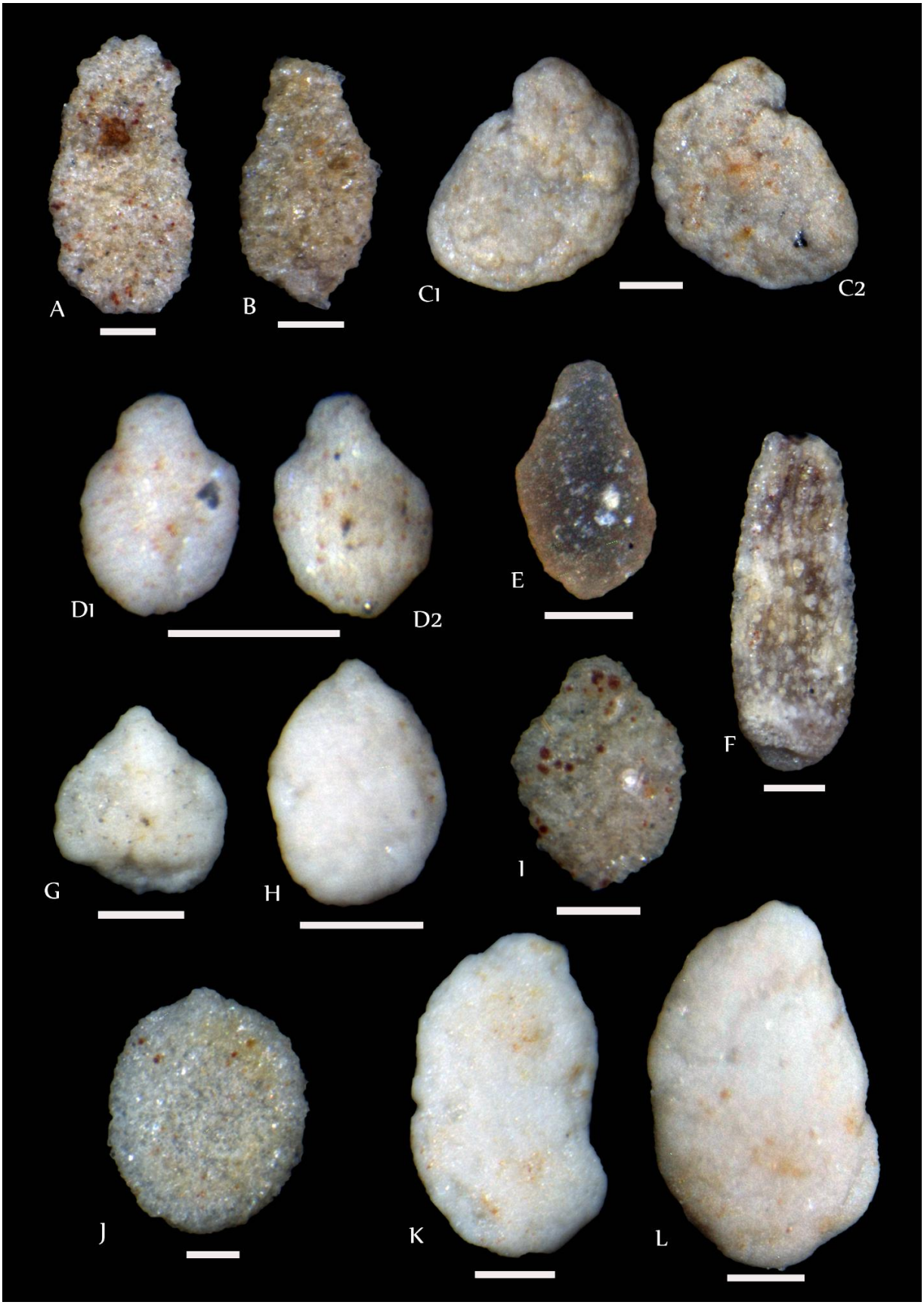
A
B
C1
C2
D1
D2
E
F
G
H
I
J
K
L

Fig. 10. Photomicrographs of agglutinated foraminifera from the Lower Silurian Qusaiba Formation. Scale bars = 100μm.

A–D. *Saccamminita galinae* Kaminski and Perdana, 2017

E. *Thurammina arcuata* Moreman, 1930

F. *Thurammina holcovae* Kaminski and Perdana, 2017

G. *Thurammina papillata* Brady, 1879

H–J. *Thurammina pentagona* Kaminski and Perdana, 2017

K. *Thurammina* (?) sp. 1

L. *Psammosphaera* (?) sp. 2

M. *Psammosphaera* (?) sp. 3

N. *Psammosphaera cava* Moreman, 1930

O. *Psammosphaera* sp. 1

P. *Sorosphaera bicella* Dunn, 1942

Q. *Sorosphaera tricella* Moreman, 1930

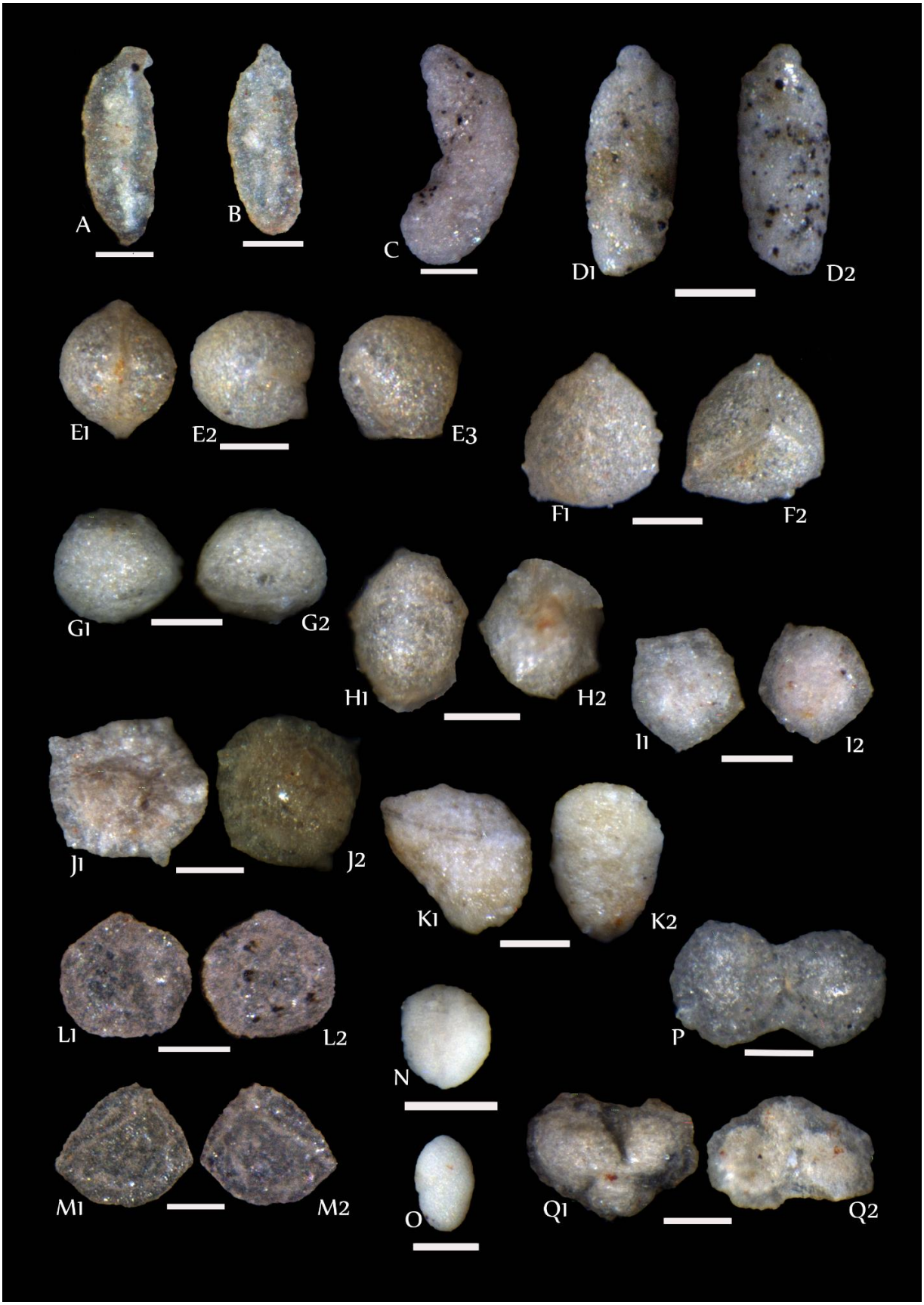
A
B
C
D1
D2
E1
E2
E3
F1
F2
G1
G2
H1
H2
I1
I2
J1
J2
K1
K2
L1
L2
N
P
M1
M2
O
Q1
Q2

Fig. 11. Photomicrographs of agglutinated foraminifera from the Lower Silurian Qusaiba Formation. Scale bars = 100μm.

A, B. Webbinelloidea sp. 1

C, D. *Kechenotiske* cf. *expansa* (Plummer, 1945)

E–G. *Hyperammina sinuosa* Kaminski and Perdana, 2017

H. *Hyperammina* sp. 1

I. *Hyperammina* sp. 2

J. *Ammovertella* sp. 1

K. *Ammovertella* sp. 2

L. *Ammovertella* sp. 3

M. *Ammovertella* sp. 4

N. *Tolypammina aihemerensis* Said and Eissa, 1969

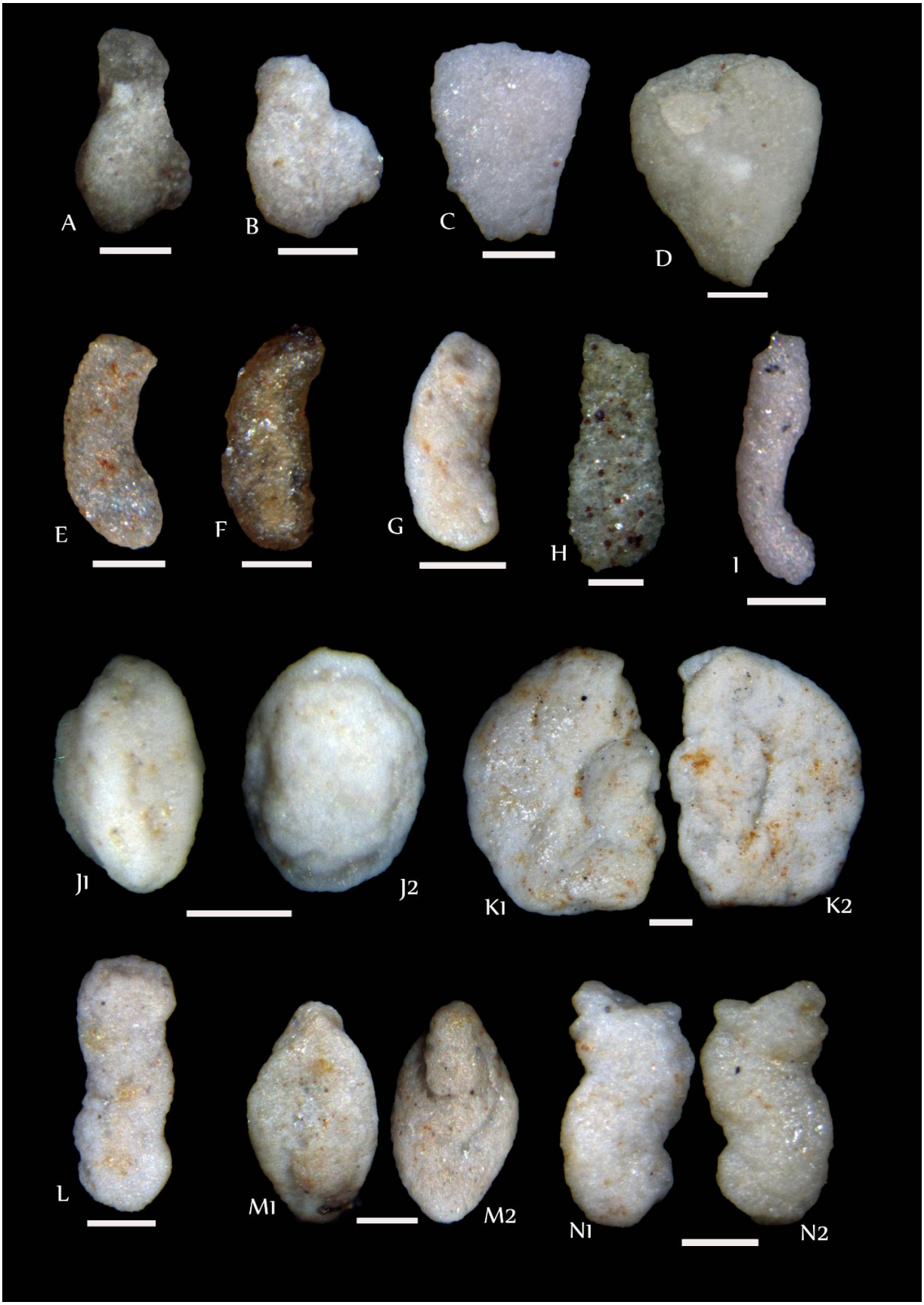
A
B
C
D
E
F
G
H
I
J1
J2
K1
K2
L
M1
M2
N1
N2

Fig. 12. Photomicrographs of agglutinated foraminifera from the Lower Silurian Qusaiba Formation. Scale bars = 100μm.

A. *Tolypammina aihemerensis* Said and Eissa, 1969

B. *Tolypammina* cf. *bulbosa*

C–F. *Tolypammina howchini* (Ludbrook, 1967)

G, H. *Tolypammina* aff. *jackobchapelensis* Conkin, 1961

I. *Tolypammina* aff. *serpens* Ireland, 1956

J. *Tolypammina tornella* (Ireland, 1956)

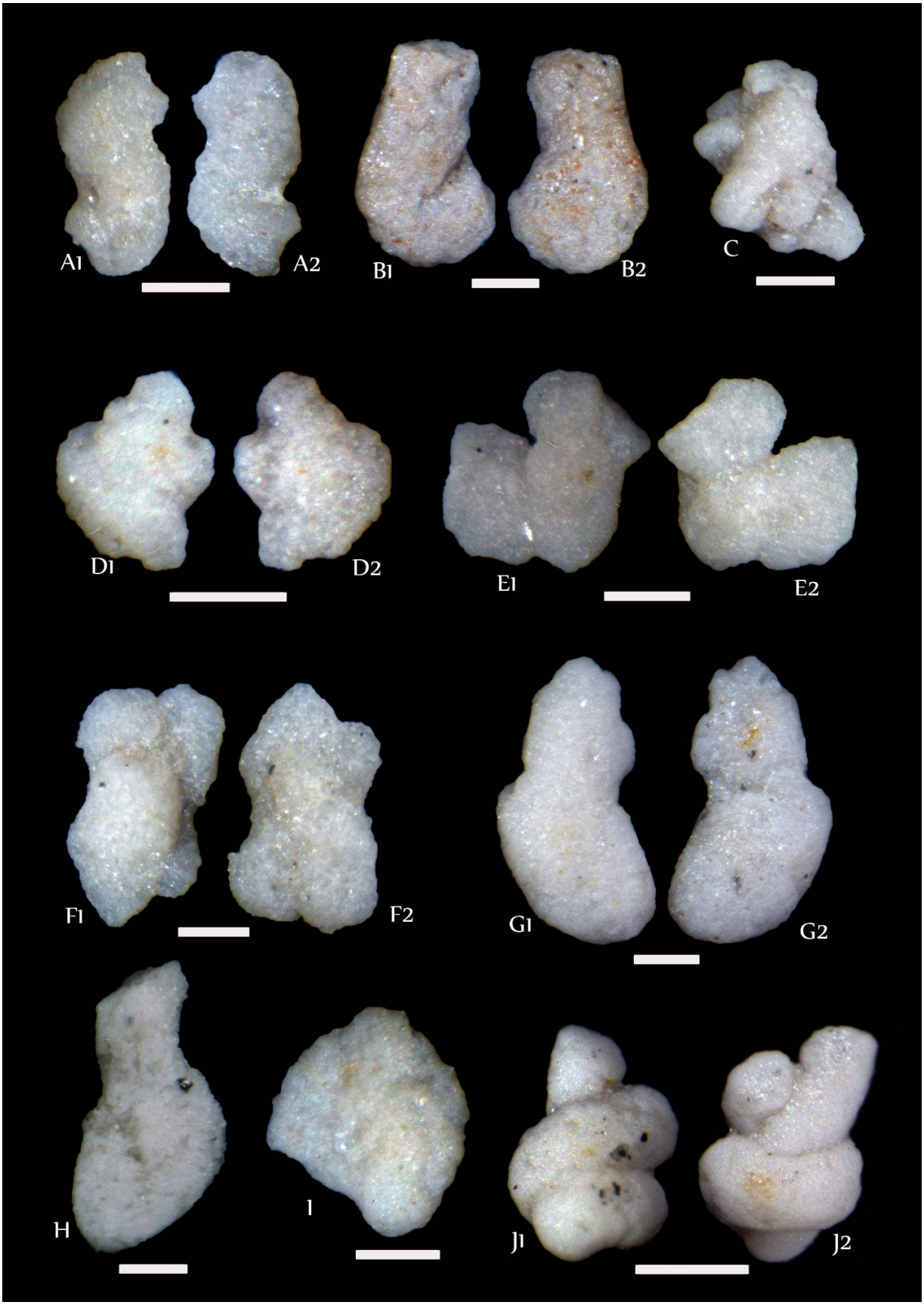
A1
A2
B1
B2
C
D1
D2
E1
E2
F1
F2
G1
G2
H
I
J1
J2

Fig. 13. Photomicrographs of agglutinated foraminifera from the Lower Silurian Qusaiba Formation. Scale bars = 100μm.

A–C, E. *Tolypammina tornella* (Ireland, 1956)

D. *Tolypammina* cf. *tortuosa* Dunn, 1942

F–H. *Tolypammina* sp. 1

I. *Tolypammina* sp. 2

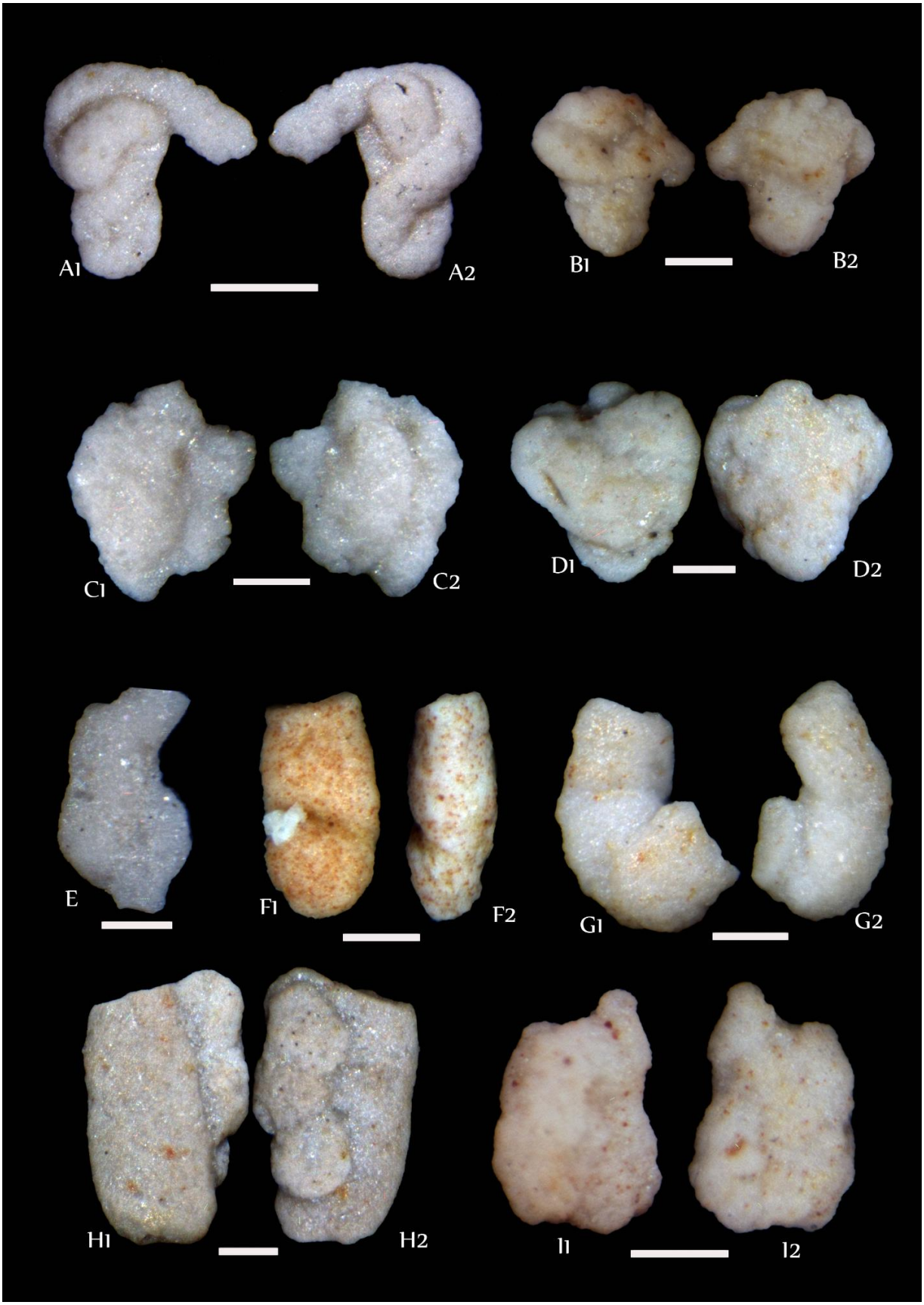
A1
A2
B1
B2
C1
C2
D1
D2
E
F1
F2
G1
G2
H1
H2
I1
I2

Fig. 14. Photomicrographs of agglutinated foraminifera from the Lower Silurian Qusaiba Formation. Scale bars = 100μm.

A–F. Tolypammina sp. 3


A1
A2
2a
2b
C1
C2
D1
D2
E1
E2
F1
F2

Fig. 15. Photomicrographs of agglutinated foraminifera from the Lower Silurian Qusaiba Formation. Scale bars = 100μm.

A, B. *Tolypammina* sp. 3

C. *Tolypammina* sp. 4

D. *Tolypammina* sp. 5

E. *Tolypammina* sp. 6

F, G. *Turritellella* sp. 1

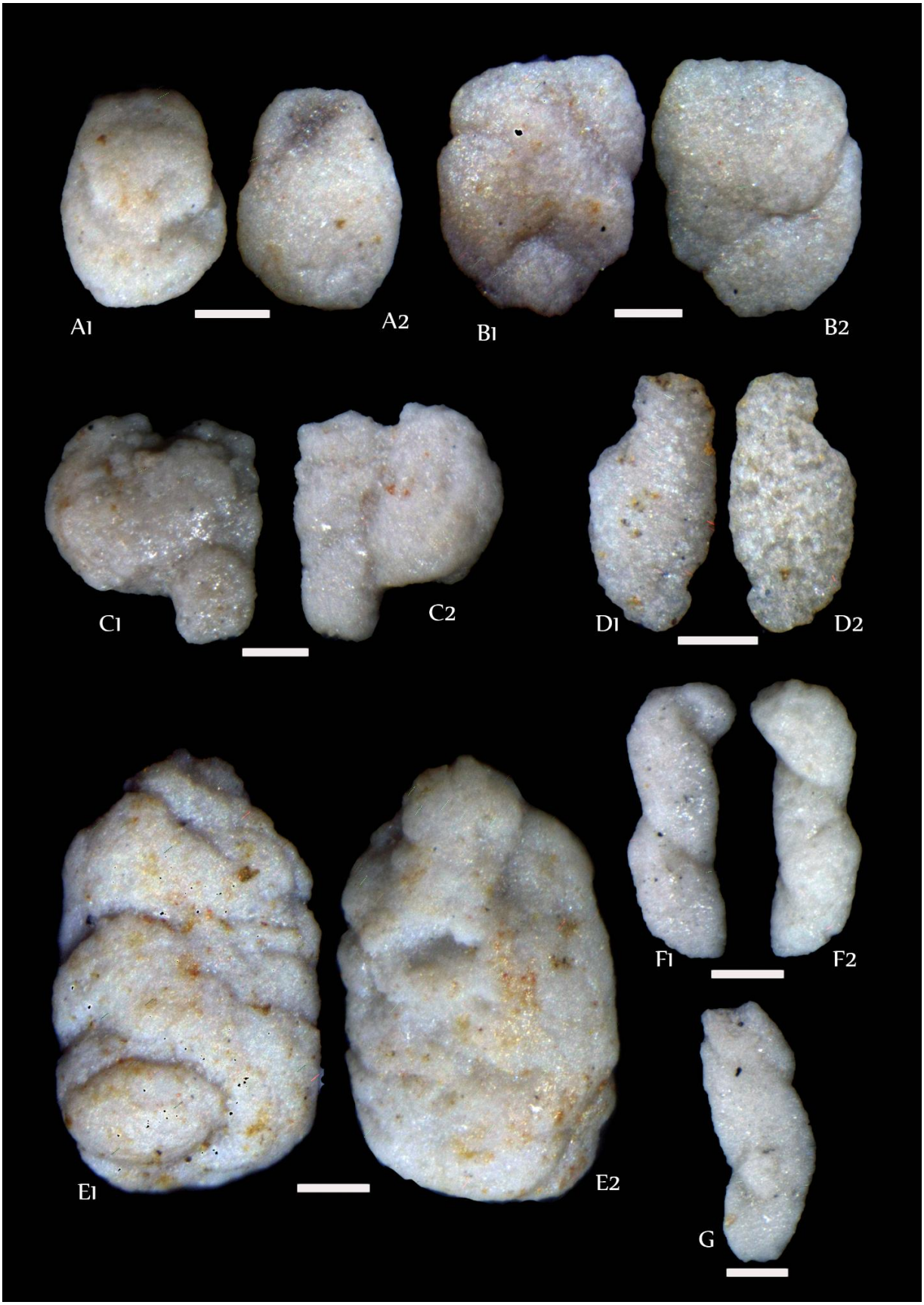
A1
A2
B1
B2
C1
C2
D1
D2
E1
E2
F1
F2
G

Fig. 16. Photomicrographs of agglutinated foraminifera from the Lower Silurian Qusaiba Formation. Scale bars = 100μm.

A–C. *Ammobaculites qusaibaensis* Kaminski and Perdana, 2017

D–F. *Simobaculites* sp. 1

G. *Stacheia trepeilopsiformis* Conkin, 1961

H–I. *Stacheia* sp. 1

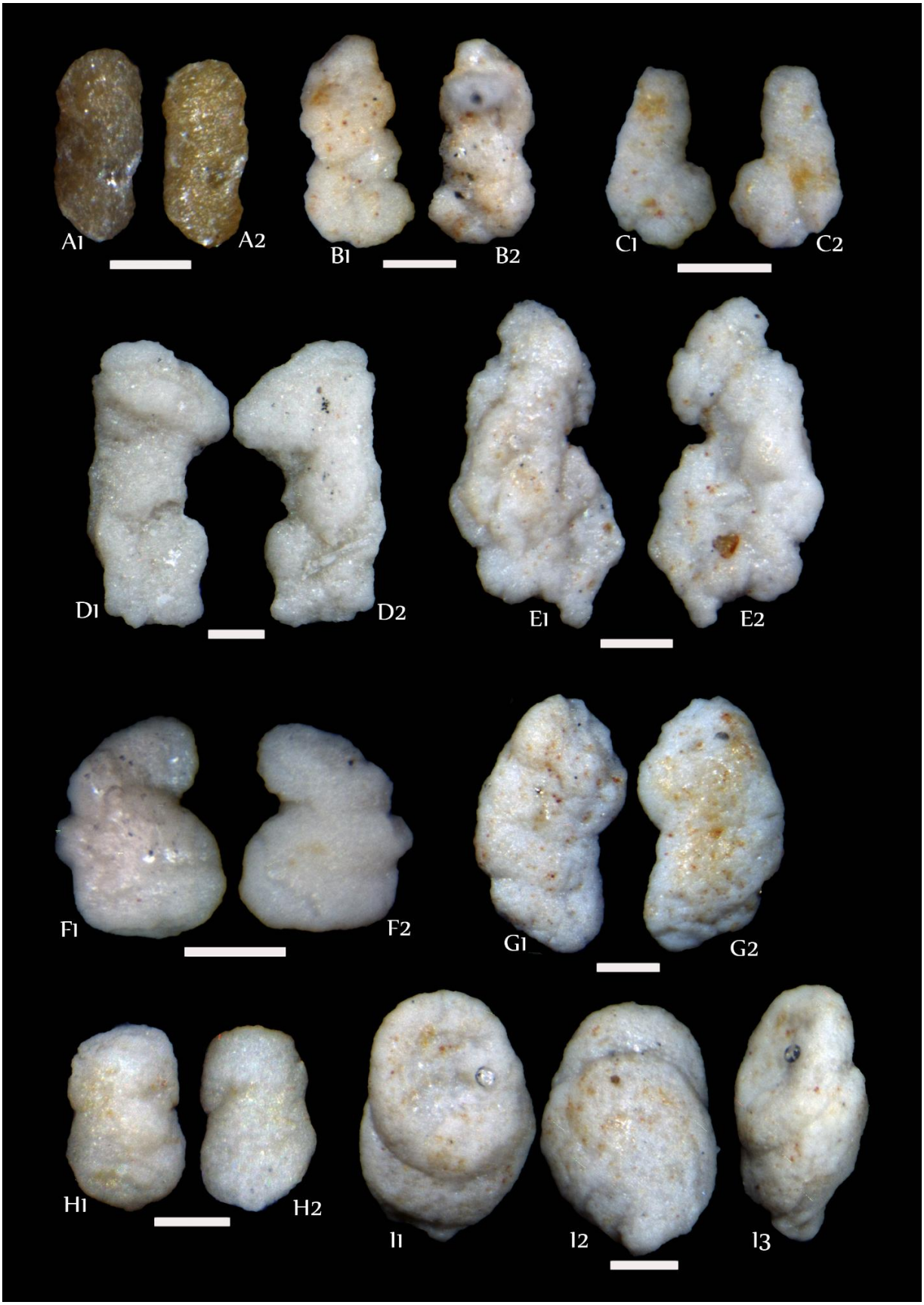
A1
A2
B1
B2
C1
C2
D1
D2
E1
E2
F1
F2
G1
G2
H1
H2
I1
I2
I3

C. Recoverable Conodonts

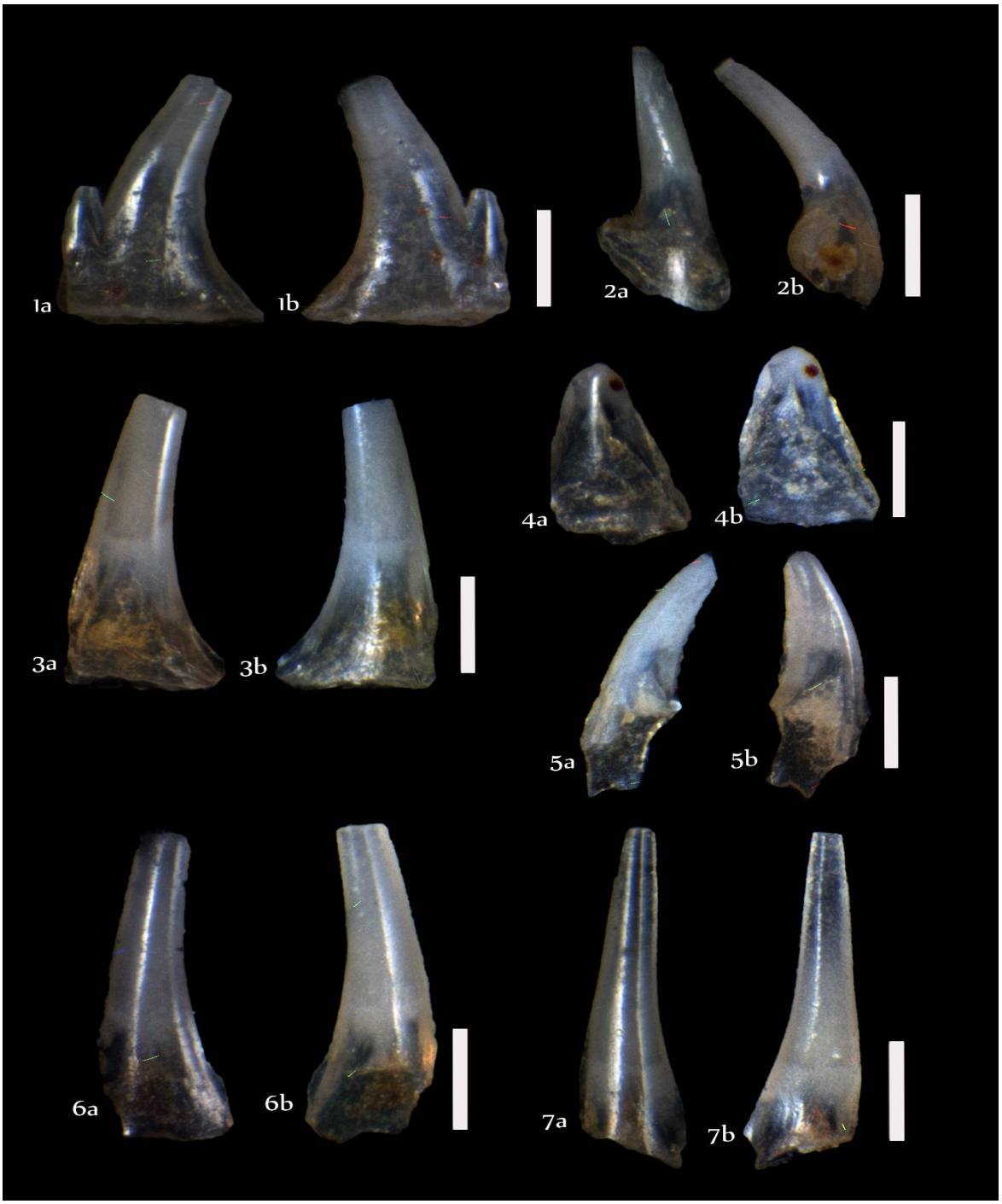

D. SEM-EDS

Lithofacies Mdg

Sample Q13

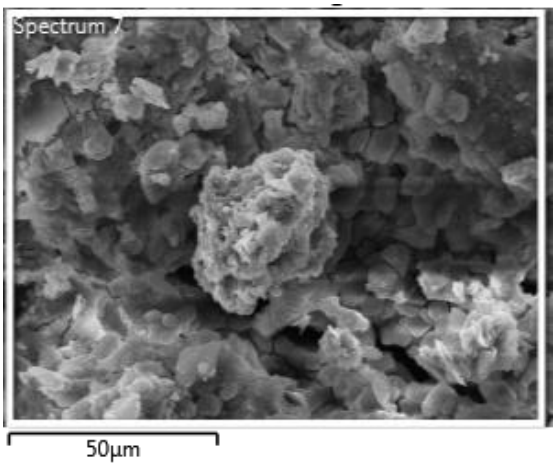

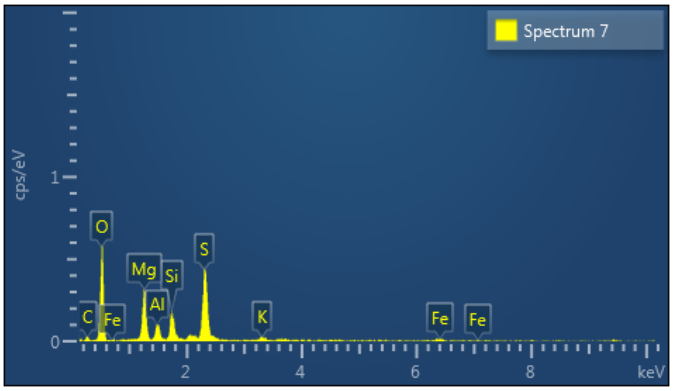

Sample Q16

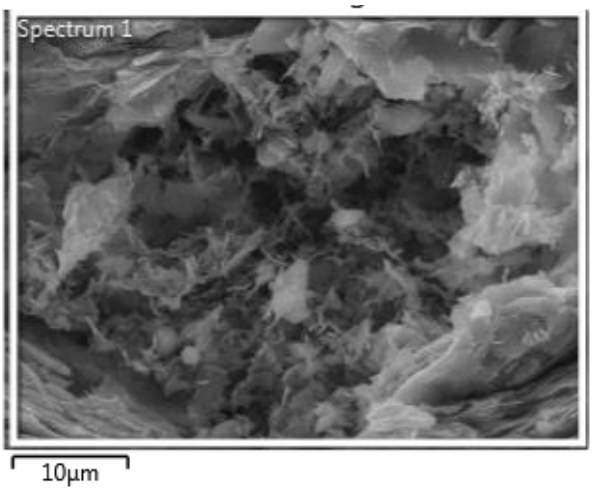

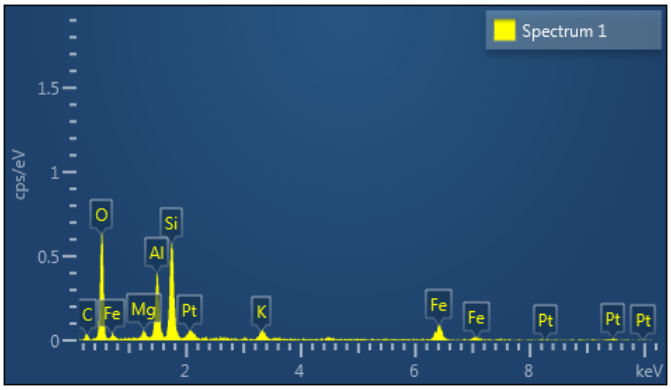

Sample Q17

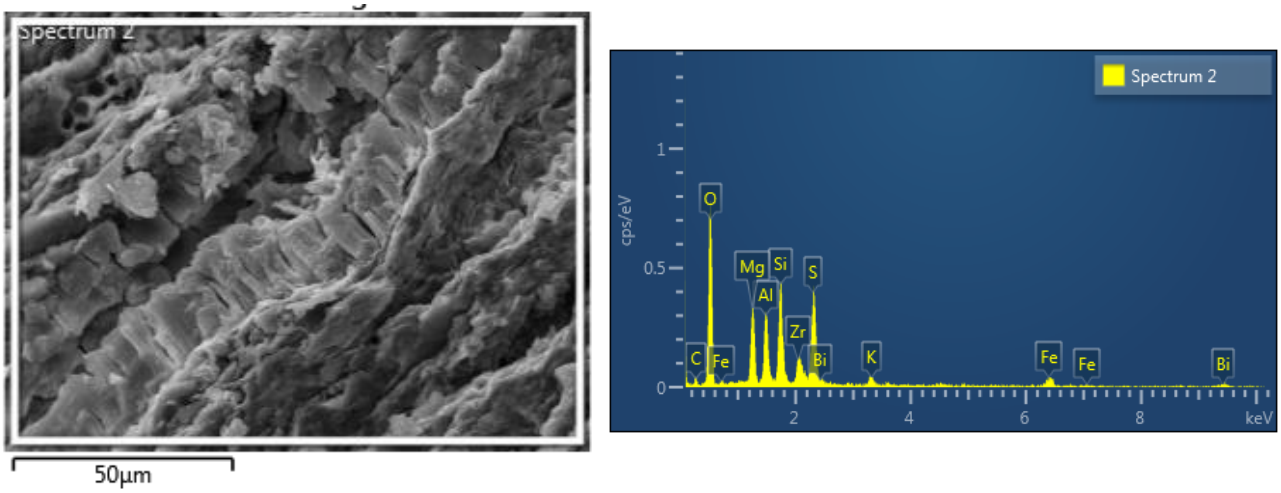

Lithofacies Mlg sample Q8

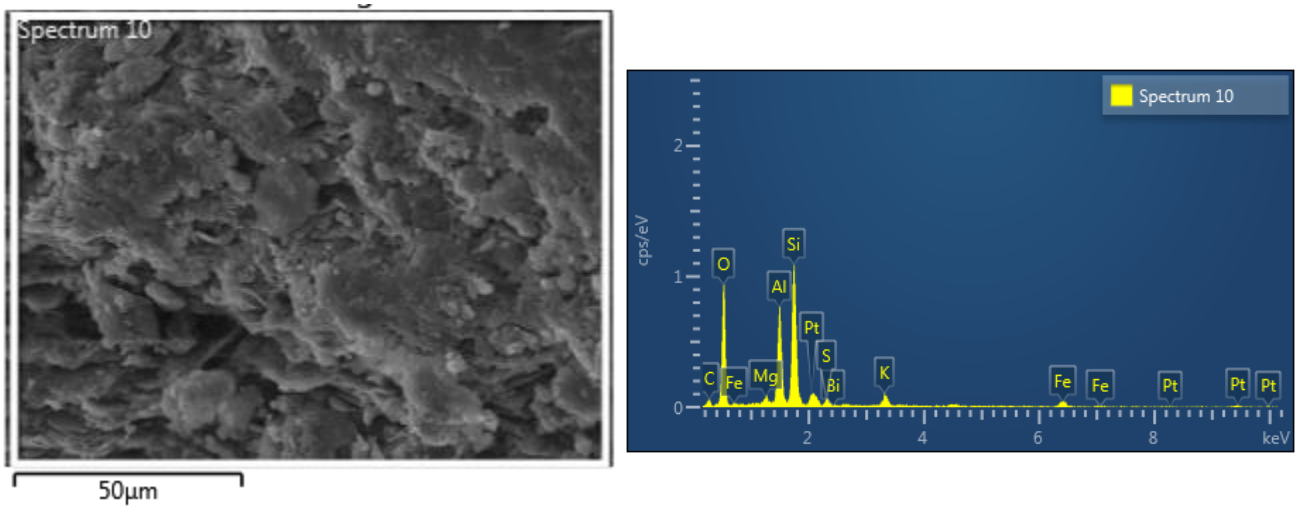

Lithofacies Mzr sample Q1F

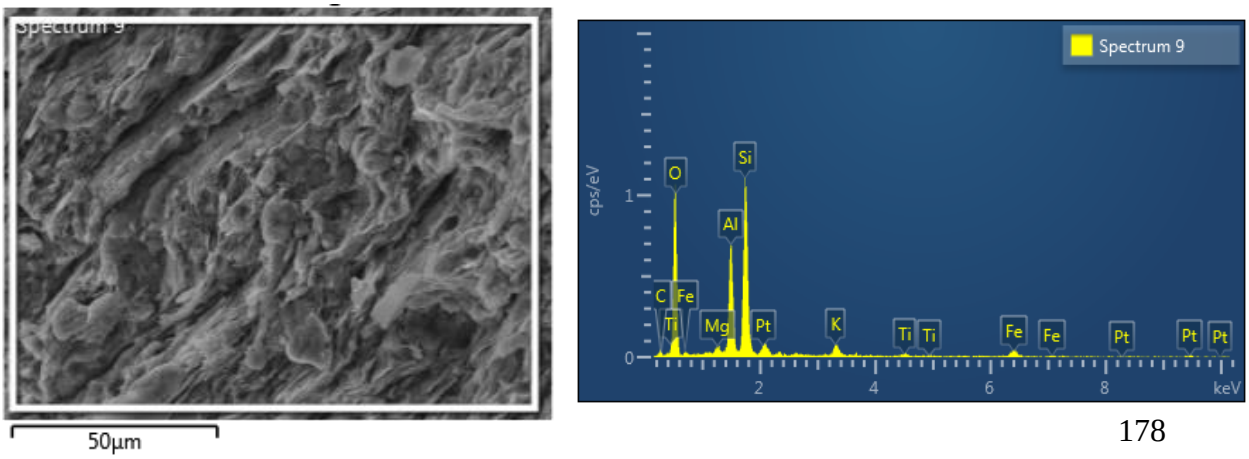

Lithofacies Sfc 2 sample Q0

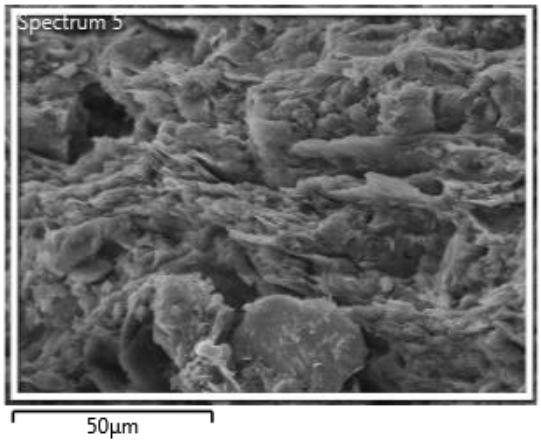

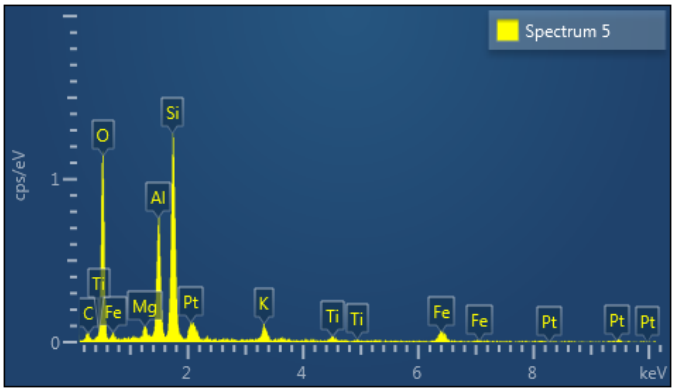

Curriculum Vitae

PRAMUDYA RINENGGA DATU PERDANA

Email : pramudyarinengga@gmail.com

Mobile : **+966 530846752**

PERSONAL DETAILS

Place, Date of Birth	: Madiun, 12 March 1987
Gender	: Male
Address 1	: Housing Building 815, King Fahd University of Petroleum & Minerals, Dhahran, Saudi Arabia, 31261.
Address 2	: RT.13 RW.3 Jatimulyo TR 1/759 Kel. Kricak Kec. Tegalrejo, Yogyakarta, 55242.
Marital Status	: Married
Nationality	: Indonesian

EDUCATION BACKGROUND

Geosciences Sciences Department **King Fahd University of Petroleum & Minerals**	**M.Sc.** **in *Geology***	**2018**
Geological Engineering Department **Gadjah Mada University**	**B.Eng. in *Geological Engineering***	**2013**

ACADEMIC AND RESEARCH EXPERIENCES

September 2015 – March 2017	*Quantification of Silurian Qusaiba Shale Source Rock* The National Science and Technology Innovation Plan Project **King Abdulaziz City Sciences and Technology**
February-May 2017	*Teaching assistant of Seismic and Sequence Stratigraphy* **King Fahd University of Petroleum and Minerals**

September 2017-January 2018	*Teaching assistant of Regional Geology* **King Fahd University of Petroleum and Minerals**

TRAINING, WORKSHOP, AND COURSES

11 – 30 June 2017 **Urbino, Italy**	10th International School on Foraminifera **Organized by the Grzybowski Foundation**
26 – 28 March 2016 **Dhahran, Saudi Arabia**	5th Center for Energy and Geo Processing Workshop *"Seismic Data Processing and Interpretation"* **Organized by Center for Energy and Geo Processing** ***King Fahd University of Petroleum & Minerals in Collaboration with Georgia Institute of Technology***
8 – 9 April 2015 **Dhahran, Saudi Arabia**	2nd Digital Rock Physics Workshop *"Mineral Fluid Interaction"* **Organized by Center for Petroleum and Minerals** ***King Fahd University of Petroleum & Minerals***

PUBLICATIONS

Kaminski, M.A. and **Perdana, P**. 2017. *New Foraminifera from the Lower Silurian Qusaiba Shale Formation of Saudi Arabia*.

Published in: Micropaleontology, volume 63, no. 1, 59–66.

CONFERENCE PRESENTATIONS

Michael Kaminski, **Pramudya Perdana**, Marco Vecoli, and Stefan Jozsa**. 2018.** An assemblage of primitive monothalamids (Foraminifera) from the Lower–Middle Ordovician Klabava Formation in the Czech Republic: implications for foraminiferal diversification. **EGU General Assembly 2018, Vienna, Austria.**

Perdana, P.R.D, Kaminski, M.A, Chan, S.A., Abdullatif, O.M. *The Role of Foraminiferal Biofacies as a Paleo-oxygenation and Paleoenvironmental Proxy of the Lower Silurian Qusaiba Shale, Qasim Region, Saudi Arabia*. **GEO 2018, Manama, Bahrain.**

Perdana, P. and Kaminski, M. 2017. *First Discovery of Early Silurian Foraminiferal Assemblages from the Upper Qusaiba and Lower Sharawra members, Qasim Region, Saudi Arabia, and their paleoenvironmental implications*. **EGU General Assembly 2017, Vienna, Austria.**

Kaminski, M.A. and **Perdana, P.** 2017. *Early Silurian Agglutinated Foraminifera from Saudi Arabia*. **10th International Workshop on Agglutinated Foraminifera, Smolenice, Slovakia.**

Kaminski, M.A. and **Perdana, P.R.D.** 2016. *Early Silurian Foraminifera from the Qusaiba Shale, Qasim Region, Saudi Arabia*. **7th Checkz-Slovak-Poland Paleontological Conference, Krakow, Poland**.

PROFESSIONAL MEMBERSHIP

2014 - Present	**Dhahran Geosciences Society (DGS)**
2015 - 2017	**European Association of Geoscientists and Engineers (EAGE)**
2015 - 2017	**American Association of Petroleum Geologists (AAPG)**